TAMPEREEN TEKNILLINEN YLIOPISTO
TAMPERE UNIVERSITY OF TECHNOLOGY

MUKESH KUMAR

MODELLING AND SIMULATION OF COMPOUND PV-BESS SYSTEMS

Master of Science thesis

Examiner: Prof. Enrique Acha
Topic and Examiner approved by the Faculty Council of the Faculty of Computing and Electrical Engineering on 1st March, 2017

ABSTRACT

MUKESH KUMAR: Modelling and simulation of compound PV-BESS systems
Tampere University of technology
Master of Science Thesis, 79 pages
Dec 2017
Master's Degree Programme in Electrical Engineering
Major: Smart Grids
Examiner: Professor Enrique Acha

Keywords: Photovoltaics, Battery energy Storage, DC/DC converters, DC-AC Inverters, Simulink, PV-BESS

The thesis reports on the modeling and simulation of PV systems with grid-connection. The research carried out assesses the impact of key parameters of Photovoltaic systems on power generation and power quality. It also examines a utilization of Battery energy storage system (BESS) which serves the purpose to support the active power production by charging and discharging the surplus and reduced power generation from PV.

The use of renewable energy systems, such as Photovoltaic (PV), is becoming highly popular in modern power systems. However, the random and fluctuating nature of the solar resource increases the possibility of power mismatches between power generation and power demand in the grid. A large penetration of such a fluctuating energy resource can degrade the reliability of supply, the stability of system operation and introduce adverse power quality phenomena. Battery Energy Storage Systems (BESS) are recognized to be a viable solution to overcome the fluctuations present in PV systems. Hence, the integration of BESS with grid-connected PV systems will greatly enhance the reliability of the overall power grid.

In this thesis, the modeling and simulation of PV-BESS is carried out using the MATLAB/Simulink environment. A test system comprising a 100 KW PV panel is connected through a DC-DC converter in tandem with a DC-AC inverter to a Point of Common Coupling (PCC) of an equivalent power grid. The effects of changes in solar irradiance and temperature, on the output power of the PV system, are assessed in the first part of the thesis. The integration of a BESS model in parallel with a PV system model is carried out in the second part of the thesis, where the overall intermittent behavior of the combined system is assessed.

It should be stressed that the key purpose of integrating a BESS and a PV system is to provide constant power supply to the load system under varying environmental conditions. The outcome of this investigation shows that the integration of the BESS into the PV system yields very encouraging results in counteracting the fluctuation of the PV installation, helping to ensure a constant power supply to the load.

PREFACE

This Master thesis was written in partial fulfillment of the requirement of Master of Science degree in Electrical Engineering at the Tampere University of Technology under the supervision of Professor Enrique Acha.

First, I would like to show my most sincere gratitude to my thesis supervisor Professor Enrique Acha for his continuous support, encouragement and his valuable feedback during my thesis. I am very grateful for his patience and kindness during course of thesis.

I would also like to thanks to all my friends for their support and encouragement during my studies in Finland.

I would like to express my heart-felt gratitude to my parents, my siblings, my wife and kids for their unconditional love, support and encouragement.

Tampere, 09.12.2017

Mukesh Kumar

CONTENTS

LIST OF FIGURES

NOTATIONS AND ABBREVIATIONS

NOTATIONS

B_i	A constant independent of the operating temperature of a solar cell
D	Duty cycle
F_F	Fill factor of a photovoltaic cell
$f_{switcihing}$	Switching frequency (Hz)
I	Output current of a photovoltaic cell
I_d	Diode current
I_L	Light generated current in a photovoltaic cell
I_{MP}	Current of a photovoltaic cell at the maximum power point
I_o	Dark saturation current of a diode
I_{SC}	Short-circuit current of a photovoltaic cell
K	Boltzmann's constant
m_a	Amplitude modulation ratio
m_f	Frequency modulation ratio
n	Ideality factor of diode
R_s	Series resistance of a photovoltaic cell
R_{sh}	Shunt resistance of a photovoltaic cell
t_{off}	Turn-off time
t_{on}	Turn-on time
T_s	Switching time
$V_{control}$	Peak amplitude of the control signal in a PWM controlled inverter
V_{MP}	Voltage of a photovoltaic cell at the maximum power point
V_{OC}	Open-circuit voltage of a photovoltaic cell
Vt_{ri}	Amplitude of the triangular signal in a PWM controlled inverter

ABBREVIATIONS

AC	Alternating current
BESS	Battery energy storage system
CCM	Continuous conduction mode
CSI	Current source inverter
DC	Direct current
DOD	the depth of discharge
IGBT	Insulated Gate bipolar transistor
MPPT	Maximum power point technique
NPC	Neutral-Point-Clamped Inverter
PLL	Phase locked loop
PV	Photovoltaic
P-V	Power Voltage
PWM	Pulse width modulation
SOC	state of charge

STC	standard test condition
V-I	Voltage-current
VSC	Voltage source converter
VSI	voltage source inverter

1. INTRODUCTION

Electricity has become one basic commodity in today's world owing to key advancements in technology, population growth, raising standards of living in most parts of the world and widespread industrialization. It has become one of the parameters by which the economic growth of a country is measured. Figure 1-1 shows the worldwide energy consumption from 1800-2015 in TW-h [1].

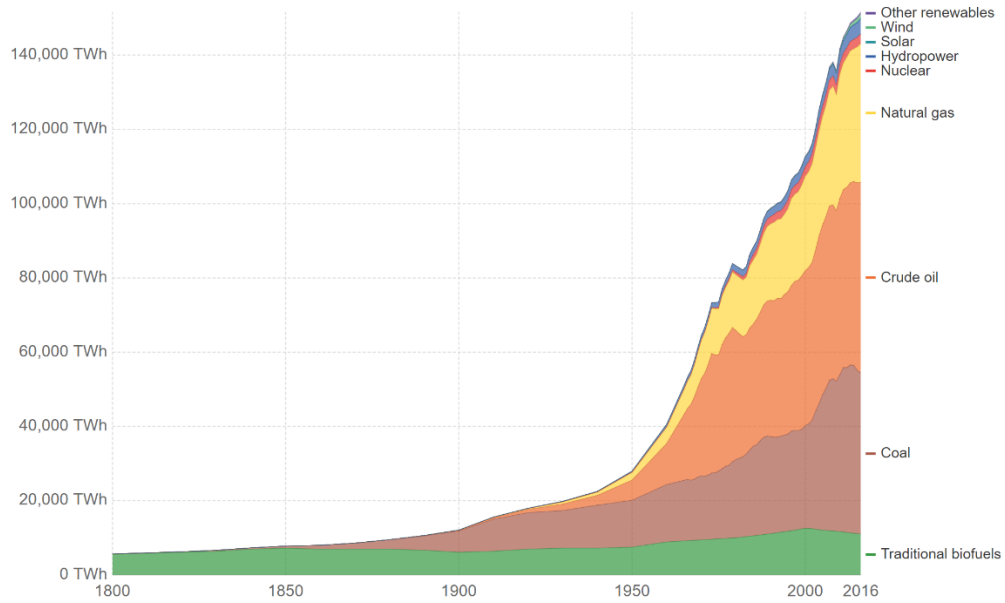

Figure 1-1. *The global primary energy consumption in TW-h* ***[1]****.*

Electrical energy is produced using different sources of electricity mainly categorized as non-renewable and renewable energy sources. Non-renewable sources use fossil fuels, coal, gas and nuclear resources, which are finite and increase the greenhouse effects and ocean waters pollution, posing a serious threat to the earth's environment. In order to mitigate the threat posed by continuing using non-renewable sources of electricity, the electricity supply industry is gradually moving to the use of renewable energy sources, which represent a sustainable path. To help to implement the consumption and production of green energy, the European Union (EU) has set major targets to be accomplished by 2020. To reduce the greenhouse gases by as a minimum 20% below the levels of 1990, to increase by 20% the use of renewable energy resources in the overall energy consumption within the EU, to reduce by 20% the use of primary energy resources by improving energy efficiency [2, 3].

In 2016, there has been a global increase of 75GWdc of solar photovoltaic (solar PV) capacity according to the International Energy Agency (IEA) [4]. In 2016, as seen in

Figure 1-2, at least 74.4 GW of PV power was added to the global PV market. This figure could in fact be higher, say, 75.4 GW, since a few countries do not report figures. This represents 50% more than the 50 GW growth of 2015 [5].

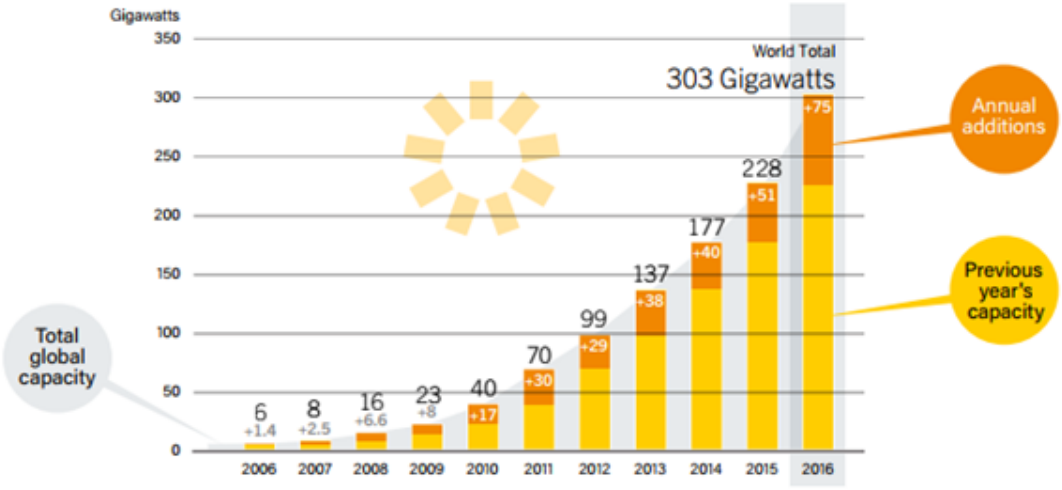

Figure 1-2. *PV annual addition and global capacity, 2006-2016* ***[5]****.*

Although the PV power generation has enormous potential to reduce CO_2 emissions very effectively, the solar resource is quite unpredictable and power can only be produce during daytime. The irregular behavior of moving clouds can cause fluctuations in the output power of PV generators. If a large amount of photovoltaic power is injected into the power grid then large power fluctuations will be expected, which have the potential to cause voltage imbalances, frequency instabilities and power imbalances in the power grid [6]. To supplement the output power of PV generators, in-situ energy storage devices are often used. This allows excess power to be stored and used at times when there is insufficient PV power generation due to cloudy weather or no PV power generation at all, such as at night.

Such intermittence of the solar energy resource is the reason why solar PV power is considered to be an intermittent source of power and to be classified as non-firm generation. Energy storage turns this on its head, as it compensates very effectively for the fluctuating power outputs of the PV generators, provided the BESS has been properly rated at the design stage. The BESS technology has the potential to improve the reliability and power quality of the electrical energy fed into the utility grid [7].

This thesis focuses on the analysis of the output power of PV generators during changing solar radiation and temperature conditions and on the compensation of the ensuing active powers by means of a battery energy storage system.

1.1 Research objectives and outline of thesis

The major objectives of the work represented in the thesis are listed below

- To design the system model of a PV generator in MATLAB/Simulink and integrate it with the load and the power grid model.
- To design a BESS system in MATLAB/Simulink, for suitable integration with the grid-connected PV system
- To assess the impact of environmental parameters on the output power of PV generators and the utilization of the BESS storage option to compensate the fluctuations in power output of the PV plant, to enable a quasi-constant power supply to the load/grid.

The thesis comprises of following chapters

Chapter 1 is the introductory chapter, which outlines issues of electrical energy consumption, the importance of renewable energy and PV power, technical issues associated with grid-connected PV systems and the strategic importance of battery energy storage systems.

Chapter 2 provides an overview of the fundamentals of PV systems, the basics of a photovoltaic cell, the impacts of environmental effects on the operation of PV systems and an introduction of grid-connected PV system.

Chapter 3 presents a classification of the kinds of batteries available and discusses some key battery parameter and key points of the model used in Simulink.

Chapter 4 deals with the power electronics concepts and control techniques, which are of paramount importance to the integration of renewable energy into the power grid, in particular, PV generation. The different types of DC-DC converters, a MPPT algorithm, and a DC-AC inverter along with the associated control technique, are all discussed in this chapter.

Chapter 5 addresses the modeling of PV systems and BESS system within the Simulink environment.

Chapter 6 presents the simulation results pertaining to the PV system and the PV-BESS system, obtained with Simulink.

2. PHOTOVOLTAIC SYSTEM

2.1 Introduction

PV is the technology which permits direct conversation of solar energy into electrical energy. A semiconductor material-based device used to convert sun energy into electrical energy is a called solar cell or a photovoltaic cell. The physical phenomenon of converting sun energy into electrical energy is also known as a Photovoltaic effect, which was first observed by Becquerel in 1839 [8].

2.2 PV cell

A photovoltaic system is the combination of PV modules grouped in series and parallel combinations to meet a specified voltage, current and power rating. A PV cell is made up of semiconductor materials, such as silicon or germanium. A typical PV cell is composed of n-type and p-type semiconductor materials exhibiting different electrical properties. When a PV cell absorbs a photon of sunlight, free electron and holes are created at the positive and negative junctions of the semiconductor assembly and generates DC power. The structure of a basic PV cell is shown in Figure 2-1, the power generated by the PV cells are collected through metallic contacts connected on both sides of the cell.

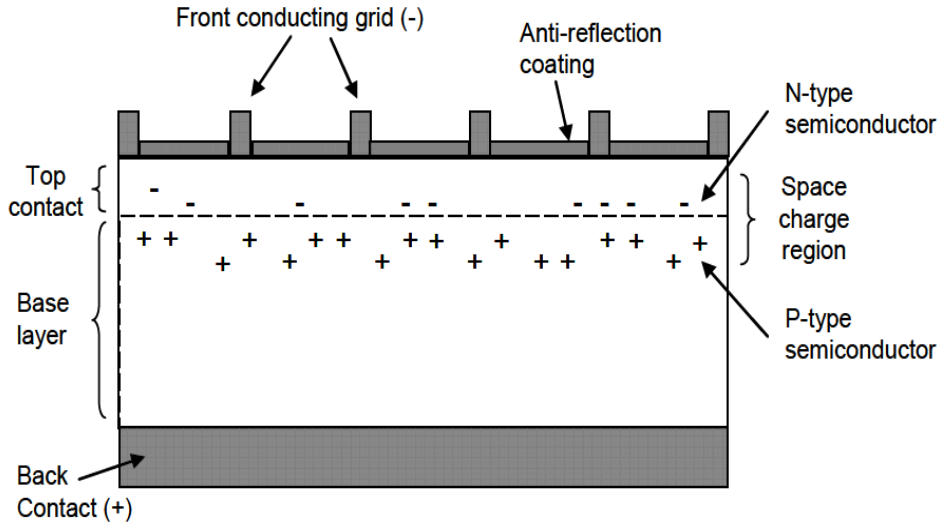

Figure 2-1. *The structure of PV cell* ***[9]****.*

The output of PV cell under various operating conditions generally represented by V-I curve and P-V curve is shown in Figure 2-2, where, V_{oc} is open circuit voltage, I_{sc} is short circuit current and $V_{mp}I_{mp}$ is maximum voltage and current at maximum power point.

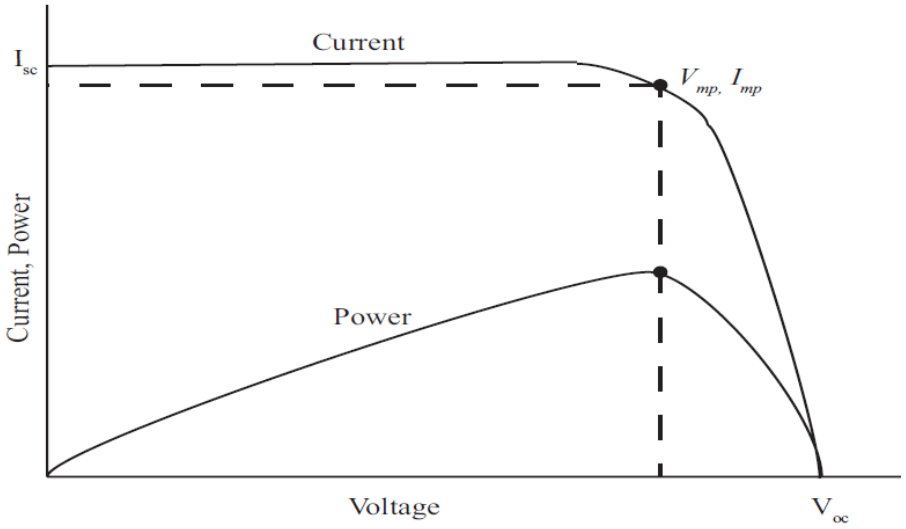

Figure 2-2. *The typical I-V and P-V curve of PV cell* ***[8]***.

To model the PV cell, it is important to understand the properties of I-V characteristics. The DC current generated by PV cell generally given as

$$\mathrm{I} = I_L - I_o\left[exp\left(\frac{\mathrm{qV}}{nkT}\right) - 1\right] \tag{2.1}$$

Where, I_L is short circuit current, I_o is saturation current, V is the voltage of PV cell.k is the Boltzmann constant, q is the electron charge, T is the temperature. The electrical model of single diode PV cell represented by Figure 2-3 .

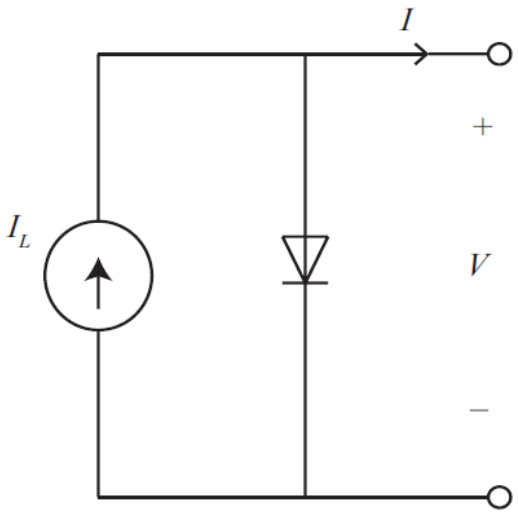

Figure 2-3. *Single diode of PV cell* ***[8]***.

The short circuit current is the maximum current available when the voltage is zero and the open circuit voltage (V_{oc}) is the maximum voltage obtain at zero current and the open circuit voltage is given as

$$V_{oc} = \frac{nkT}{q} \ln\left(\frac{I_L}{I_o} + 1\right) \tag{2.2}$$

The fill factor is also one of the essential parameter which measure the performance of PV cell and quality of junction and it is given as,

$$F_F = \frac{V_{mp} I_{mp}}{V_{oc} I_{sc}} \tag{2.3}$$

The ideal fill factor value of the solar cell is 1, which defines the highest quality of PV cell. Due to existence of parasitic elements in the PV cell, the value of fill factor decreases. The circuit of PV cell with parasitic elements is shown in Figure 2-4.

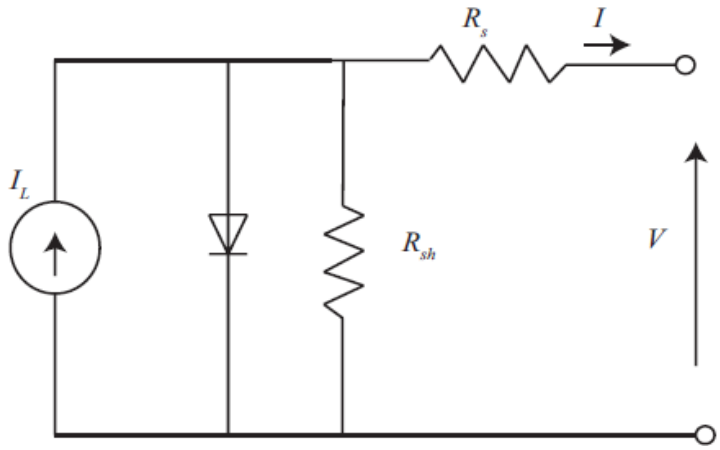

Figure 2-4. *The single diode of PV cell with parasitic elements* ***[8]****.*

The practical PV cells also contain parasitic elements, series resistance (R_s) and shunt resistance (R_{sh}). The presence of shunt resistance is due to impurities near the p-n junction and series resistance is due to high resistance of metal contacts, interconnections and, semiconductor material. The higher value of shunt resistance is desirable and thus it increases the performance of PV cell and the lower value of series resistance increases the output power of PV cell as shown in Figure 2-5.

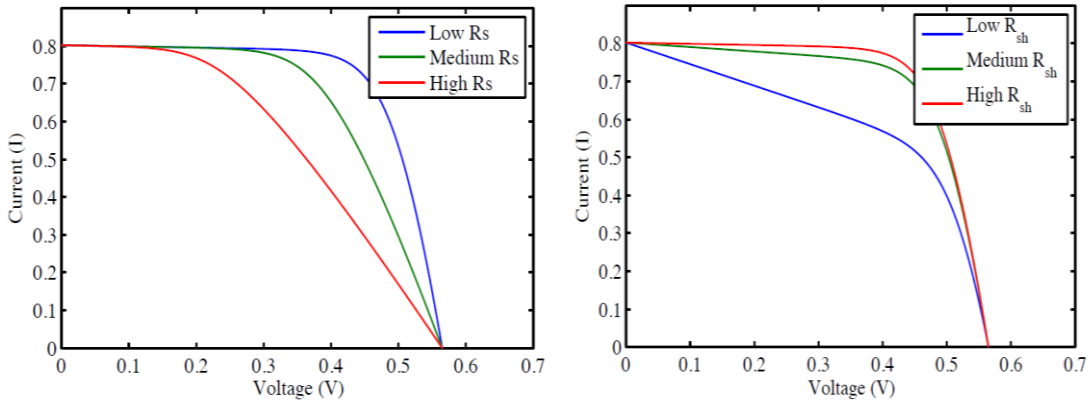

Figure 2-5. *The series and shunt resistance effect on V-I curve of a solar cell* ***[10]***.

The presence of shunt and series resistance in the V-I characteristics of PV cell given by:

$$\mathrm{I} = I_L - I_o \left[exp\left(\frac{\mathrm{V} + \mathrm{I}R_s}{\frac{nkT}{q}} \right) - 1 \right] - \frac{\mathrm{V} + \mathrm{I}R_{sh}}{R_{sh}} \tag{2.4}$$

2.2.1 Temperature and Irradiance effect on PV cell

The performance of PV cell affected by ambient factors such as temperature and irradiance. This section describes the dependency of both factors on the performance of PV cell. The short circuit current has an almost linear relationship to irradiance on the cell. The increase in irradiance increases the short circuit of PV cell and vice versa [11].

$$I_{SC}(G) = \left(\frac{G}{G_o}\right).I_{SC}G_o \tag{2.5}$$

Where, G_o is reference level of irradiance and G is the incident irradiance on PV cell. The dependency of irradiance and temperature also illustrated in Figure 2-6

Apparently, the environment temperature affects the operational performance of PV cell. The increase in temperature slightly increases the open circuit current due to narrow bandgap but it decreases the short circuit voltage significantly. The dependency of crystalline silicon-based solar cell on temperature is given as

$$I_{SC}(T) = I_{SC.REF} + 0.006\frac{A}{K}(T - T_{REF}) \tag{2.6}$$

And the dependency of open circuit voltage on temperature is expressed as [12]

$$V_{OC}(\mathrm{T}) = \frac{E_{go}}{q} - \frac{kT}{q} ln\left(\frac{BT^{\gamma}}{I_{SC}}\right) \tag{2.7}$$

Where γ is temperature dependent on parameter of dark saturation current, B is constant and independent of temperature, E_{go} is the linearly extrapolated zero temperature band gap energy of the semiconductor [13]. The rough estimation of the rise of every degree centigrade of silicon cell decreases the output power by 0.5%. The dependency of temperature and irradiance on the V-I characteristics of PV cell is shown in Figure 2-6

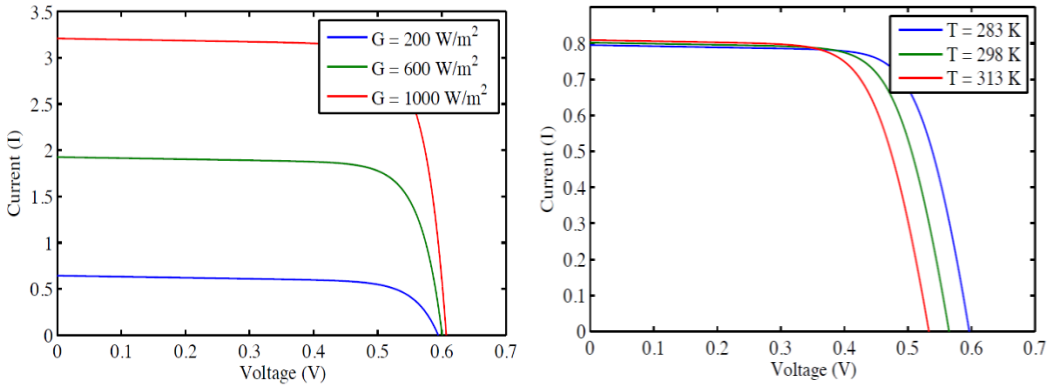

Figure 2-6. *The irradiance and temperature effect on V-I characteristics of PV cell* ***[8]***.

2.3 PV module and array

The typical PV cell generates less than 3W of power at 0.5V DC, therefore it is not used for most practical applications. Multiple PV cells in parallel-series combination to generate suitable power for most application purposes and known as PV modules. Individual cells are typical (36 or 72) connected in a series string to achieve the desired output voltage.

A typical layout of 36 PV cells connected in series shown in Figure 2-7. In this combination, the voltage across the terminal is the sum of all individual PV cell and current is same across all the cells. In parallel connection of PV cells, the output voltage across each cell is same and the output current is the sum of each individual cells [11].

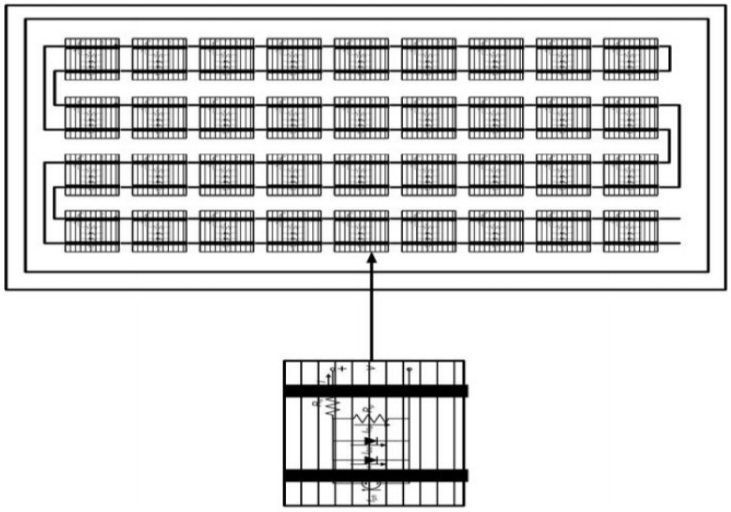

Figure 2-7. *The structure of PV module with 36 cells connected in series* ***[9]****.*

When number of PV cells are connected series, it is possible cell becomes entirely or partially shades and thus degrade the performance of the overall module. The shaded cell can be reversed biased and acts as load instead of a generator. As shown in Figure 2-8 the bypass diode connected in an anti-parallel combination individual cell or set of cells to avoid the negative impact of the shaded cell on whole module [11].

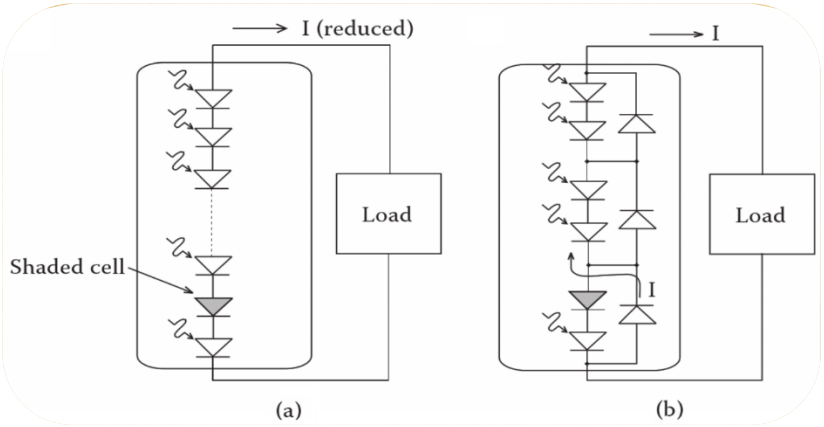

Figure 2-8. *PV module (a) cells without bypass diode (b) cells with bypass diode* ***[11]****.*

A PV array is the combination of PV modules connected electrically, mounted on the same plate to generate desired output power to the certain application. PV modules are connected in series to increases the voltage capacity of PV array and it is connected in parallel to increases the current capacity of the system. The typical series-parallel combination of PV modules shown in Figure 2-9.

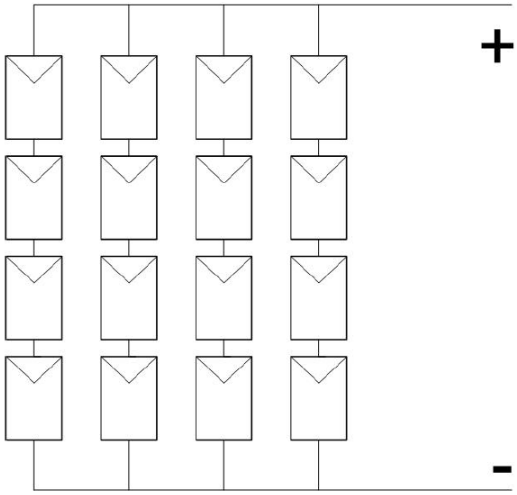

Figure 2-9. *A serial-parallel combination PV module to form PV array.*

2.4 Grid-connected PV system

The energy generated from PV system and feed to the utility grid is called grid-connected PV system. PV generators produce dc power, it requires some interfaces to connected it to the grid. The inverters are used in case of PV generator to convert DC power into AC power to connect to the power grid. Depending on the interface of the grid, the PV generators can be configured in different ways as shown in Figure 2-10 and some of them are string technology, centralized technology [14].

The traditional setup is centralized technology as shown in Figure 2-10(a), where a numeral amount of PV modules connected to the power grid via an inverter. The string of PV modules is connected in parallel via protecting diode. Centralized technology is sensitive to mismatch losses and partial shading [15].

Each string of PV module with a separate inverter is connected to the grid in parallel combination in String technology as shown in Figure 2-10(b). It is less sensitive dc power losses and partial shading but. It has the flexibility to add new strings to the system. Due to the smaller size of inverters in string technology the overall efficiency.

The multi-string technology is combination centralized and strings technology as shown in Figure 2-10c. It has the advantage of both technologies. The system is modular, it is easy to add another string and it has almost zero dc side loss [15].

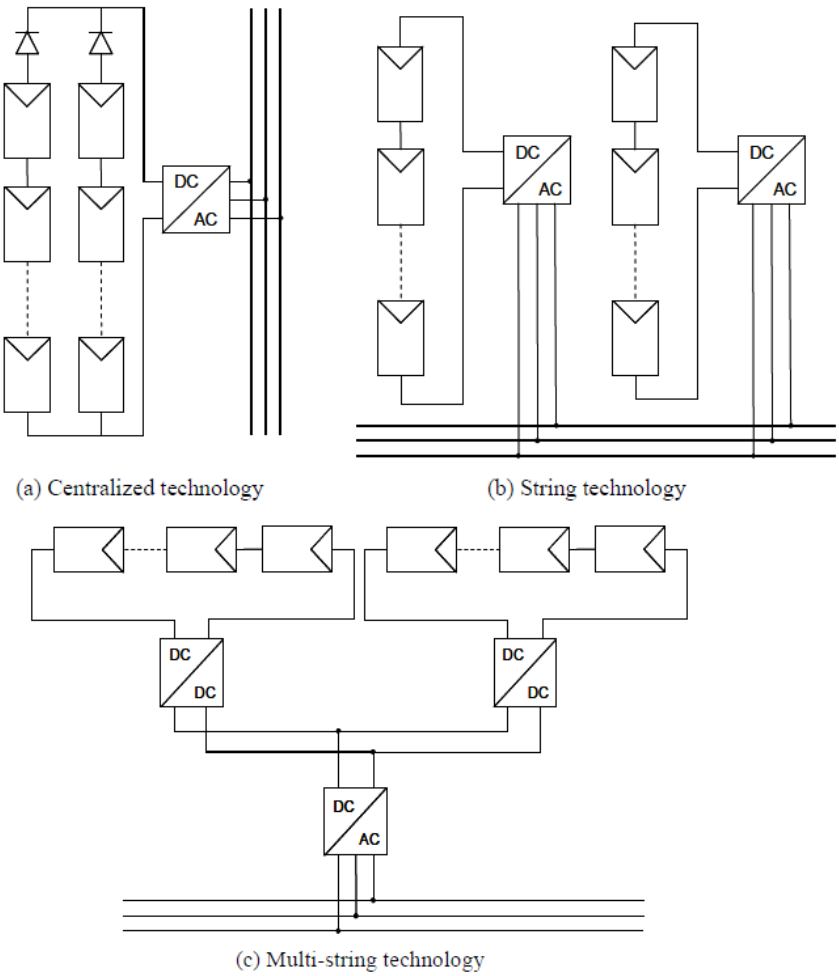

Figure 2-10. *Different configuration of grid-connected PV generators* ***[16]***.

3. BATTERY ENERGY STORAGE

3.1 Introduction

Amongst the various energy storage methods commercially available to store electrical energy, batteries are perhaps the better developed. Due to continuous development of this technology, batteries are providing a vital role in storing electrical energy especially when energy is being generated from intermittent renewable energy resources. Batteries store and release energy using electrochemical reactions: when electrical energy is converted into chemical energy, the battery is in charging mode (it stores energy). The chemical compound within the batteries acts as a storage medium. While in discharging mode, the stored chemical energy is converted into electrical energy [17].

3.2 Components of batteries and cells

A cell, the elementary battery unit, consists of four major components:

1. The *Positive electrode* or cathode (during discharging reaction) is oxidizing by absorbing electron from the external circuit or oxidized (during charging reaction) by supplying electron to the external circuit
2. *Negative electrode* or anode (during discharging reaction) is oxidized by supplying electron through the external circuit or oxidizing (during charging reaction) by accepting electrons from the external circuit. The electrode because of its shape can also be referred as positive of negative plates.
3. *The Electrolyte* is a material which conducts electric current as separation into positively (anions) and negatively (cations) charged particles called ions. The electrolyte can be either acidic solution or alkaline solution to conduct current.
4. A *Separator* is commonly used to isolate the electric path between positive and negative plates.

Typical design of cell is shown in Figure 3-1

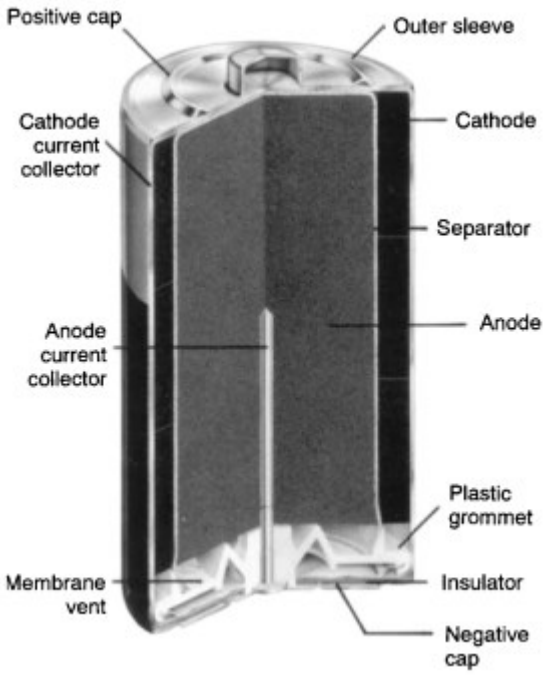

Figure 3-1. *Typical configuration of cell design* ***[18]****.*

3.3 Charging and discharging operation of cell

The electrons start to flow from anode to cathode when the battery cells are connected through the load. The formation of electric circuit occurs in the electrolyte due to the flow of cations (positive ions) and anions (negative ions) to the cathode and anode, respectively [18]. The operation of discharging shown in Figure 3-2.

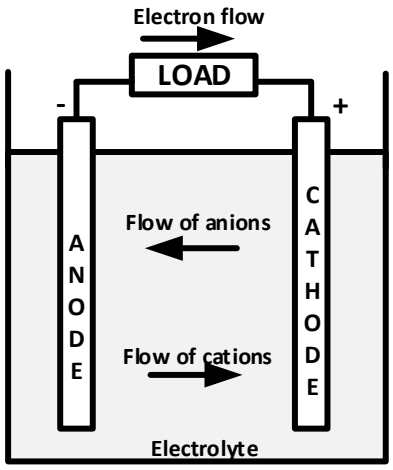

Figure 3-2. *Electrochemical operation of a cell (discharge)* ***[18]****.*

The discharging phenomenon can be expressed as following equations

Positive electrode: anodic reaction (oxidation, loss of electrons)

$$Cl_2 + 2e \rightarrow 2Cl^- \quad (3.1)$$

Negative electrode: cathodic reaction (reduction, gain of electrons)

$$Zn \rightarrow Zn^{2+} + 2e \quad (3.2)$$

Overall reaction (discharge): $Zn + Cl_2 \rightarrow Zn^{2+} + 2Cl^-(ZnCl_2)$ (3.3)

During the recharging of a battery cell, the current flow is reversed. This can be seen is Figure 3-3.

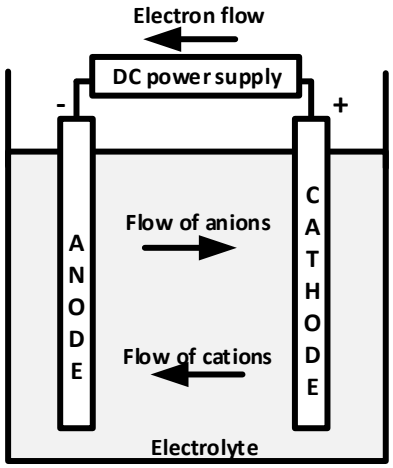

Figure 3-3. *Electrochemical operation of cell(charge).*

The charging can be expressed as following equations

Positive electrode: anodic reaction (oxidation, loss of electrons)

$$2Cl^- \rightarrow Cl_2 + 2e \quad (3.4)$$

Negative electrode: cathodic reaction (reduction, gain of electrons):

$$Zn^{2+} + 2e \rightarrow Zn \quad (3.5)$$

Overall reaction (charge): $Zn \rightarrow Zn^2 + 2e$ (3.6)

3.4 Classification of batteries

According to the classification, two distinct system of battery are described in [19].

1. Primary Batteries:
   Primary Batteries are irreversible batteries because of its chemical reaction and hence can only use once. These batteries are common for small usage because they are easy to use and cheap.

2. Secondary Batteries
   Secondary batteries are reversible batteries and they can be used over many cycles because of its charging/discharging capability. They possess true nature of electrochemical batteries. These batteries are highly used in industries and automotive application because of its rechargeable characteristics and have the capability to deliver high currents. Most common secondary batteries are Lead-Acid, Nickle/cadmium and lithium ion.

Depending on the material types some different types of electrochemical batteries are describe below [20] and characterized in Table 3-1

Table 3-1. *The summarized chart of state of art of electrochemical batteries* ***[20]***.

	Energy density (Wh/kg)	Power density (Wh/kg)	Life time (cycle)	Operating temperature (°C)
Lead-acid	20 - 35	25	200 - 2000	15 - 25
Lithium-ion	100 - 200	360	500 - 2000	-40 to 60
Lithium-polymer	200	250 - 1000	>1200	-40 to 60
Nickel-cadmium	40 - 60	140 - 180	500 - 2000	-20 to 60
Nickle-metal hybrid	60 - 80	220	<3000	-20 to 60
Sodium-sulfur	120	120	2000	

3.4.1 Lead-acid batteries:

Each individual cell of lead-acid battery consists of a lead(Pb)negative electrode, lead dioxide(PbO_2) positive electrode, and a separator that keeps electrodes electrically apart. The sulfuric acid used as the electrolyte. Lead-acid batteries are typical low-cost batteries used typically as UPS (uninterruptible power supply) and car starters.

3.4.2 Lithium-ion batteries:

The positive electrode of Li-ion batteries is made up of graphite carbon and the negative electrode is made of lithium metal oxide (($LiXO_2$). The electrolyte is made of lithium salts dissolved in organic carbonates. The V_{oc} of the cell is 4V [20].
The higher energy storage capability of Li-ion is the vital differentiate characteristics compared to the other conventional batteries. For the similar size of cells of different systems, Li-ion yields the higher energy density and specific energy [21] as shown in Figure 3-4.

Table 3-2 shows the notable advantage and disadvantages of Li-ion and Li-ion polymer batteries.

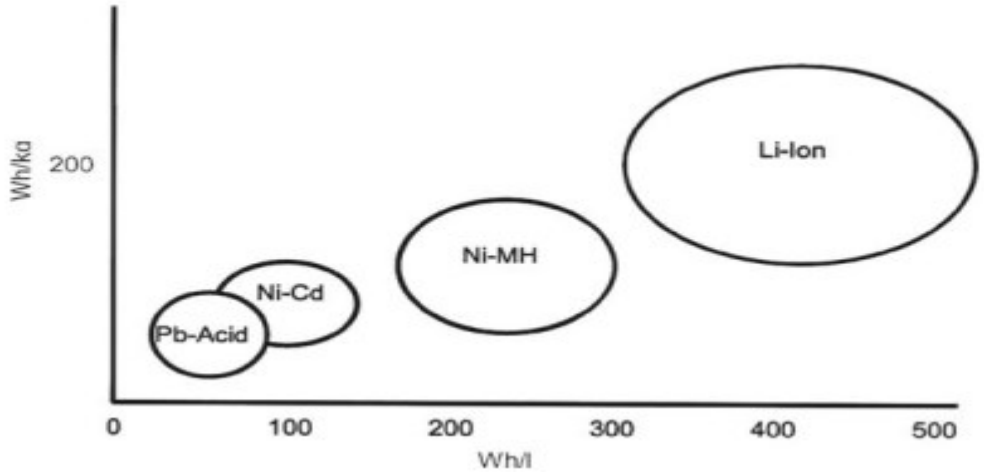

Figure 3-4. *The specific energy (Wh/kg) and energy density (Wh/l) for the main small-sealed rechargeable cells* ***[21]****.*

Table 3-2. *Advantages and disadvantages of Li-ion and Li-ion polymer rechargeable cells* ***[21]****.*

Advantage of Li-ion	**Disadvantages of Li-ion**
• Chemistry with the highest energy density(Wh/kg) • Good life cycle • High energy efficiency • Good high-rate capability • No Memory effect	• Nominal 3h charge • Relatively expensive • Thermal runaway concerns • Requires protection circuitry for safety and to prevent overcharge and over discharge

Advantages and disadvantages of Li-ion Polymer/laminate cells	
• Internal boding of anode, cathode and separator • Flexible footprint • Plasticized electrolyte	• More expensive • Limited high rate capability • Poor low-temperature performance

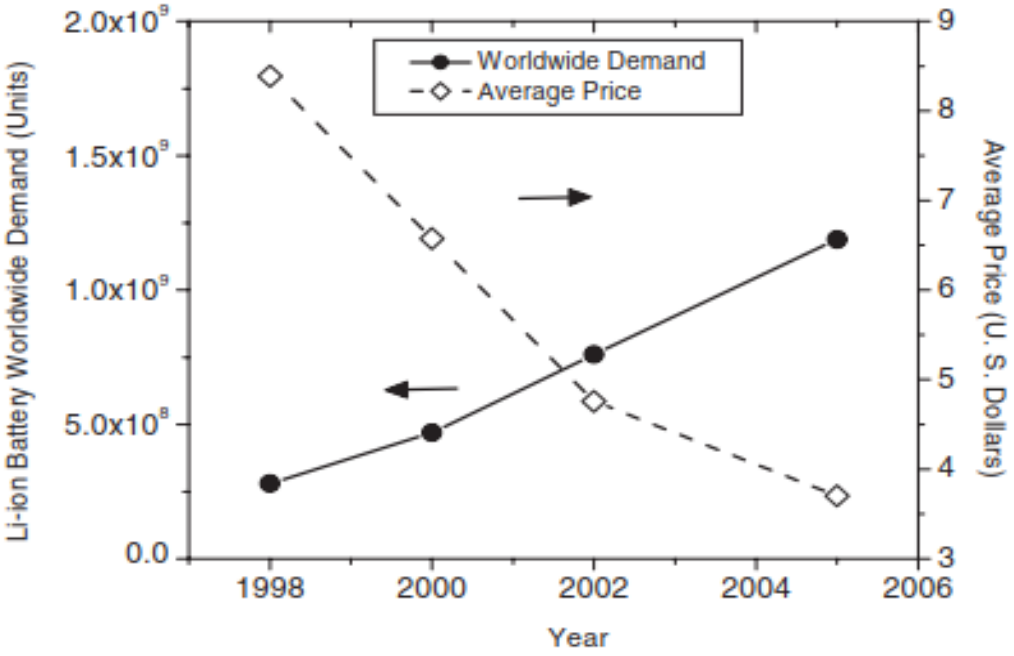

Figure 3-5. *Global demand and mean price for Li-ion batteries* ***[22]****.*

3.5 Important features and parameters of batteries

State of charge (SOC): The SOC is referred as the relative capacity of the battery as the percentage of maximum capacity of the battery. The 100% represents battery is fully charges. The capacity of the battery deteriorates over the period of time (battery aging). Many techniques are described to determine the status of SOC in [23, 24] but the commonly used method is the current drawn/supplied to demonstrate the variation in the battery over a certain period of time.

Depth of discharge (DOD): Depth of discharge usually describe the how deeply the battery is discharged. It is opposite of the state of charge(SOC). If the battery is considered as fully charge i.e. 100% SOC then of DOD of the battery is 0%.

Ageing: Ageing of the batteries often quantified by the number of charging and discharging cycles. Ageing reduces the performance of battery by reducing capability to store energy and it depends on the many external factors such as depth of discharge, discharge rate, temperature conditions.

Self-discharge: Self-discharge is gradual discharge in the available capacity over time even when no load is connected or during open circuit condition. The rate of discharge varies according to the condition of the battery. It depends on various factors such as temperature, aging, electrode material and manufactures [19].

Voltage: When the batteries charges/discharges to provide the electric energy, voltage is one of the most parameters is to be considered. The open circuit voltage (OCV) is determined by chemical reaction of the internal parameters of the cell. In actual use, this value is different from theoretical value and it depends on many kinetic factors [25]. The power delivered to load depends on the voltage of the battery as seen in the equation.

$$P = \frac{E^2}{R} \tag{3.7}$$

The high voltage energy is more supervisor then low voltage energy due to the square relation of power and voltage. The voltage is also determined by current density, when more current drawn from the battery, it reduces the voltage and the charge capacity of the battery as shown Figure 3-6 [25]

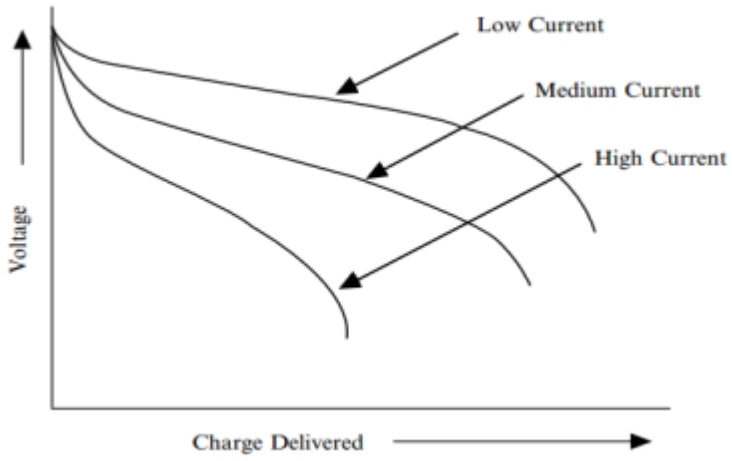

Figure 3-6. *The effect of the current density over the discharge curve.*

Some parameters also affect the OCV like the concentration of the electrolyte, battery aging, temperature, status of health, the concentration of electrolyte and depth of discharge [26, 27]. OCV as a function of DOD shown in Figure 3-7. The dotted line represents negative electrode discharge cell [19].

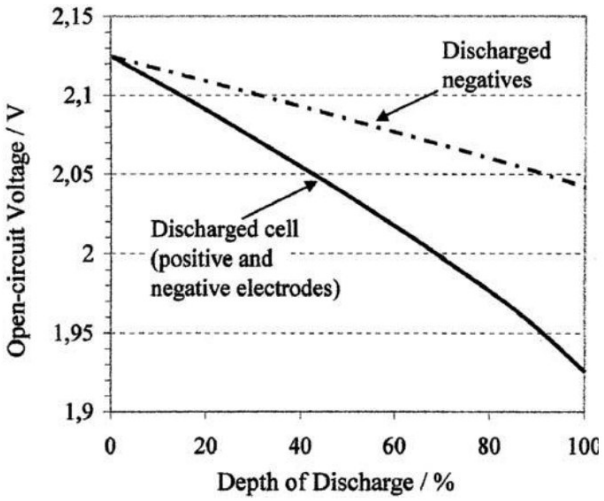

Figure 3-7. *The relationship of DOD and OCV of lead-acid batteries.*

Capacity: When the electric charge units in Ah drawn from the battery is termed the capacity of the battery.

$$Q_{ah} = \int_{o}^{t} I(t).dt \tag{3.8}$$

The energy contained in battery or cell is the integral of the multiplication of voltage and charge capacity.

$$Energy = \int E.dq \tag{3.9}$$

Where output voltage is denoted by E, it can diverge with kinetic parameters, and state of charge and q is the electronic charge, which supplies to an external circuit. Therefore, it is necessary to identify the maximum capacity and the theoretical value of charge which can be stored in a battery [28].

3.6 Model of battery in Simulink (MATLAB)

The battery block available in Simulink, which common generic model for many re-chargeable batteries is shown in Figure 3-8 [29]. The charging and discharge equation of lithium-ion battery in term of voltage is written below [30] . The equivalent circuit of the battery based on the discharge characteristics.

Charge mode (i*<0)

$$V_{batt} = E_o - R.i - K\frac{Q}{it - 0.1Q}.i^* - K\frac{Q}{Q - it}.it + A.e^{-B.it} \quad (3.10)$$

Discharge mode (i*>0)

$$V_{batt} = E_o - R.i - K\frac{Q}{Q - it}.(it + i^*) + A.e^{-B.it} \quad (3.11)$$

Where,

V_{Batt} = Battery voltage (V)
E_0 = Battery constant voltage (V)
K = Polarization constant (V/(Ah)) or polarization resistance (Ω)
Q = Battery capacity (Ah)
It = ∫i.dt = actual battery charge (Ah)
A = Exponential zone amplitude (V)
B = Exponential zone time constant inverse $(Ah)^{-1}$
R = Internal resistance (Ω)
i = Battery current (A)
i* = Filtered current (A)

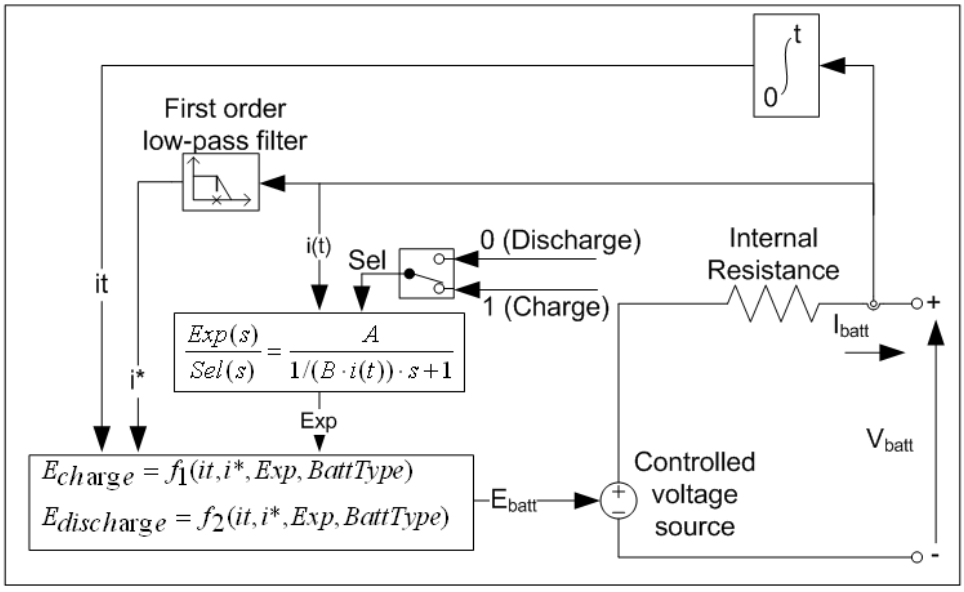

Figure 3-8. *Battery equivalent circuit.*

A discharge curve categorized into three sections shown in Figure 3-9. The exponential voltage drops when the battery is charged. The next section exhibits the charge that can be taken out from the battery until the voltage drops below its nominal voltage and the entire discharge of the battery is represented in last section when the voltage drops promptly. The charging of battery as shown in Figure 3-10. [29].

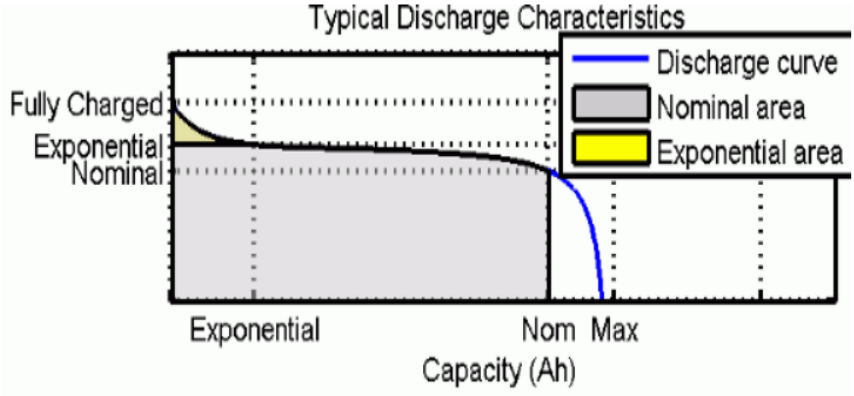

Figure 3-9. *The discharge characteristics of typical Li-ion battery.*

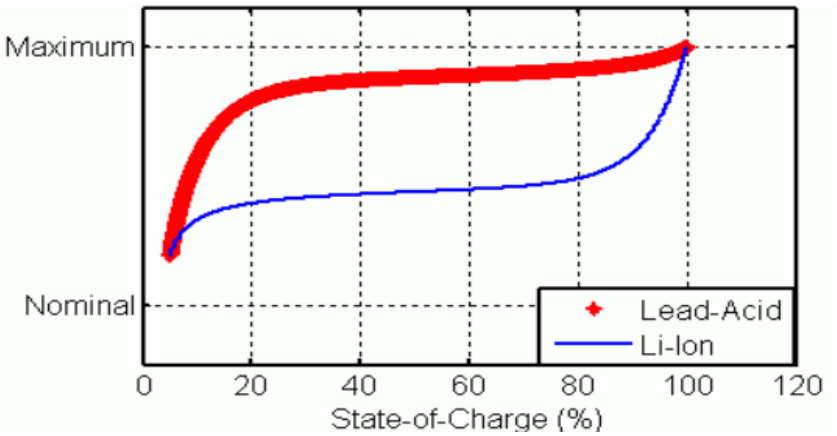

Figure 3-10. *Typical charge curve of Li-ion and lead-acid battery.*

The model has some limitation and assumption according to the [30].

Model limitations:

- The minimum OCV of the battery is 0 and $2 \cdot E_0$ the maximum battery voltage.
- The maximum capacity is Q and the minimum capacity is 0.

Model assumptions:

- The parameter of the model is not altered by charging and discharging cycles.
- The effect of temperature is not considered in the model's behavior.
- The capacity of battery doesn't affect by the amplitude of the current.
- The self-discharge is not considered in the model.

4. POWER ELECTRONICS

Power electronics is essential for the grid integration of PV and BESS systems, as it helps in controlling the voltages and flow of power in the integrated PV and BESS system, as well as in converting the DC voltage and current waveforms into AC voltage and current waveforms. In this thesis, the PV system employs two power stages, a DC-DC (boost type) converter with an MPPT algorithm and DC-AC inverter. Likewise, the BESS system also employs a bi-directional DC-DC converter (Cuk type) and a DC-AC inverter. In general, a DC-DC converter serves the purpose of controlling the output DC voltage at a specified level, whereas in PV applications is used to enable MPPT control and the task of the DC-AC inverter is to convert the DC power into AC power.

4.1 Fundamentals of DC-DC converters:

The key function of the DC-DC converters is to regulate the voltage level around a particular value at the output. The voltage regulation is also carried out against load and line variations. These converters also help to avoid the electromagnetic interference phenomenon that may arise from the source and the supplied system [31]. These incredible capabilities enable the implementation of DC-DC converters in various useful applications. In PV-BESS system applications, the DC-DC converters play the pivotal role in controlling the output power flow at a specified level by use of the various techniques. Thus, the high standards of stability at the output are achieved by mitigating any fluctuation from the input source of PV system.

4.2 Applications and Types of Semi-Conductor Devices:

The voltage regulation at the output can be easily achieved with the help of one or more semiconductor devices. These devices must be connected to each other in a suitable arrangement to be able to generate the expected results at the output. The arrangement of such type enables the devices to generate the desired output more efficiently. For initial design and analysis purposes, it is assumed that the behavior of these devices is equivalent to the ideal switch. One of the descriptions states that the semiconductor devices in modern power electronics can be divided into three major sections. These are Diodes, Thyristors and Controllable Switches [32].

1. Diodes: The on and off state of such devices is governed by the normal operational behavior of the electrical circuit which implements it.
2. Thyristors: The power-on state of this device is enabled with the help of an input control signal whereas power off state totally depends on the operational behavior of the power circuit under normal circumstances.

3. Controllable Switches: These devices offer the capability to switch between the on and off states with the help of control signals.

The controllable switches incorporate the comprehensive range of semiconductor devices. Some of them are the gate-turn-off thyristors (GTO), bipolar junction transistor (BJT), metal-oxide-semiconductor field effect transistors (MOSFET) [32].

4.2.1 Pulse Width Modulation:

The Pulse width modulation or PWM is one of the most widely implemented mechanisms to achieve the regulated voltage at the output. This scheme has many advantages over the other methods known to today. It offers the simple control, high efficiency, high conversion ratio, and constant frequency switching mode of operation. The pulse width modulation technique makes use of a control signal to regulate the *off* and *on* state of the switch. The control signal is generated in accordance with the reference voltage and a repetitive sawtooth waveform as shown in Figure 4-1 [33].

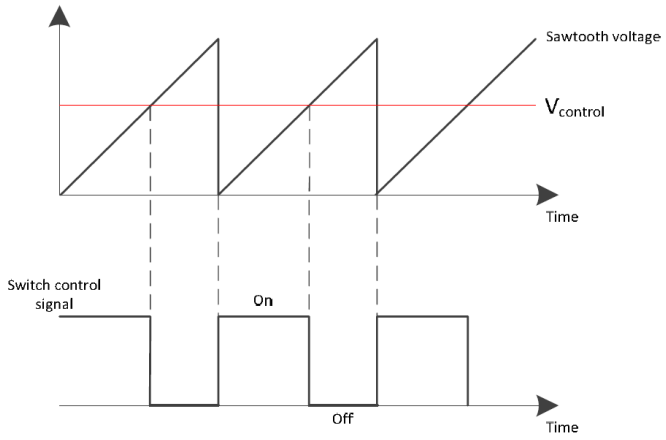

Figure 4-1. *Comparator signal of PWM.*

We can generate the reference voltage using the various techniques. It can either be done by comparison of desired and actual value of the voltage or by the amplification of the error value. The switch will operate in power on the mode in case the value of reference voltage is greater than the sawtooth waveform and will power off otherwise. The duty cycle ratio and switching time of the converter are governed by the below equations [32]:

$$D = \frac{T_{on}}{T_s} \tag{4.1}$$

$$T_s = \frac{1}{f_s} \tag{4.2}$$

4.3 DC-DC converters:

The DC-DC converters are widely used in renewable energy applications. To keep the output voltage at a specific level is the major purpose of the converter. Some of the DC-DC converters are discussed in the chapter.

4.3.1 Buck Converter:

The Buck converter or step-down converter reduces the input voltage to get desired output voltage. The circuit diagram and the output waveform of the buck converter are shown in Figure 4-2. When the inverter current is above zero all the time then it is operating in continuous conduction mode (CCM). Buck Converter operates in two states When the switch is *on* state, the diode is reverse biased and input energy is supplied to charge inductor. When the switch is in *off* state, the diode is forward biased and inductor current discharge through the diode as shown in Figure 4-2(b).

The transfer function of the buck converter is the ratio of output voltage to the input voltage, it can be given as:

$$D = \frac{V_o}{V_s} \tag{4.3}$$

. Where V_o is output voltage, V_s is input voltage and D is duty cycle.

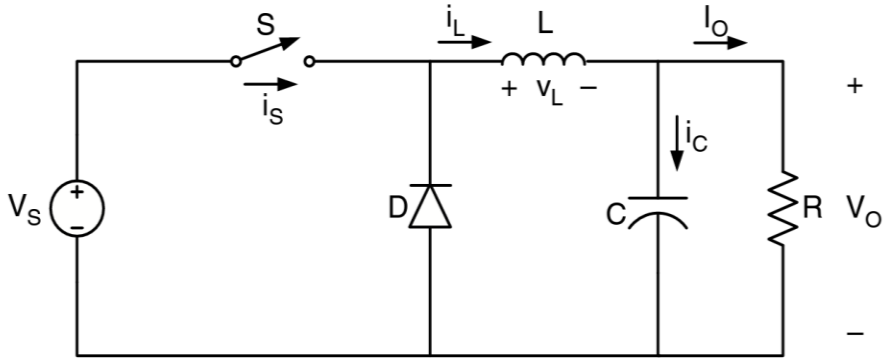

(a)

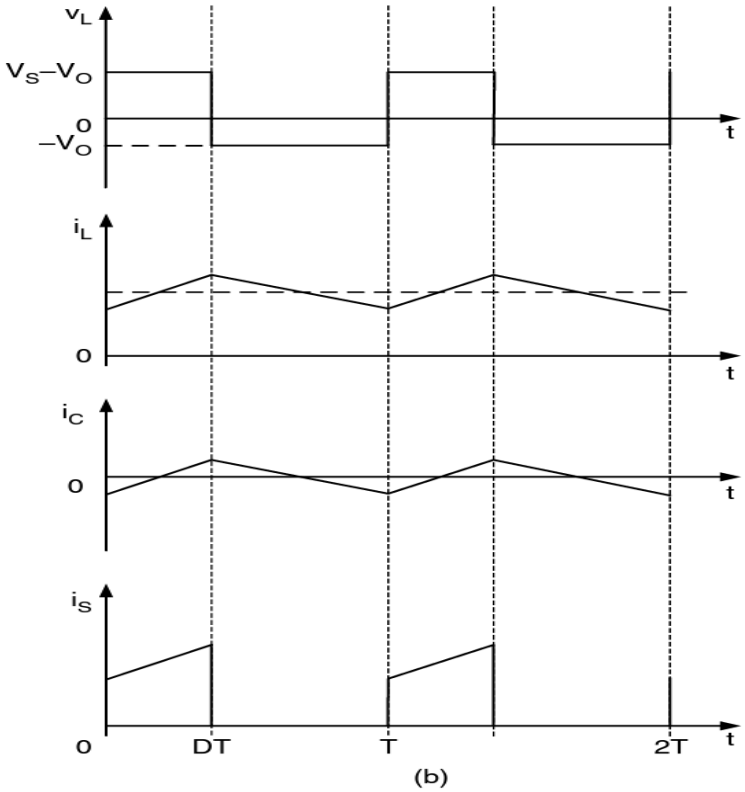

Figure 4-2. *Buck Converter (a). circuit diagram (b) waveform* ***[31]****.*

4.3.2 Boost Converter:

The boost converter or step-up converter increases the input voltage to get desired output voltage. The circuit diagram and current and voltage waveform is shown in Figure 4-3 Boost Converter also operate in two states When the switch is *on* state, the diode is *off* that time and current is inductor increases linearly. When the switch is in *off* state, the stored energy in the inductor, as well as the power from input supplies the energy to load, the waveform of current and voltage, are shown in Figure 4-3(b).

The transfer function is the ratio of output voltage to the input voltage, it can be given as:

$$\frac{1}{1-D} = \frac{V_o}{V_s} \tag{4.4}$$

. Where V_o is output voltage, V_s is input voltage and D is duty cycle

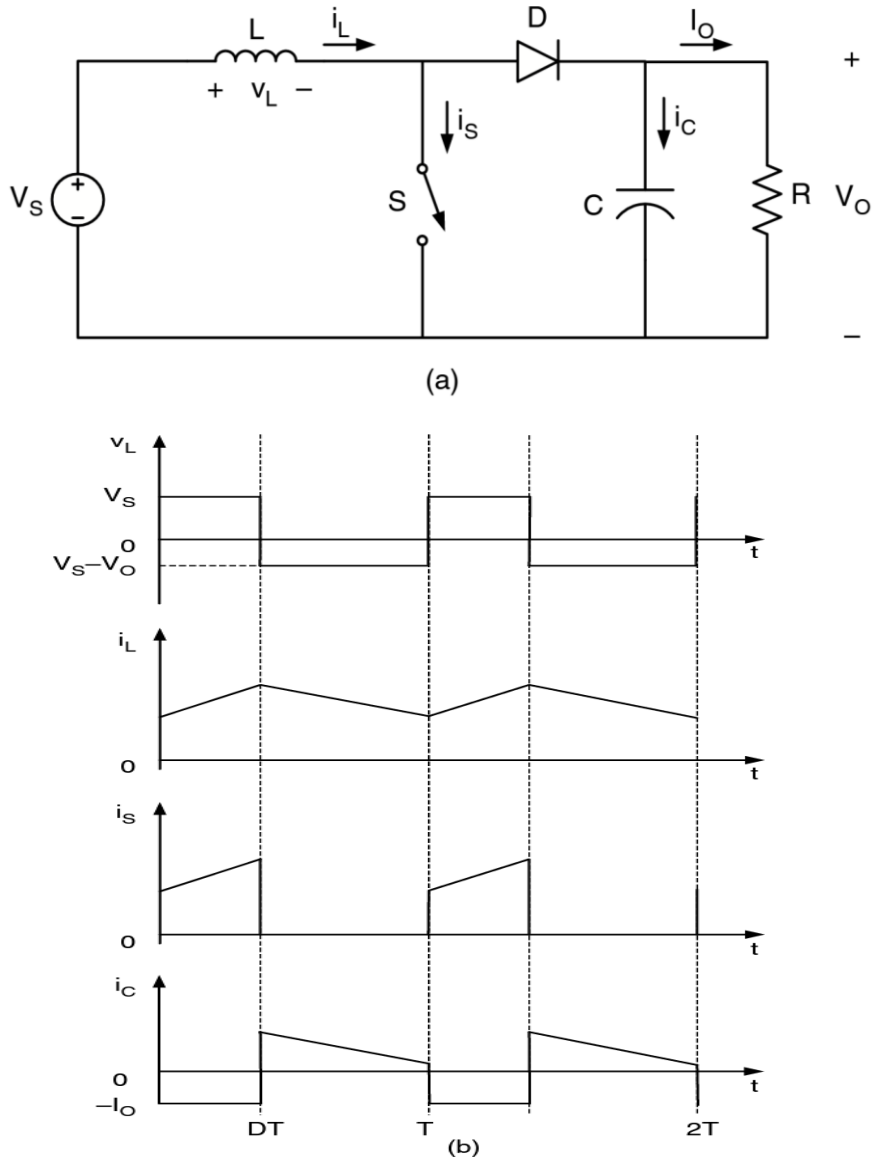

Figure 4-3. *Boost Converter (a) circuit diagram (b) waveform* ***[31].***

4.3.3 Buck-Boost Converter:

The buck-boost converter is the combination of DC-DC buck and boost converters. They are seemed cascaded with each other in this arrangement. It enables the buck-boost converter the greater flexibility. It can both step-up and step-down the output. It also incorporates the functionality to invert the voltage at the output. Thus, the voltage obtained at the output will be of the opposite polarity to that of the input voltage. The circuit diagram and output waveform is shown in Figure 4-4.

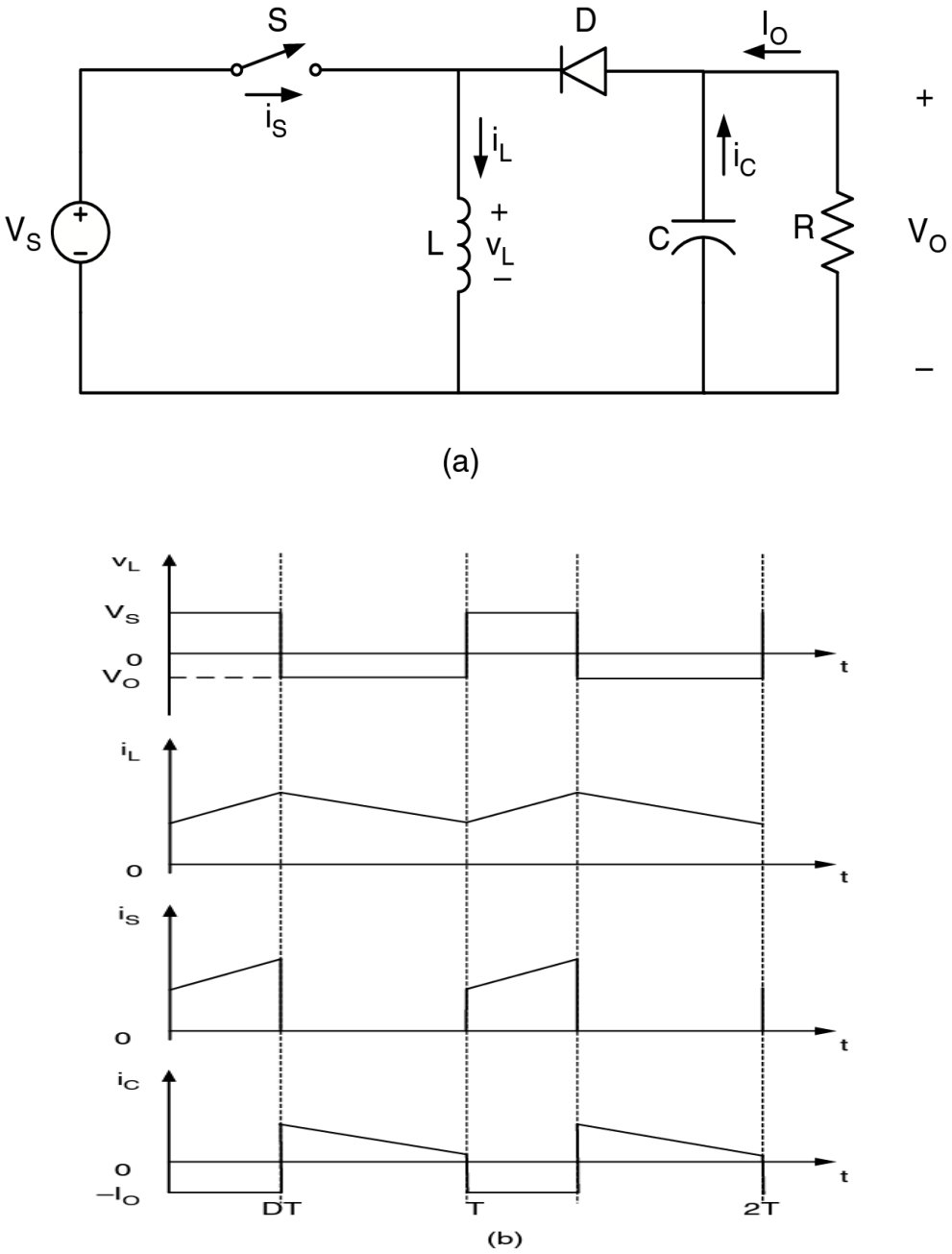

Figure 4-4. *Buck-Boost Converter (a) circuit diagram (b) waveform* ***[31].***

When the switch is closed, the diode acts as reverse biased and inductor stores the energy from the input power. The load at the output is powered by the already charged capacitor. On the other hand, when the switch is open the inductor acts as the source of the energy. It supplies the power for the capacitor and load at the output. The diode operates in forward biased mode in this state.

4.3.4 Cuk Converter:

The Cuk converter is the modified and advanced version of the buck-boost converter. It comes with the capability to the high or low voltage at the output as compared to the input voltage. The polarity of the voltage is also reversed at the output. The diagram of Cuk converter and output waveform as illustrated in Figure 4-5.

The transfer function of the buck-boost converter is:

$$-\frac{D}{1-D}=\frac{V_o}{V_s} \tag{4.5}$$

The Cuk converter offers many advantages over the buck-boost converter. The C_1 capacitor stores the energy from the input and has the capability to transfer at the output. The output current offered by the Cuk converter is continuous or smooth at the output which is not the case for the buck-boost converter. The complexity of the Cuk converter is much more than that of the buck-boost converter. The one drawback of the Cuk converter is that, it uses the large value of C to maintain the V_C voltage at the output.

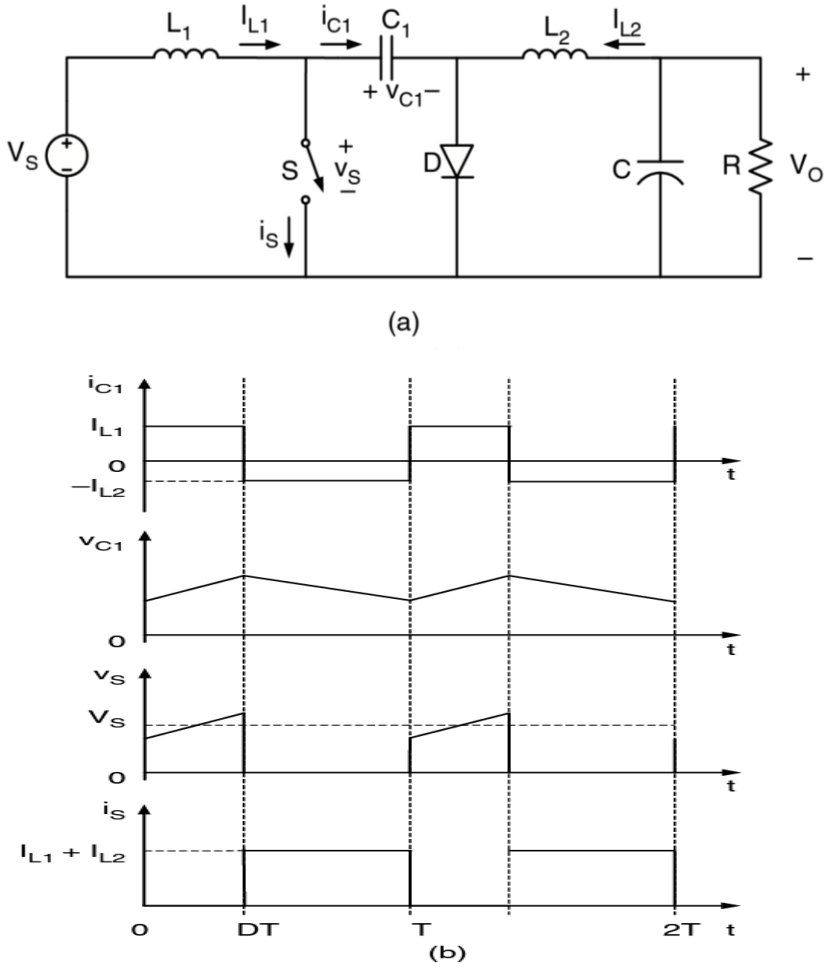

Figure 4-5. *Cuk Converter (a) circuit diagram (b) waveform* ***[31]****.*

4.4 Techniques for Tracking the Maximum Power Point:

The key area of focus during the design of a photovoltaic generation system is to identify the maximum operating point. It is also called the maximum power point. It enables to ensure that highest level of output efficiency is achieved for PS system which is usually being impacted by the environmental conditions, i.e. temperature and irradiance. The Figure 4-6 shows a comparison of I-V and P-V curve and explains the non-linear behavior of the solar cells. The MPP tracking techniques enable to identify the maximum operating point that is in accordance with the corresponding changes in the operational environment. The power converter also plays the pivotal part in determining maximum power operating point of the PV system.

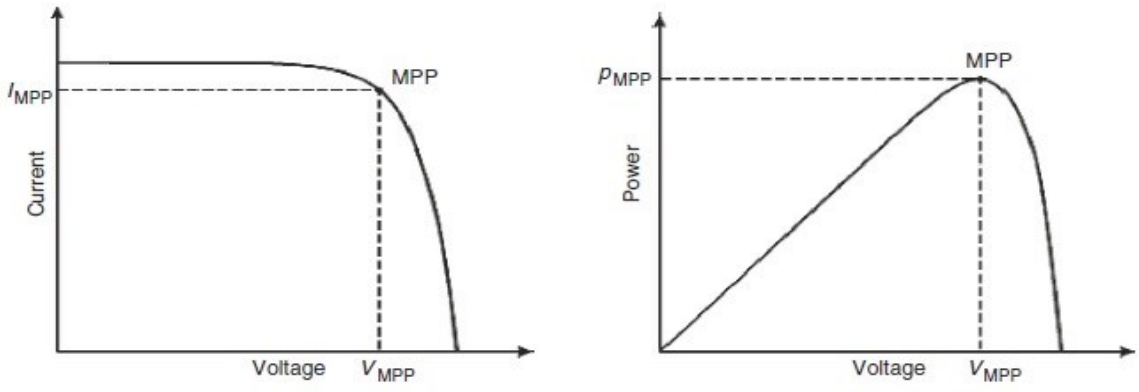

Figure 4-6. *Current and voltage characteristics of a PV cell* ***[31]****.*

The Figure 4-7 gives the brief idea about the algorithm implemented for MPPT. The algorithm makes use of the continuous power measurements. The controller analyzes the input power signal to determine if the system is operating at maximum power point and adjusts duty cycle in accordance in order to achieve the optimal operation point for the whole system.

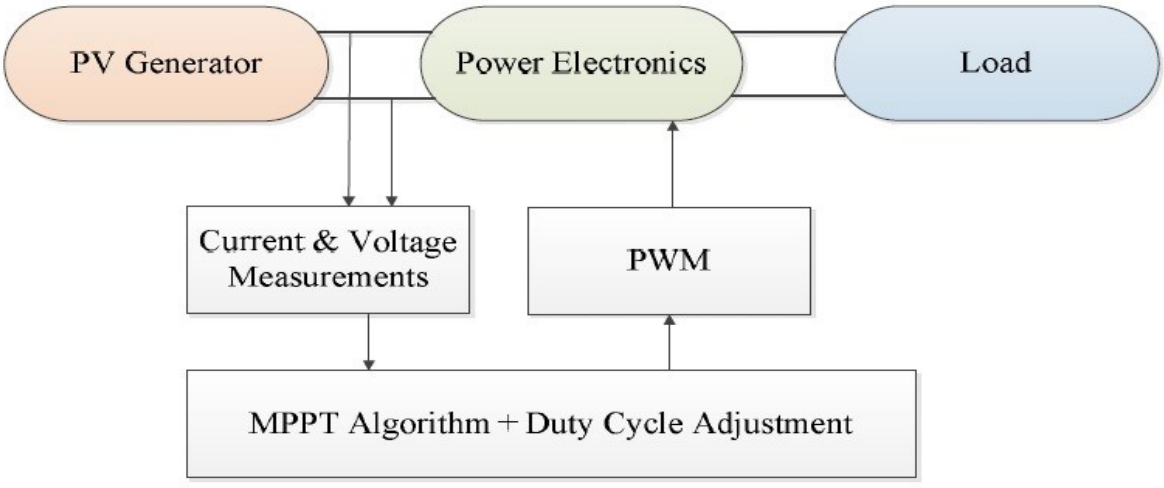

Figure 4-7. *The high-Level Schematics of MPPT Method* ***[33]****.*

There are numerous MPTT techniques in use today. Each technique implements different algorithms and offers different levels of efficiency in terms of determining the best possible maximum power point. The following chapter discussed the two main techniques.

4.4.1 Perturb and Observe Technique:

This technique implements the comparison between old and new values of the output power of the PV system to determine the optimal operating point to achieve maximum power efficiency at the output. The control signal increments or decrements the current or voltage accordingly along with the variation in duty cycle. The phenomenon is known as perturbing. The old values of the output power are stored in the memory of the control systems for later comparison and analysis requirements. The primary focus of the whole process is to achieve zero value of the derivative of the voltage at MPP. The perturbation pattern remains same if the power at the output is at increasing end and changes if the output power is decreased due to any reason until the maximum power point is achieved with dP/dV=0. The Figure 4-8 represents the flow chart of perturb and observation method.

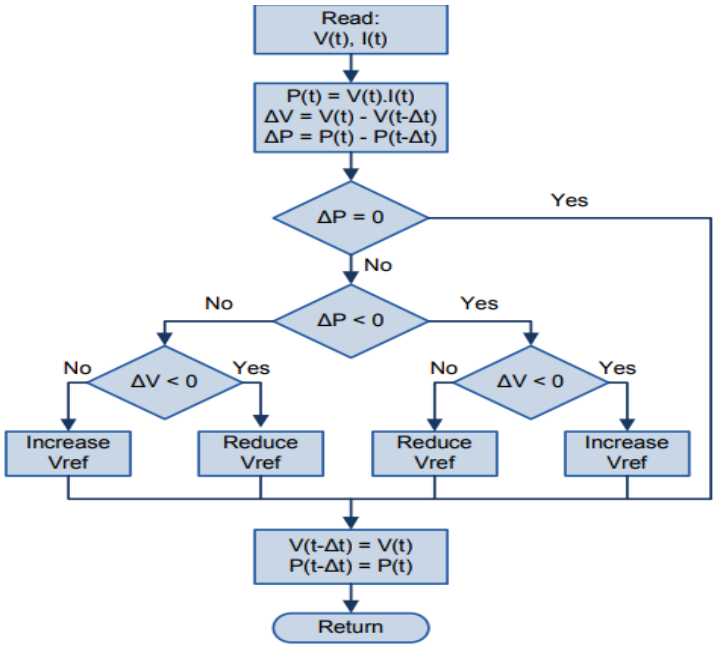

Figure 4-8. *The perturb and observe algorithm* ***[34]****.*

This method does not stop the calculations even if the maximum power point is achieved. It is the drawback of the algorithm despite its simplicity and smooth implementation. This behavior sometimes causes hindrance to achieve and sustain maximum system efficiency. However, the algorithm is commonly implemented because of the simplicity in its application for research and analysis requirements.

4.4.2 Incremental Conductance & Integral Regulator Technique:

This method implements the comparison between incremental and instantaneous conductance values. It enables to determine the direction of the voltage change at the output. Once the maximum power point for PV system is achieved, this algorithm stops the further calculations. The algorithm will not carry out any further calculation until or unless there is some change in the conditions of the operating environment. The flowchart in Figure 4-9 briefly explains the algorithm for internal conductance [35].

The maximum operating point measured by calculating the change in voltage and change in current until the change becomes zero. The increase or decrease in the intensity of the radiation will impact the normal operation of the PV system at the maximum operating point. The control system behaves in accordance to increase or decrease the operating voltage to achieve the desired or maximum power point [35].

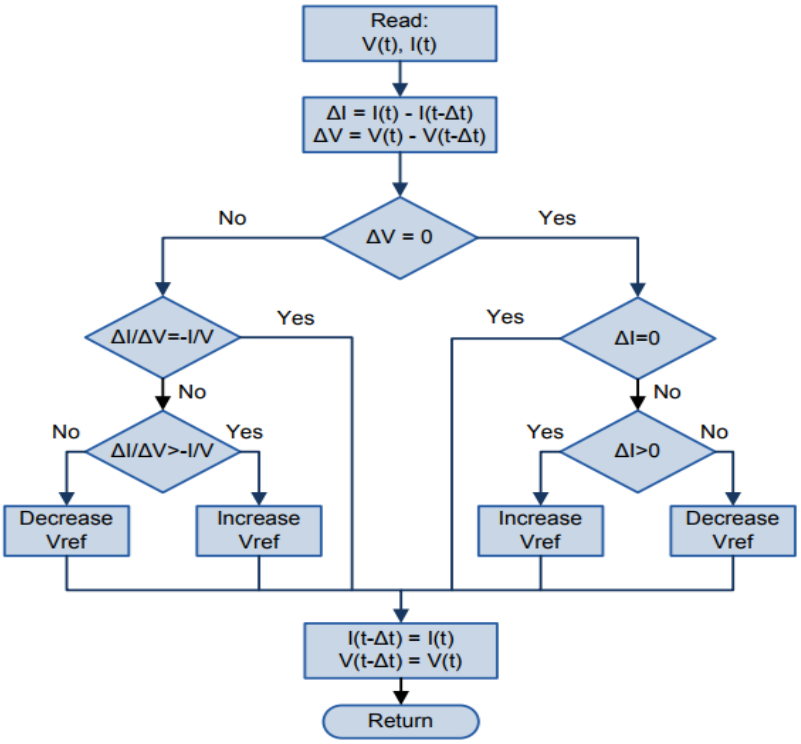

Figure 4-9. *Incremental conductance algorithm flow chart* ***[34]****.*

4.5 DC-AC Inverters Fundamentals:

Most of the renewable energy produces DC power output. The inverter is required to convert DC power to AC that can be directly interconnected with utility grid and it can use for consumption application. The control of inverter is a significant part to enhance the quality of power and meet the requirement of grid integration. The inverters are of two types mainly which includes the voltage source inverter and current source inverter. The VSI comes with the zero or minimal impedance at the input whereas CSI comes with the very high impedance. These inverters can work in single phase or three phase system which entirely depends on the circuit arrangement of these inverters. This thesis focusses on PWM controlled voltage source inverter. The basic full bridge single-phase inverter shown in Figure 4-10.

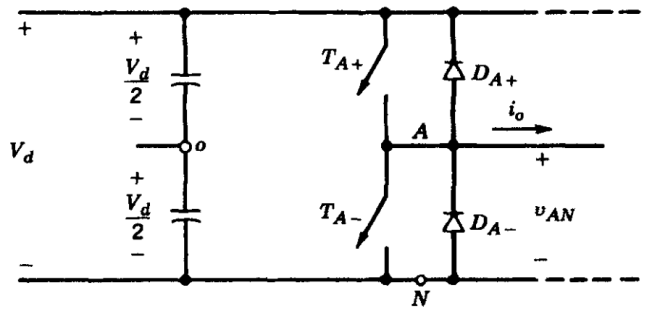

Figure 4-10. *Basic full bridge single leg inverter* ***[32]****.*

4.5.1 Modulation technique for inverter

The switches in the inverter needs to be turn *off* and *on* by triggering pulses at the gate to get AC signal from DC signal. Several technical have been used to general the pulses. Space vector based pulse width modulation and sinusoidal pulse width modulation are the most common in Voltage source inverters. Sinusoidal pulse width modulation has been used in this thesis.

4.5.2 Pulse Width Modulation

The PWM helps to produce sinusoidal output with controlled magnitude and frequency. A sinusoidal control signal is compared with the triangular waveform to produce the sinusoidal output voltage as shown in Figure 4-11. The switching frequency(f_s) and amplitude of a triangular waveform(V_{tri}) generally kept constant. The switching frequency established from the frequency of the triangular waveform. The control signal $V_{control}$ helps to module the duty ratio. The control signal ($V_{control}$) has a frequency (f_1), which related to the fundamental frequency of the required voltage. The f_s is also known as carrier frequency and subsequently, f_1 is also known as modulating frequency [32].

The amplitude modulation ratio(m_a) and frequency modulation ratio(m_f) are two essential parameters of PWM. These parameters greatly impact the performance of the system, it is important to select frequency modulation ratio carefully while designing the inverter. The amplitude and frequency modulation ratio can be defined as:

$$m_a = \frac{V_{control}}{V_{tri}} \tag{4.6}$$

$$m_f = \frac{f_s}{f_1} \tag{4.7}$$

The switches T_{A+} and T_{A-} as shown in Figure 4-10 are controlled by comparing the $v_{control}$ and v_{tri}. As the switches, T_{A+} and T_{A-} cannot turn on simultaneously, the output voltage

of lies between $\frac{1}{2}V_d$ and $-\frac{1}{2}V_d$. When $v_{tri} > v_{control}$, the switch T_{A-} is on and output voltage v_{Ao} is $-\frac{1}{2}V_d$ and vice versa. The peak amplitude of output fundamental shown in Figure 4-11(b) can be given as:

$$v_{Ao} = m_a \frac{V_d}{2} \tag{4.8}$$

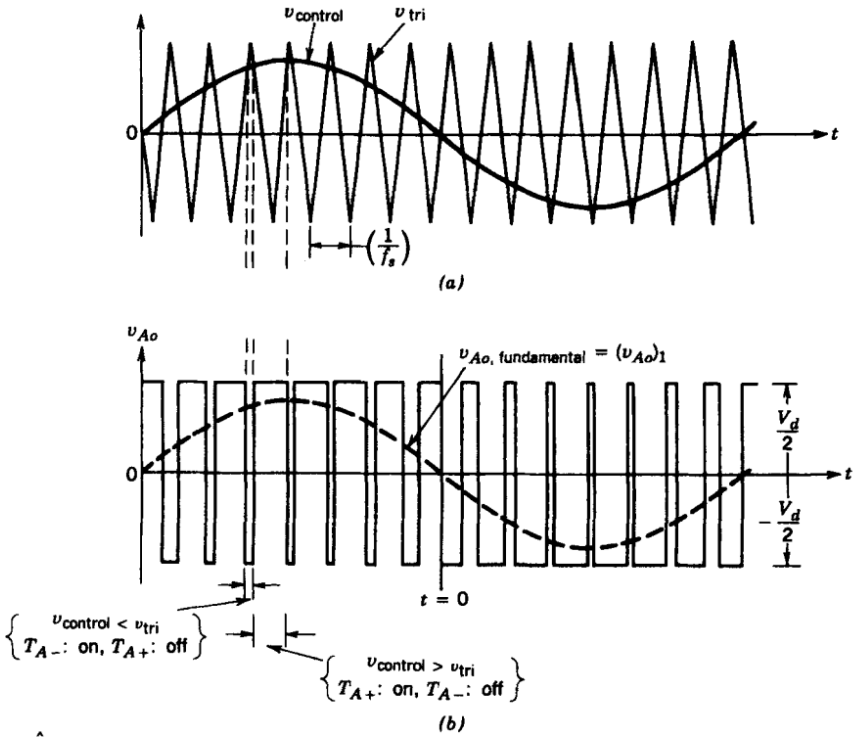

Figure 4-11. *Behaviour of PWM* ***[32]****.*

4.5.3 Three Phase VSI and PWM

The single-phase inverter preferably used in low power application and three phase inverters used for the high lower application. The full bridge and half bridge are most popular inverter topologies used for commercial purpose. The full bridge requires half the input voltage to get required output voltage as compared to half-bridge inverter. The Figure 4-12 illustrates the three phases three-level inverter topology and Figure 4-13 illustrate the output waveform and switching behavior of various switches. The three-level inverter also known as neutral point clamped inverters (NPC). The number of level determine the output voltage level. Most common are two and three level. The three-level inverter as numerous advantages over two level inverter such as [36, 37],

- Three level has three output voltage level i.e. $V_{\frac{i}{2}+}$, $V_{\frac{i}{2}-}$ and V_0 so it provides better sinusoidal waveform and result in less THD.
- The switching frequency is required half to produce smooth output signal.
- Lower module of IGBT can be used because it required only half the bus voltage.

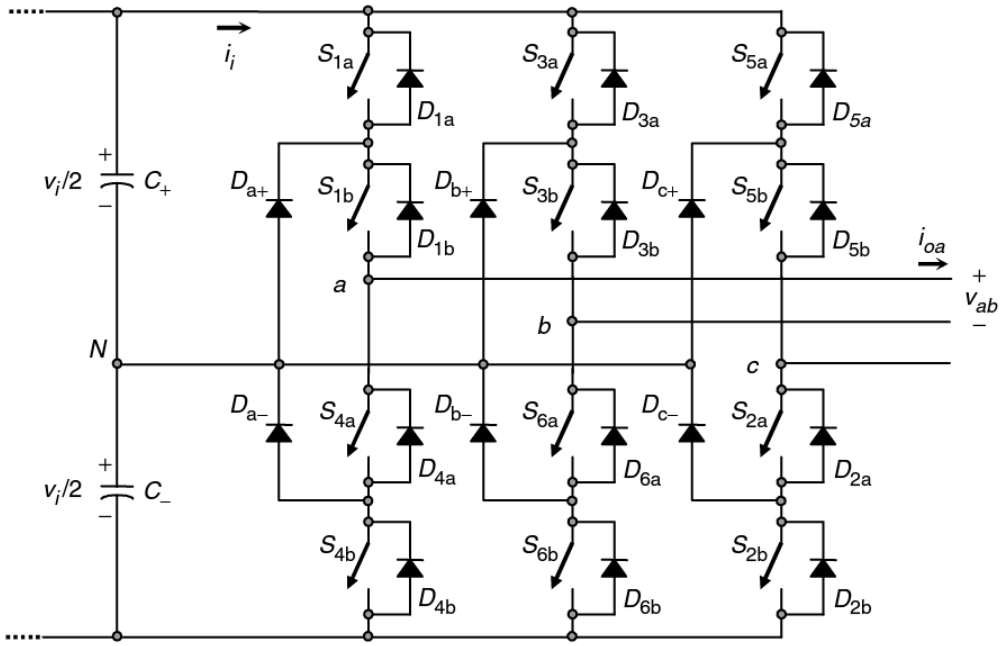

***Figure 4-12**. Three phase three-level inverter **[31]**.*

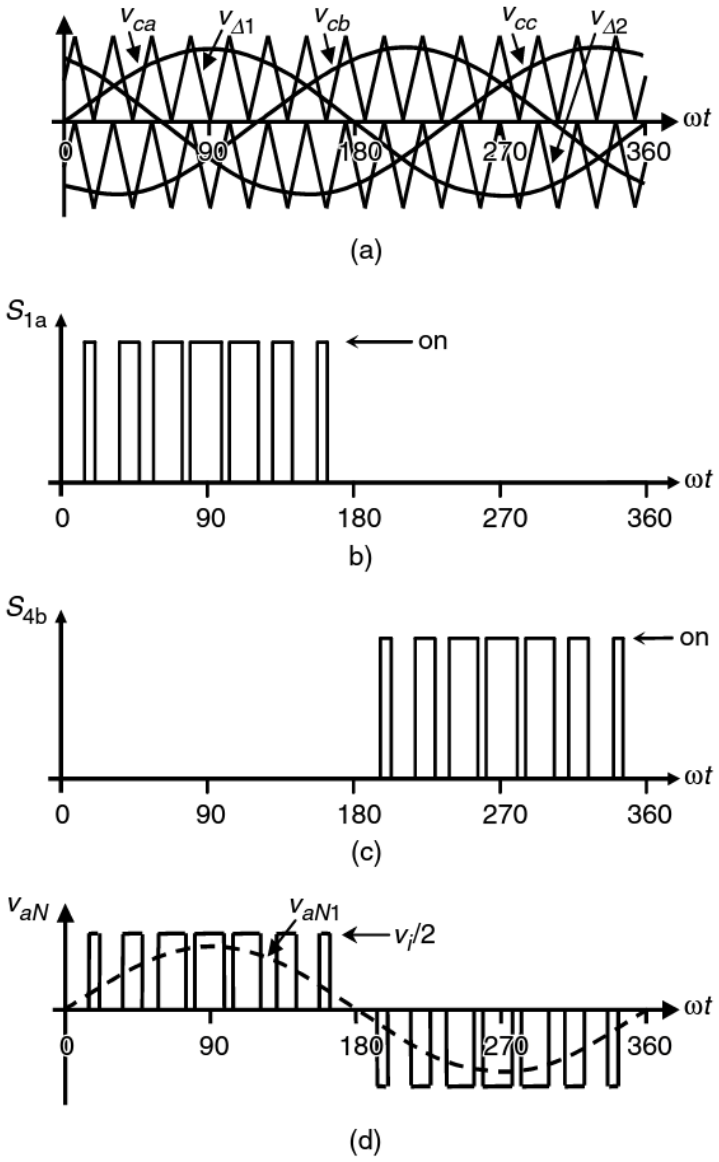

Figure 4-13 *(a) modulating and carrier signals, (b) switch S_{1a} status (c) switch S_{4b} status (d) inverter phase a voltage* ***[31]****.*

4.5.4 Control Structure of Grid Connected Inverters:

The major purpose of the grid-connected inverter is to manage the power injection into the grid extracted from distributed generation. The structure of a controller shown in Figure 4-14. The control structure mostly based on two cascaded loops for this purpose. A cascade loop can be used in many ways, but most popular strategy mentioned in [38]which uses an outer voltage loop and inner current loop.

The inner current loop regulates the power quality and decrease in harmonics in the current, which can be injected to the grid and the outer voltage loop which regulate balance the power flow of the system. It regulates the dc link voltages up to required level [38].

It is difficult to control the three-phase system, managing the control and sampling of the three-phase sinusoidal signal is the complex purpose and it required suitable transformation for sinusoidal signals. The control system can be designed into three reference frames namely, the natural frame, the stationary frame, and synchronous reference frame. The transformation diagram from reference frame shown in Figure 4-15. The approach used in this thesis is synchronous reference frame which is also known as dq0 frame. Further information on reference frame grid-connected inverter can be seen in these paper [38, 39].

In synchronous reference frame, the sinusoidal variable (abc) are converted into frame(dqo) which rotates at synchronous speed with sinusoidal variables. This transformation also known as Park's transformation which makes these values appear as DC values in a steady state condition. The PI controller can be used to get satisfactory results [38].

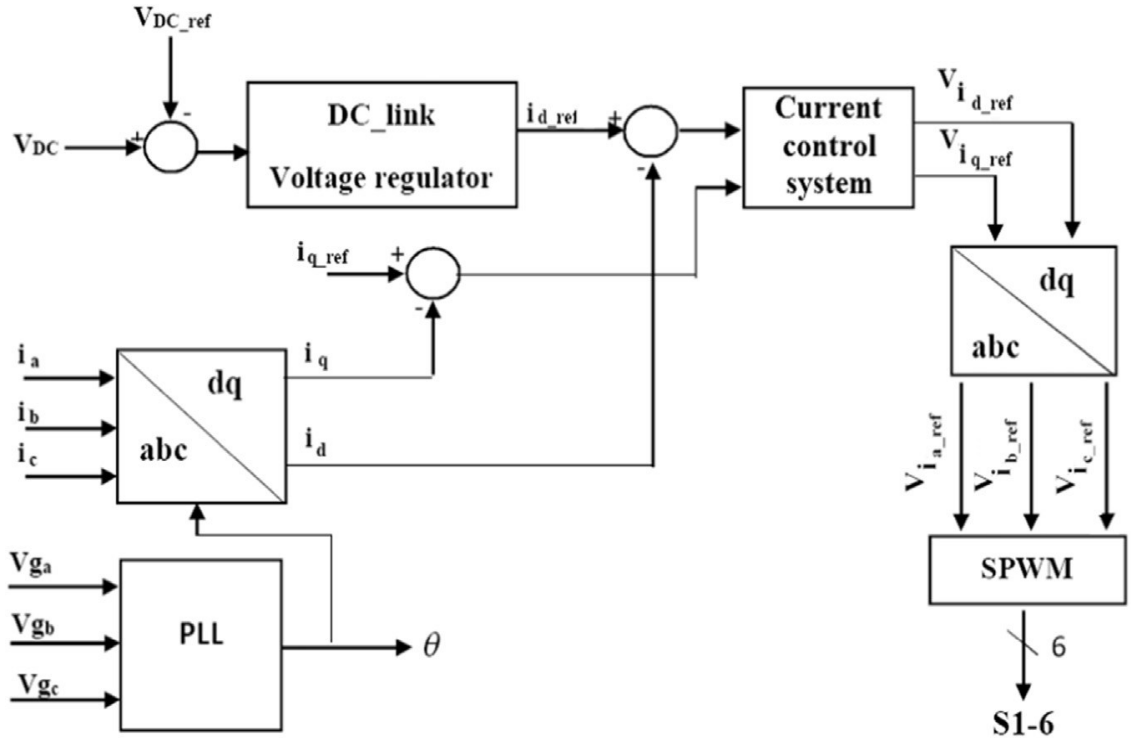

Figure 4-14. *The control system for grid-connected inverter* ***[40]****.*

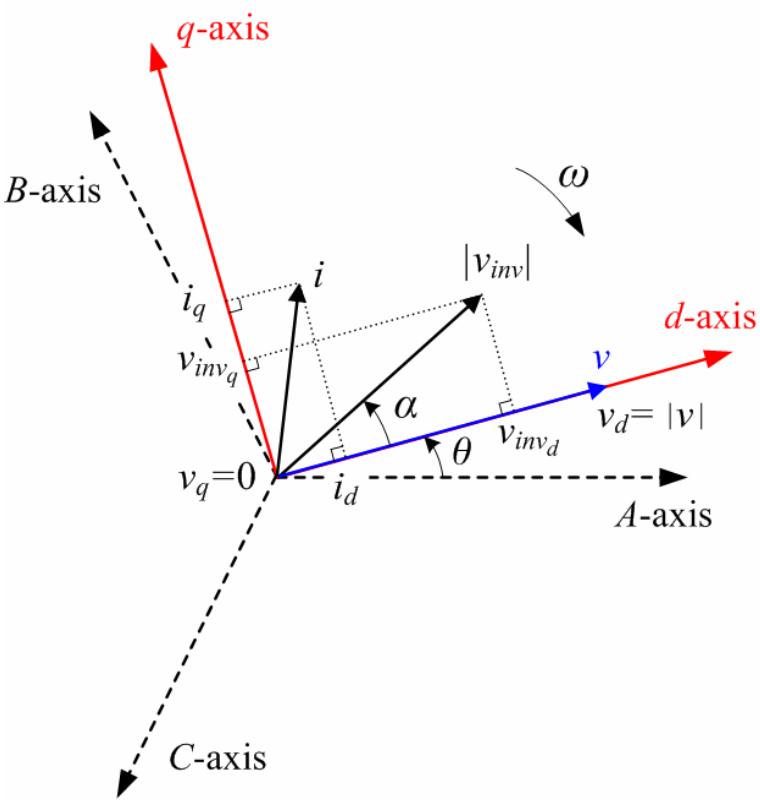

Figure 4-15. *Transformation diagram from reference frame* ***[41]****.*

4.6 Filters:

There are different types of filters available that are used in combination with the inverters to improve the overall output efficiency of the system. These filters are placed in different configuration schemes. It helps to remove the odd harmonics at the output. It also enables to compensate the voltage distortion from unbalanced or non-linear loads. The design of filter for such applications depends on various factors. It is ensured that filters have lowest possible power loss at the output to meet efficiency of the system at different levels of load voltages. The availability of components, size, and cost of the filter also has an impact on the overall low pass filter design. However, the voltage at the output and total harmonic distortion are the driving factors for optimal design and application of the filters [42]. There are commonly three kinds of passive filters used i.e. L, LC, and LCL as represented in Figure 4-16.

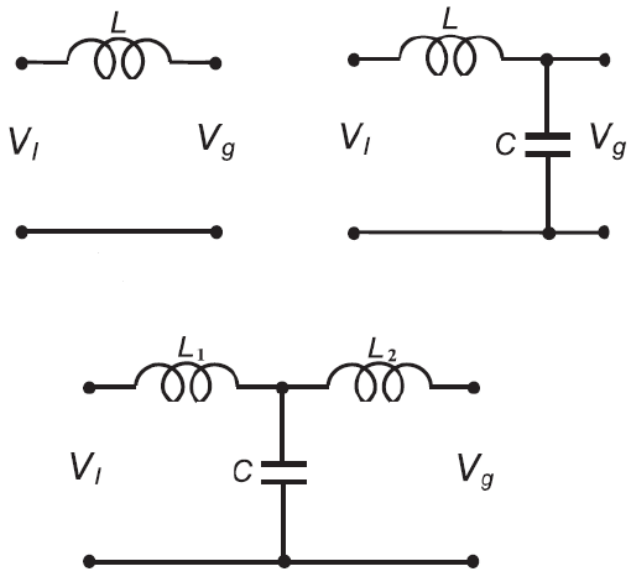

Figure 4-16. *L, LC and LCL filters* ***[42]****.*

5. MODELLING OF PV-BESS SYSTEMS

5.1 Introduction

This chapter provides the modeling and control techniques employed by all the components of the compound PV-BESS system put forward in this thesis. The two main subsystems of the compound PV-BESS are shown in Figure 5-1, namely: (a) the PV subsystem comprising a DC-DC converter and the MPPT control, in tandem with the DC-AC converter with its associated VSC control; (b) the Battery Energy Storage sub-system comprises a bi-directional DC-DC Cuk converter, in tandem with the DC-AC (VSC) inverter. Each subsystem connects to a point of common coupling with the AC power grid and a load point, as illustrated in the Figure 5-1.

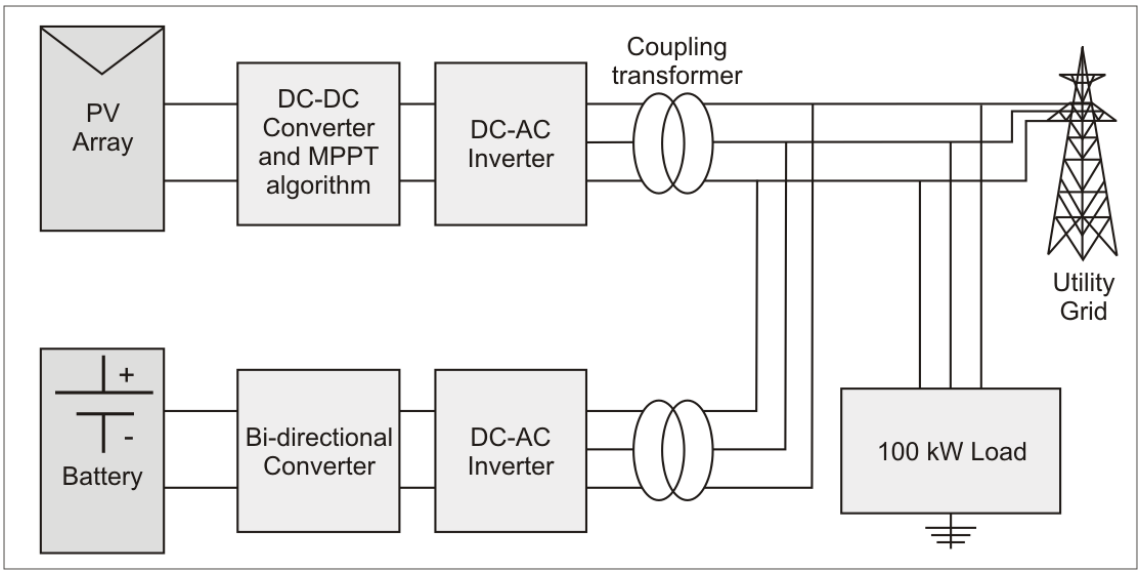

Figure 5-1. *Proposed PV-BESS system.*

5.2 About MATLAB Simulink

MATLAB Simulink has been extensively used for simulation of the PV-BESS. Simulink is a modeling and calculation platform is extremely flexible and provides the opportunity to design models. For this thesis, several tool boxes from MATLAB Simulink have been used to model different components that allow testing of the PV system under different test conditions. The Simulink implementation of this system facilitated the simulation, for example, it allowed modeling the value of irradiance (and its variation) that computed the output current produced by the photovoltaic module.

5.3 PV System Modelling

In this thesis, a base model considered for this work available in [43] as shown in Figure 5-2. A PV array of 100-kW has been connected to a load and 25-kV AC grid via a DC-DC boost converter and a 3-phase 3-level VSC followed by 260V/25kV three-phase coupling transformer.

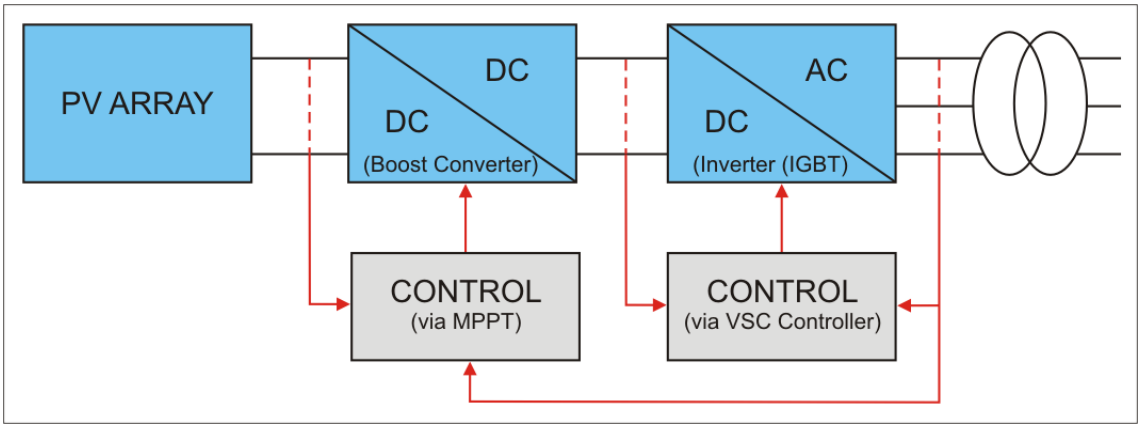

Figure 5-2. *Modelling of PV system.*

The description of all components given in Table 5-1**.**

Table 5-1. *Components used in the PV system modeling.*

Components	Brief description
PV array	Capable of producing 100 kW at STC (1000 W/m^2 at 25 ºC)
DC-DC boost converter (5-k Hz)	Used to increase PV output (273 V DC) voltage to 500 Volt DC. The MPPT controller optimizes the duty cycle of boost converter.
3-level 3-phase VSC type DC-AC inverter	The DC to AC inverter able to convert the 500 V DC link voltage to 260 V AC. The power factor is maintained as 1 (one). It operates using two control loops. The external control loop controls DC link voltage to +/- 250 V. The internal control loop adjusts active and reactive current components.
10-kVAR capacitor bank	It is capable of filtering harmonics which are created by VSC

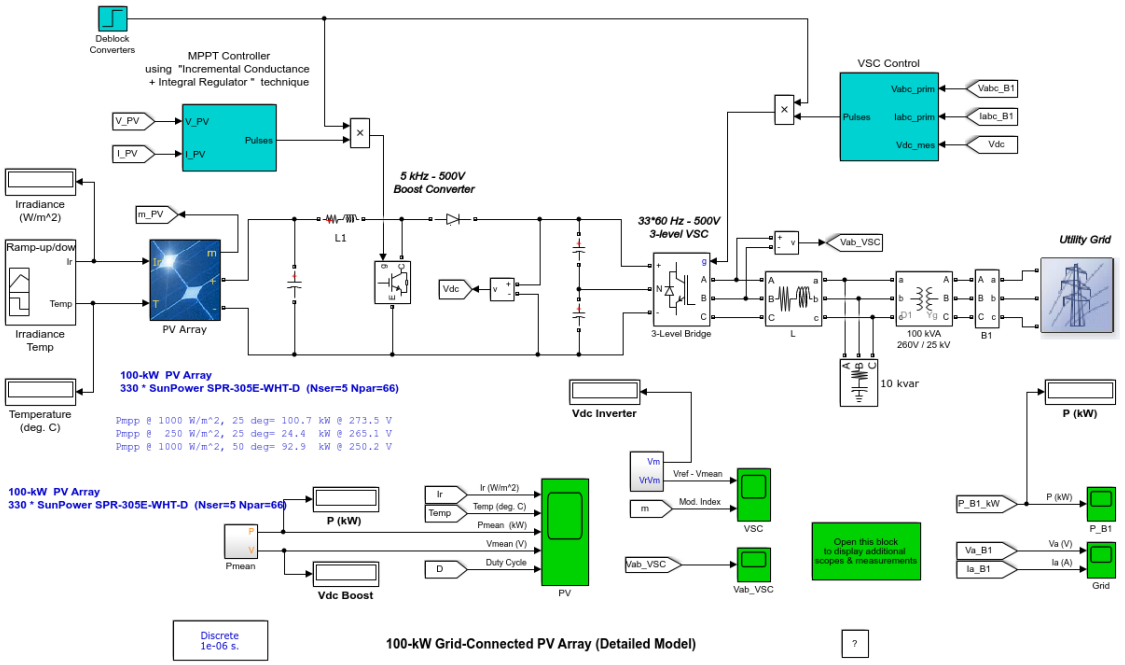

Figure 5-3. *MATLAB Simulink modeling of the PV system used in this thesis.*

5.3.1 Modeling of PV Array

Although the modeling of PV array can be done from Simulink using simpower components, MATLAB has built-in PV array block which can be used. The PV array comprises a total of 330 solar modules that provide 100.7 kW under standard test conditions (STC). The layout of the PV array consists of 66 parallel strings where each string has 5 series-connected SunPower modules (with specification SPR-305E-WHT-D). The PV array has an optimum capacity of 66*5*305.2 W = 100.7 kW at 25 ºC or STC.

The array layout is shown in Figure 5-4. Note that each string has 5 modules. There are 66 such strings. Total wattage is calculated as 66*5*305.2 W= 100.7 kW.

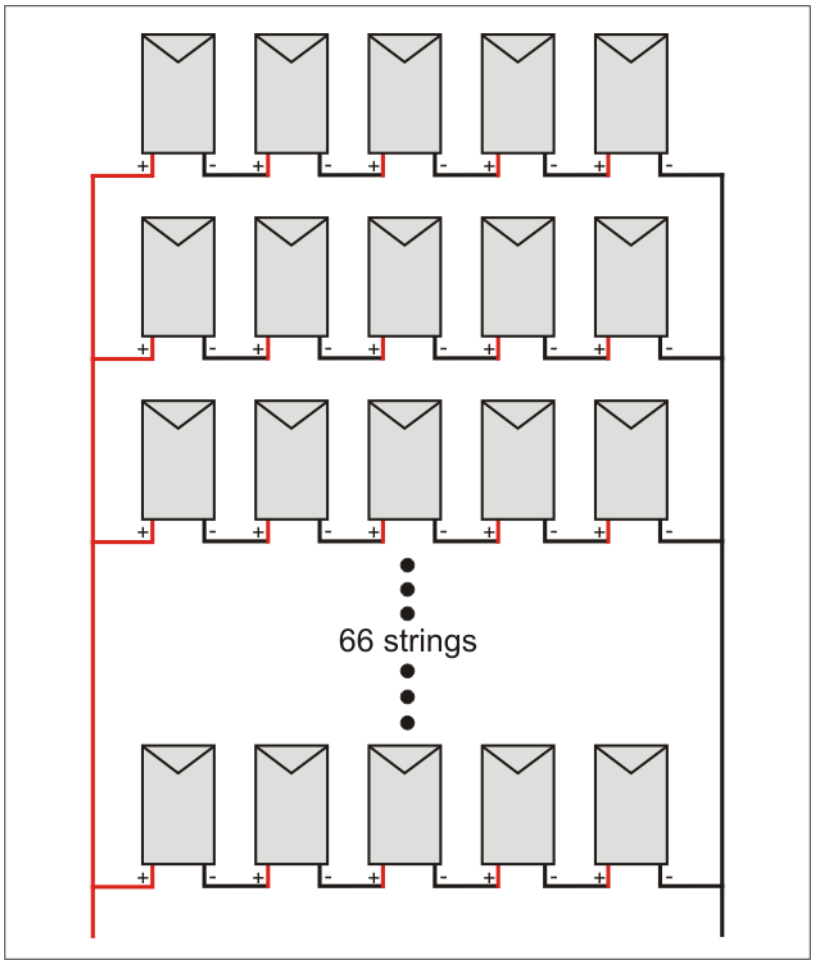

Figure 5-4. *The Series and parallel connection of PV module to form PV array of 100 kW.*

5.3.2 DC-DC Converter (Boost Converter)

In this thesis, the Boost converter is used. It has a freewheeling diode that blocks reverse current and amplifies the output voltage of PV arrays to a higher level. Control of the DC-DC converter is carried out by pulse width modulation (PWM) duty cycle. Note that the state of transistor determines the output of the converter. The optimum load impedance of the PV array is achieved by varying duty cycle. The boost DC converter steps up the input voltage by storing energy in an inductor for a certain period of time. It then uses this stored energy to boost the input voltage to a higher voltage.

The electrical circuit of the Boost converter, used for this work, has been modeled as shown in Figure 5-5. The input source charges the inductor when the switch is closed. The diode is reverse biased – this technique is used to provide isolation between the input and output of the converter. When the switch is opened, the energy stored in the inductor

and the power supply is transferred to the load. The ratio of output voltage and the input voltage is given as:

Output voltage/input voltage $= \frac{1}{1-d}$, where *d* is the duty cycle.

The modeling boost implemented by using SimPower systems tools which is the part of simscape library. The SimPower systems libraries consist of a range of basic components necessary for the construction of the boost converter. From efforts and time point of view, the simulation of the boost converter is straightforward. The simulation allowed easy addition of new block or change the properties of the existing block.

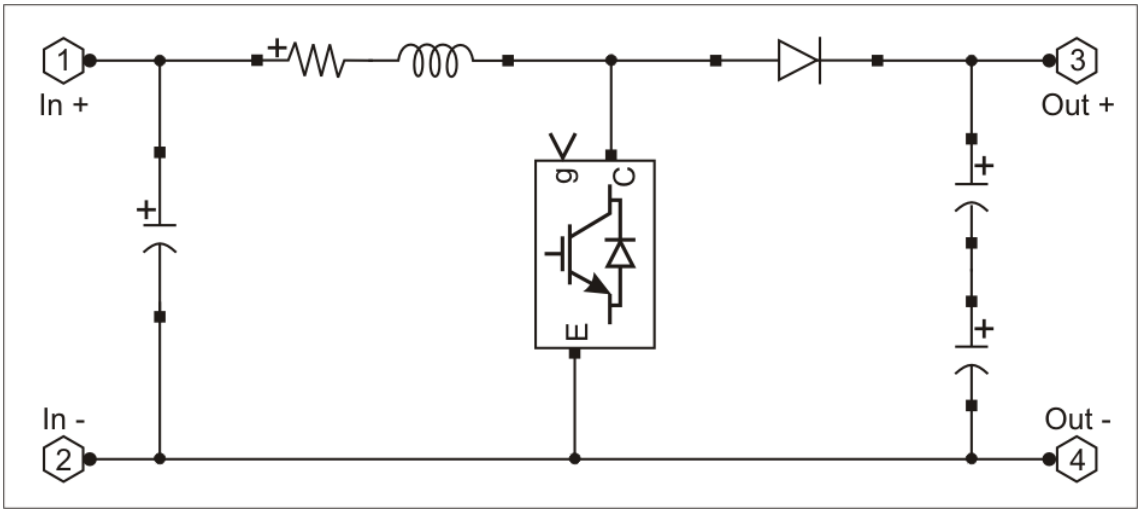

Figure 5-5. *Modeling of the boost converter.*

5.3.3 Maximum Power Point Tracking (MPPT)

The power output of the PV array is heavily reliant on the location of the sun and the direction of the sun rays (e.g., irradiation). Considering power vs voltage curve of solar modules/panels, there exist only one maxima of power on this curve corresponding to the desired value of current and voltage and the technique which is used is known as maximum power point tracking (MPPT).

There are several MPPT techniques of varying performance and two of them are discussed in chapter 4 but in this simulation, incremental conductance plus integral regulator method has been used.

The incremental conductance method is constructed on comparison and measurements of the instantaneous conductance and the incremental conductance. It also identifies deviations in the voltage direction. The differentiation of power vs voltage curve obtained by the following equations:

$$\frac{\partial P}{\partial V} = \frac{\partial (VI)}{\partial V} = I\frac{\partial V}{\partial V} + V\frac{\partial I}{\partial V} = I + V\frac{\partial I}{\partial V} \tag{5.1}$$

$$\frac{\partial P}{\partial V} = 0 \tag{5.2}$$

$$I + V\frac{\partial I}{\partial V} = 0 \tag{5.3}$$

$$\frac{\partial I}{\partial V} = \frac{I}{V} \tag{5.4}$$

Where $\frac{I}{V}$ signifies the instantaneous conductance of the PV array and $\frac{\partial I}{\partial V}$ is the instantaneous change in conductance. The maximum power point of PV system can be defined by comparison of the quantities given by (5.5).

$$\begin{cases} \frac{\partial P}{\partial V} > 0, V < V_{mpp} \\ \frac{\partial P}{\partial V} = 0, V = V_{mpp} \\ \frac{\partial P}{\partial V} < 0, V > V_{mpp} \end{cases} \tag{5.5}$$

An inclusion of integral regulator effectively increases the performance of the incremental conductance method, which will also reduce the error e, as shown in (5.6).

$$e = \frac{\partial I}{\partial V} + \frac{I}{V} \tag{5.6}$$

In this thesis, implementation of the incremental conductance and the integral regulator algorithm has been implemented in Simulink and shown in Figure 5-6, where the controller's output adjusted by the initial duty cycle. The working of the model based on [35].

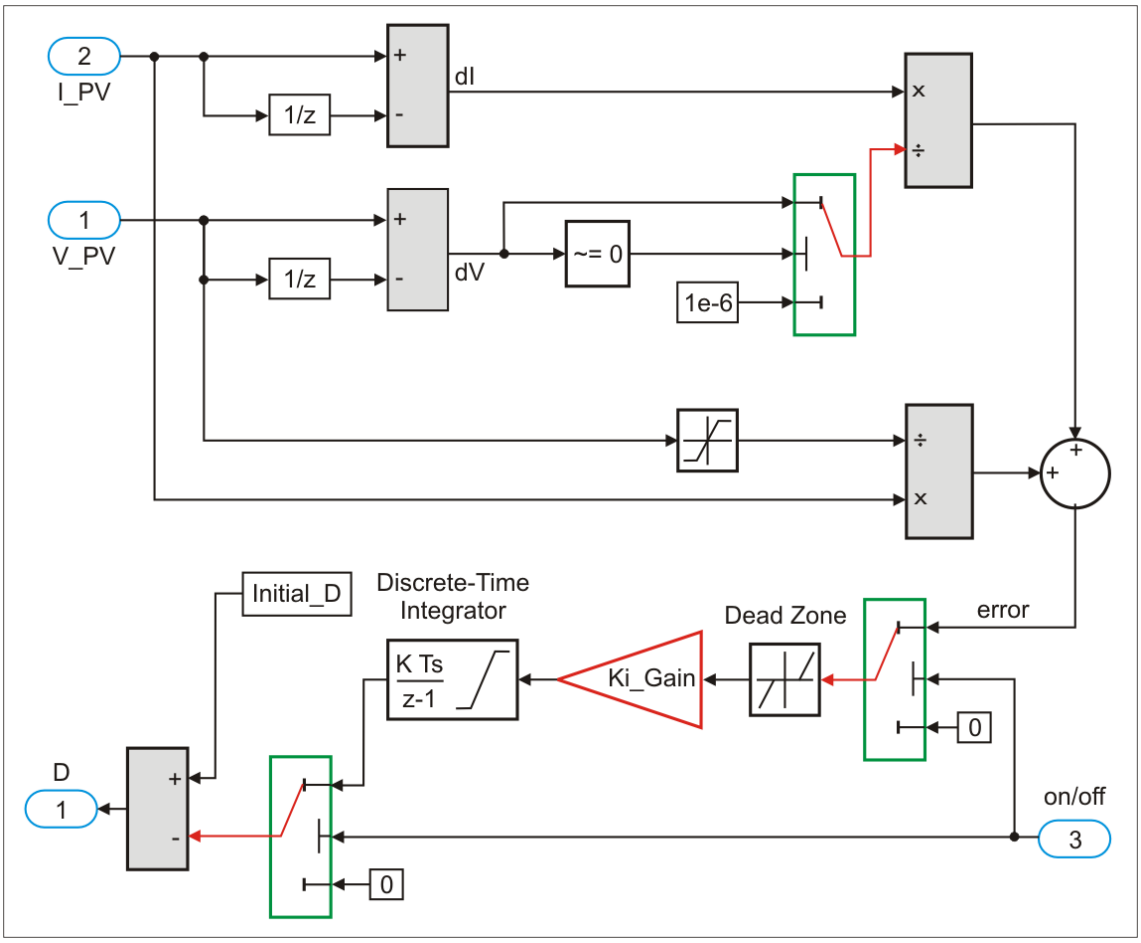

Figure 5-6. *Incremental conductance plus integral regulator method.*

5.3.4 DC-AC Inverter

This simulation used an IGBT (Insulated Gate Bipolar Transistor) based inverter that converts the dc supply (from the array and the DC-DC converter) into an AC supply. The efficiency of the inverter (e.g., less harmonic distortion) determines its ability to convert the dc into ac with the accurate waveform. These inverters use high-efficient multi-level PWM (pulse width modulation) technique for DC to AC conversion.

In this thesis, the universal bridge of MATLAB Simulink has been used as 3-level IGBT, as shown in Figure 5-7.

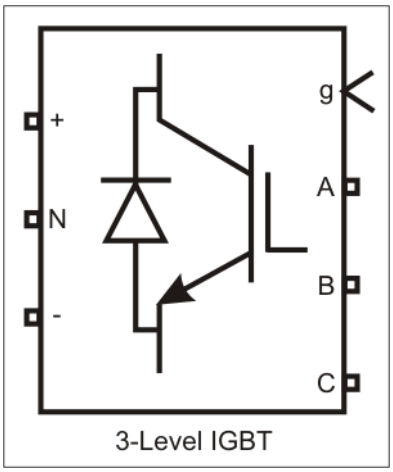

Figure 5-7. *Three level IGBT block in Simulink.*

The universal bridge block available in MATLAB Simulink can be used for various purposes and in the scope of this thesis, it has been used as IGBT and functioning 3 level, 3 phase VSC type DC-AC inverter.

5.3.5 Controller of inverter

As the PV system is connected also with the grid, which is operating at certain voltage and frequency, so controller inverter is designed in a way as shown in Figure 5-8, it synchronized the output of PV with the grid. Voltage and current are measured in abc coordinates at sending side of the transformer and pass it through phased lock loop (PLL). The PLL generates the phase angle and three phase parameters are converted into two-phase parameters, this transformation from abc frame to dq frame transformation is called as a synchronous frame. These parameters are pass-through current regulator which is designed to achieve maximum power injection to the grid. The backward transformation has been done to the natural frame which can be feed to PWM general. Details of this controller have been discussed in chapter 4.

In the simulation, 3-level 3-phase VSC converts the 500V DC to 260V AC. To minimize the harmonics generated by this VSC, a 10-kVAR capacitor bank filtering is employed.

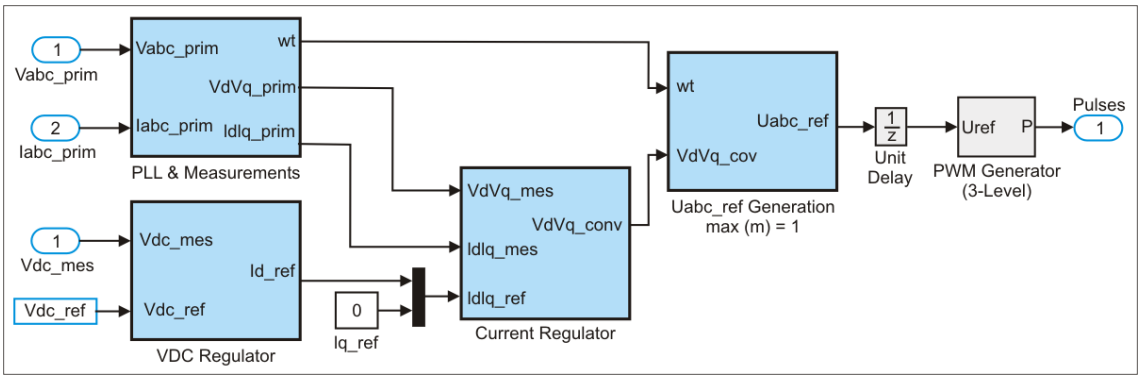

Figure 5-8*.The controller of inverter.*

5.3.6 Coupling Transformer

A transformer is subsequently used to increase the voltage from the IGBT inverter. The output voltage from the transformer becomes equal to the grid voltage. In this simulation, a 260V/25kV three-phase coupling transformer has been used. The whole system then connected to load and utility grid.

5.4 Battery Energy Storage System (BESS)

To mitigate the intermittent generation of renewable energy (for example, a PV solar system), Battery Energy Storage System (BESS) has been considered to make the system reliable and to provide operational flexibility.

BESS, as shown in Figure 5-9, has three components as follows:

- A battery bank (consisting of Lithium-ion batteries).
- A bi-directional DC-DC Converter. It is a Cuk type converter with two switches to control the flow of power.
- A DC-AC inverter. It converts the DC voltage into AC voltage and maintains the voltage level.

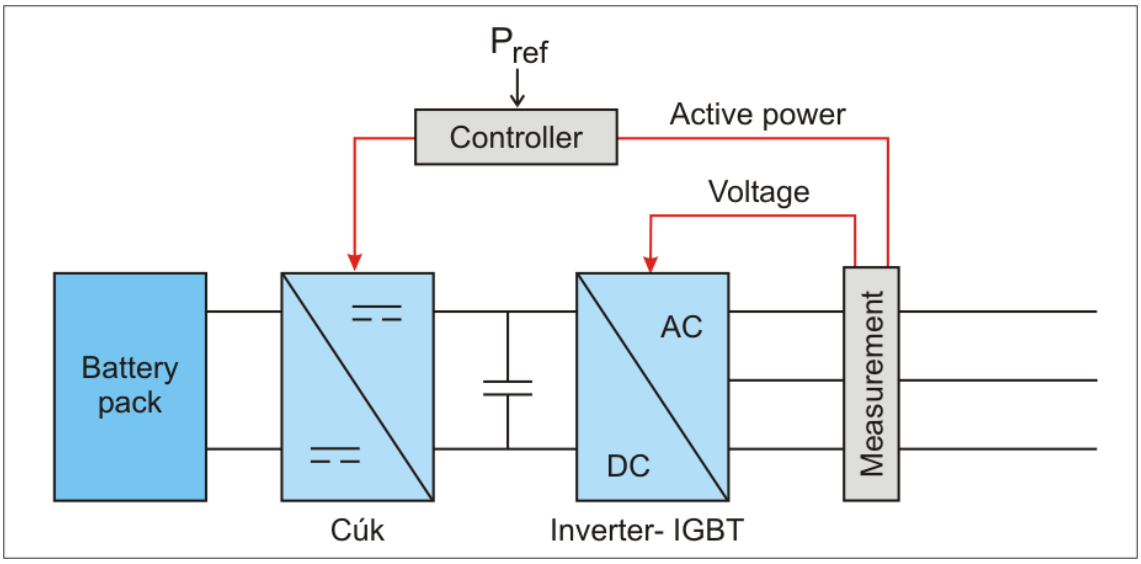

Figure 5-9. *The BESS model used in this simulation.*

The main objective of BESS is to deliver the power to the load when PV system is unable to deliver the total power required by the load. BESS complements the total power generated from the PV system. The main purpose of the battery is to supply the additional energy to the load. This increases the efficiency of the overall plant. The BESS allows controlling the flow of active power into the battery.

For simulation, all three components have been implemented in MATLAB Simulink to assess the impact of the BESS in delivering energy to the load as well as its impact to the power grid.

5.4.1 Battery Pack

MATLAB Simulink provides the simulation capability of the sophisticated battery dynamics that is very useful for this work. However, it does not incorporate battery aging and temperature dependency. Even without considering battery aging and temperature dependency, the battery modeling provided by MATLAB Simulink is considered very accurate for this work. The battery model is shown in Figure 5-10.

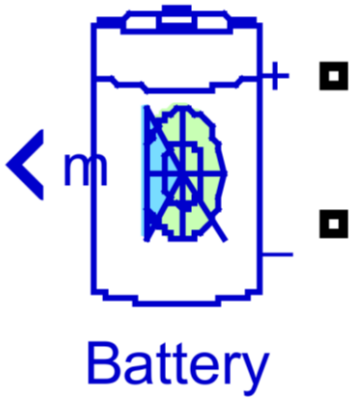

Figure 5-10. *A Battery model in Simulink.*

The parameters of battery model which is used in this thesis are shown in the Table 5-2.

Table 5-2. *The parameters of battery.*

Type	Lithium-ion
Nominal voltage (V)	500
Rated Capacity (Ah)	200
Initial state of charge (SOC)	80
Maximum capacity (Ah)	200
Cut-off Voltage (V)	375
Fully charged voltage (V)	581
Nominal discharge current (A)	86.9
Internal resistance (Ohms)	0.025
Capacity (Ah) at nominal voltage	180

5.4.2 DC-DC Converter (Cuk Converter)

The thesis has considered the following DC-DC converter, as shown in. It is a bi-directional Cuk-converter. In this simulation, the parameters of this converter are set to the following values:

C1 = 500µF	C2 = 2000µF	C3 = 8000µF
L1 = 12µH	L4= 12µH	

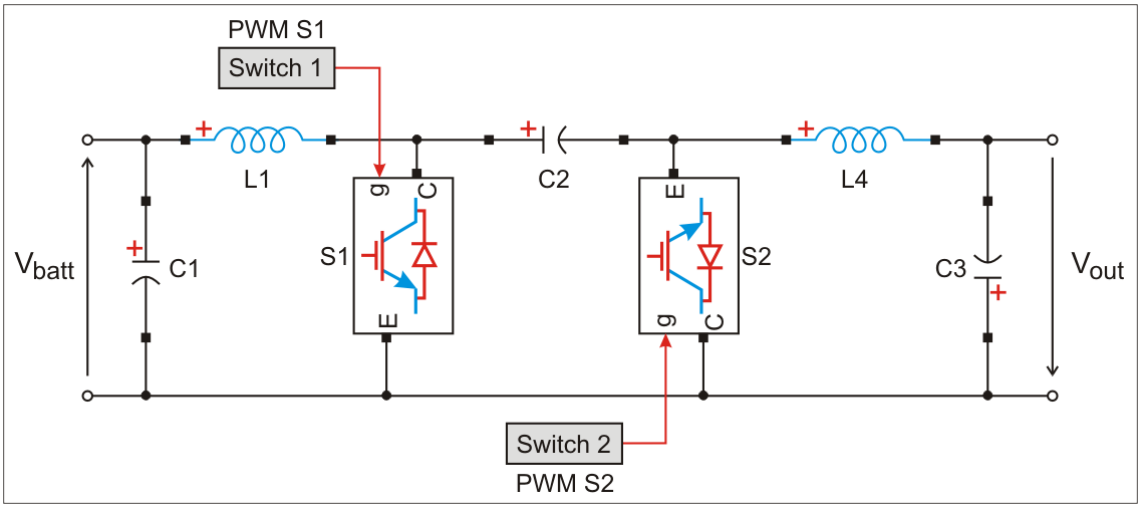

Figure 5-11. *DC-DC converter used in the BESS.*

This DC-DC converter controls the active power flow of the batteries. It charges the battery by controlling the terminal voltage. This is possible by adjusting the duty cycle. The power drawn from the battery and injected into the battery controlled by switches S1 and S2 respectively. These switches operate one at a time. The terminal voltage of the battery is also controlled by these switches. The Capacitor C3 reduce the voltage spike on the output terminal of converter.

The simulation assumes a high value for C2 and C3 to provide a large capacity. For example, capacitor C3 reduces the ripple of the output voltage. This is important as ripple needs to be small as possible. Capacitor C2 keeps the voltages between switches constant when the power is transferred from the battery bank to the VSC.

5.4.3 Operation of Cuk Controller:

The controller of Cuk converter is divided in three major stages. Initially the difference of active power calculated at the PCC. The impact of the BESS is proportional to the difference of active power. The impact of the BESS is considering to be zero if the difference of active power flow is below the threshold value to prevent continuously charging and discharging of the battery. In the next stage, the target output voltage is calculated.

The initial status of BESS is kept constant while simulation. In the last stage, the duty cycle of Cuk converter is calculated, which are transformed into PWM signal.

5.4.4 DC-AC Inverter (VSC)

For BESS, same inverter (with similar description) is used like the PV systems. However, during simulation, it is found that control is extremely difficult, and it is recommended for future study. This topic is recommended for future work. Voltage measurement is carried out in the grid and it is passed through a phase locked loop to generate a synchronized phase angle. The inverter also minimizes input power losses. To do this, it employs feedback control and regulates the DC-link voltages. The inverter also employs current control regulation that can achieve maximum power injection into the grid.

5.5 Summary

In this chapter, the modeling and control of all the necessary components of the PV system along with the Battery Energy Storage systems (BESS) has been provided. Two main subsystems have been considered in detail for MATLAB Simulink simulation: a) PV system consists of DC-DC Converter and MPPT control, DC-AC Converter with VSC control; b) Battery Energy Storage systems (BESS), consisting of a bi-directional Cuk type converter along with the DC-AC inverter.

For the modeling and control of the individual subsystems, MATLAB Simulink has been extensively used. For this thesis, several tool boxes from MATLAB Simulink have been used to model different components that allow testing of the PV system under different test conditions. The Simulink implementation of this system facilitated the simulation, test results are provided in Chapter 6.

6. SIMULATION RESULTS AND DISCUSSION

6.1 Introduction

This chapter reports on the simulation results furnished by the Simulink model of the compound PV-BESS system, discussed in Chapter 5. The MATLAB Simulink environment facilitates the modeling and simulation of rather complex engineering systems, such as the PV-BESS system, which is the object of this research project. A sample of key results have been recorded and presented in this chapter using plots and tables. The salient points of these results are brought up for discussion in suitable locations of this chapter.

6.1.1 Performance of PV module and array

To start with, simulation test results have been presented for each PV module and for the entire PV array respectively. The PV array is shown in Figure 6-1; a total of 330 solar modules provide 100.7 kW under standard test and conditions (STC). The layout of the PV array consists of 66 parallel strings where each string has 5 series-connected SunPower modules (with specification SPR-305E-WHT-D as per Table 6-1). The PV array has an optimum capacity of 66*5*305.2 W = 100.7 kW at 25 ºC or STC, as per Table 6.2.

Table 6-1. *Technical data of a PV module (SPR-305E-WHT-D) at STC.*

Short Circuit Current Isc	5.96 A
Current at maximum power point Impp	5.58 A
Voltage at maximum power point Vmpp	54.7 V
Open circuit voltage Voc	64.2 V
Number of cells in Series ns	96

Table 6-2. *Technical data of the PV array (capacity 100 kW at STC).*

Number of modules in string series Nss	5
Number of modules in string parallel Npp	66
Output Voltage rating	273.5 V
Output Current rating	368.3 A
Maximum Power Output	100.7 KW

The voltage and current characteristics of PV module under varying irradiance had been shown in Figure 6-2. The output Current PV module is linearly connected with related with the amount of irradiance. The irradiance also affects the voltage of the PV module, but it is not so significant. Due to change in irradiance, the overall power of the PV module also varies as shown in Figure 6-2. Decreasing the irradiance will reduce the overall performance of the PV module. Similarly, the impacts of temperature have been analyzed on PV array shown in Figure 6-3and Figure 6-4. The temperature impacts the voltage of the PV array. Increasing the temperature reduces the performance of the PV panel.

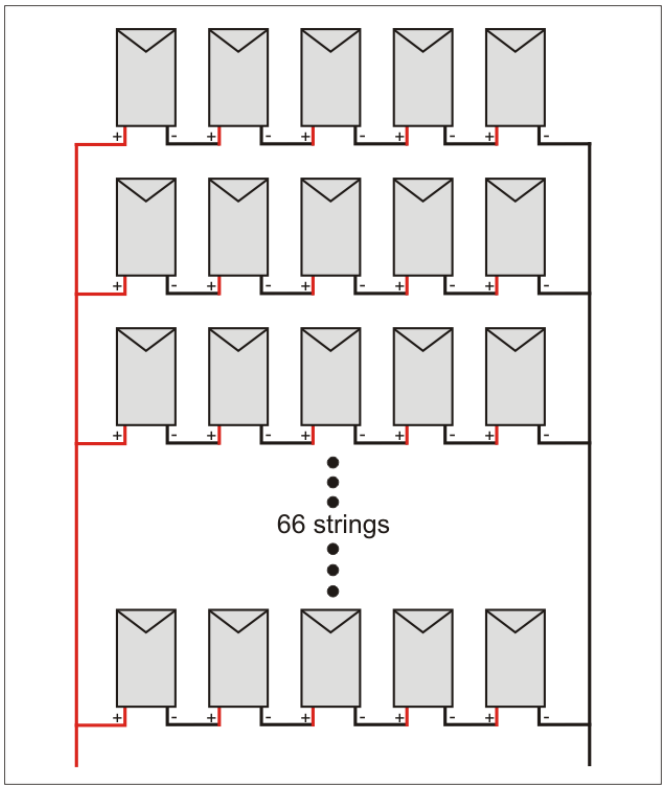

Figure 6-1*. PV module connected in series and parallel to form an array.*

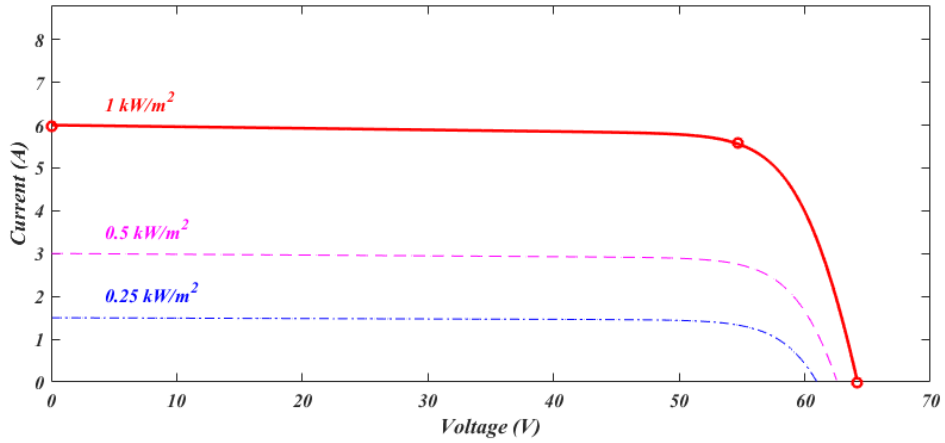

Figure 6-2. *I-V Characteristics of the PV module under varying irradiance.*

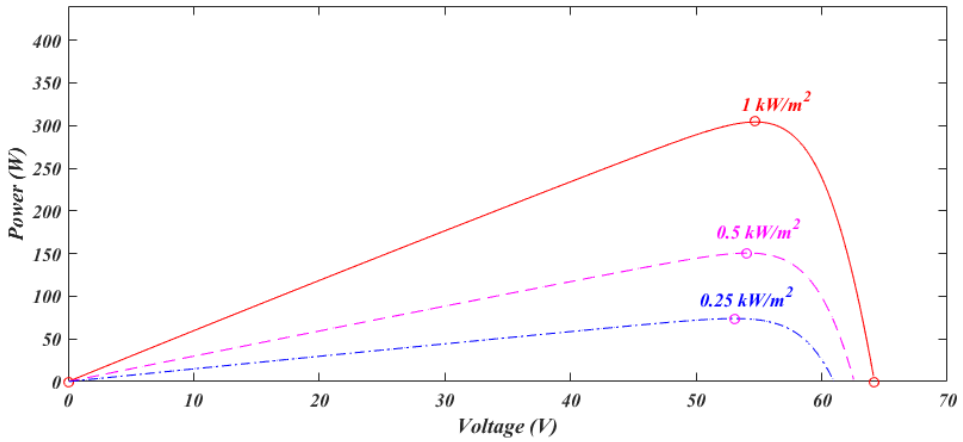

Figure 6-3. *P-V Characteristics of the PV module under varying irradiance.*

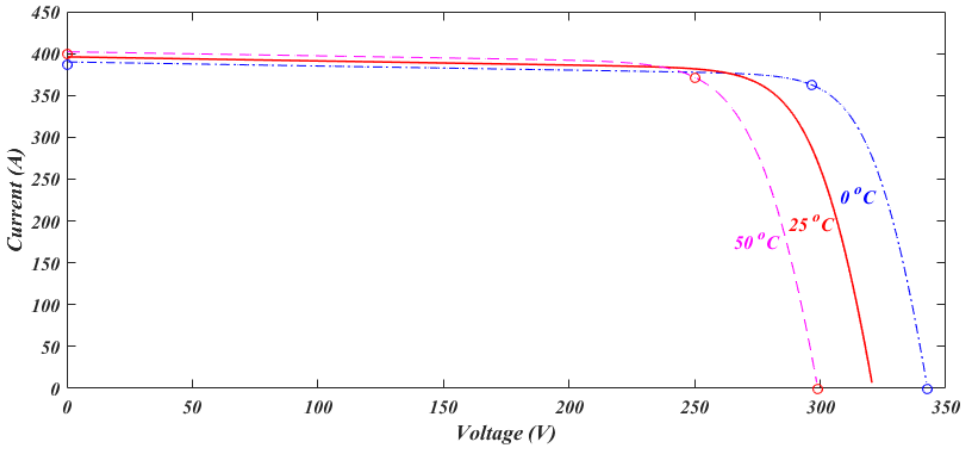

Figure 6-4. *I-V Characteristics of the PV array under varying temperature.*

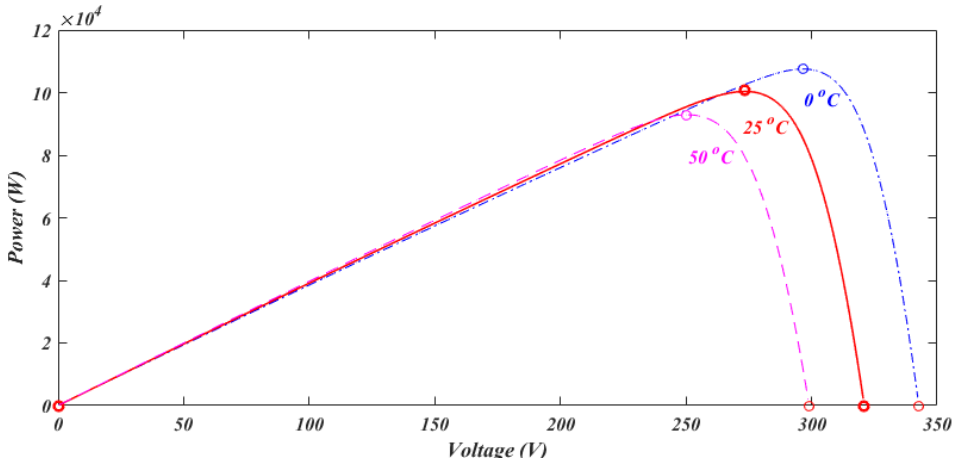

Figure 6-5. *P-V Characteristics of the PV array under varying temperature.*

Simulation test results have been organized into four cases as follows:

6.2 Case 1: PV System Performance

Performance of PV system is analyzed in this case. PV system consists of PV array, boost-type DC/DC converter, VSC type DC/AC inverter, filter, coupling transformer and it is connected to load and grid as described in chapter 5. It has two parts – in Part (a), In this case, the irradiance and temperature assumed to be constant, the PV array generates electricity delivers power to the electrical load. The simulation starts assuming standard sunlight condition (1000 W/m^2 and 25 ºC) when the maximum output power (100.7 kW) can be obtained from PV array. In Part (b), solar irradiance changes from 1000 W/m^2 to 250 W/m^2. The output from the PV array drops to 24.3 kW. The simulation also considered the temperature variation from 25 ºC to 50 ºC; affecting output power varies PV array from 100.7 kW to 93 kW.

Figure 6-6 shows Case 1 energy flow: starting from electricity generation by the PV array delivery the power to the electrical load. The electricity generated by the PV array goes to the load via the DC-AC inverter as shown in Figure 6-6.

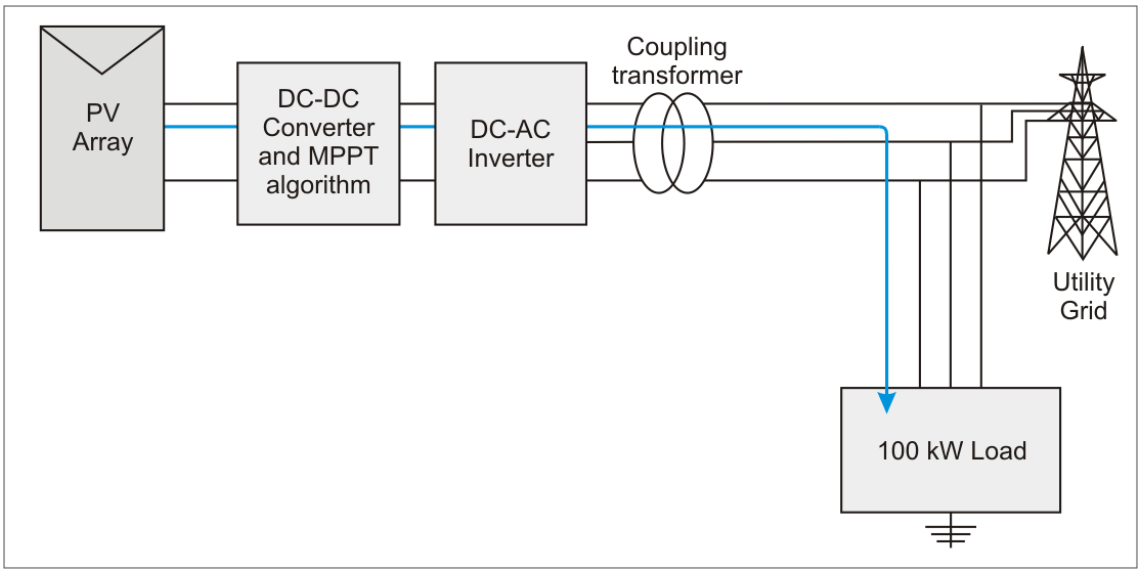

Figure 6-6. *Energy flow of PV system.*

The simulation result for Case 1 are obtained as follows:

1. Steady-state performance of PV system.
2. Performance of PV under varying operating conditions.
3. Simulation results of PV-BESS

6.2.1 Steady-State Performance of PV Array

The steady-state performance of PV system for Case 1 Part (a) is provided in Figure 6-7 to Figure 6-12. For this Simulation result, the irradiance and temperature are assumed to be constant for whole simulation time. From t = 0 sec to t = 0.05 sec, pulse to boost converter and VSC are blocked. PV voltage according to open circuit voltage reaches up to 321 V as shown in Figure 6-9. At t = 0.05 sec, the pulse to boost converter and VSC are de-blocked. Voltage is dc-link is regulated at 500v and duty cycle of the boost converter is fixed at 0.5 as shown in Figure 6-10. Steady-state operation of PV reaches at t = 0.25 sec, where to power and voltage of PV array reaches at 96kw and 250v as seen in Figure 6-8 and Figure 6-9 simultaneously. However, the maximum power of specific PV array is 100.7 KW at 1000 w/m^2. The MPPT algorithm has been enabled at t = 0.5 to get the maximum output power of PV, it starts to regulate the voltage of PV by varying the duty cycle of the boost converter to get maximum power. The maximum power (100.7kw) and voltage (274 V) are obtained at D = 0.545. The voltage and current are in phase at the 25kV bus as shown in Figure 6-12.

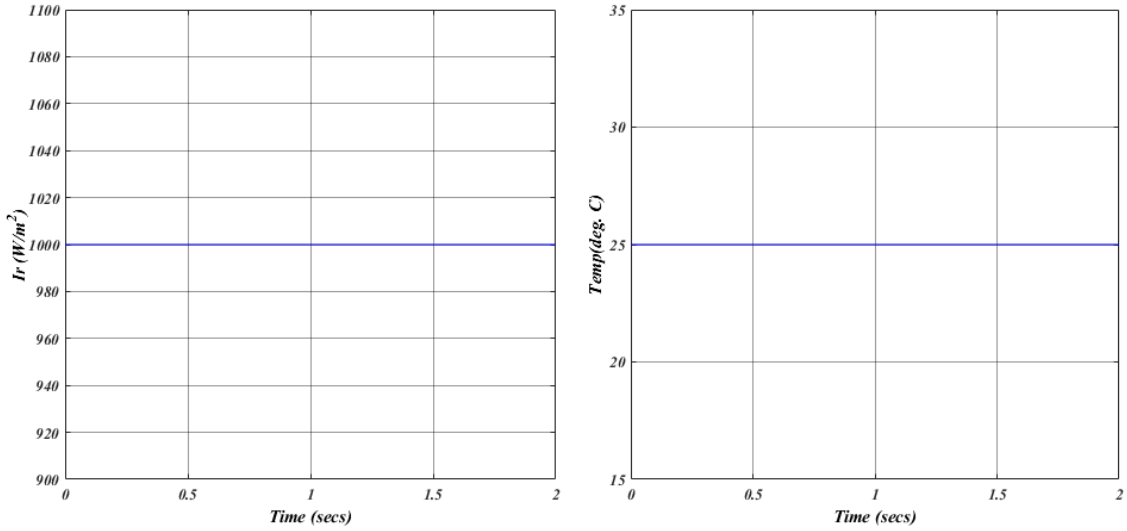

Figure 6-7. *Constant Irradiance and temperature used for Case 1, Part (a).*

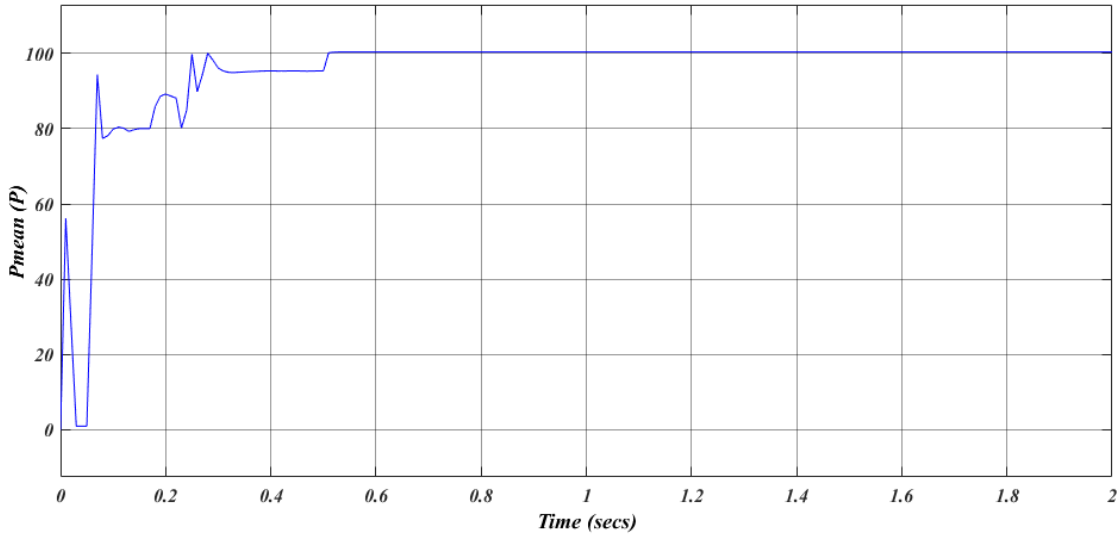

Figure 6-8. *DC Power Output from the PV.*

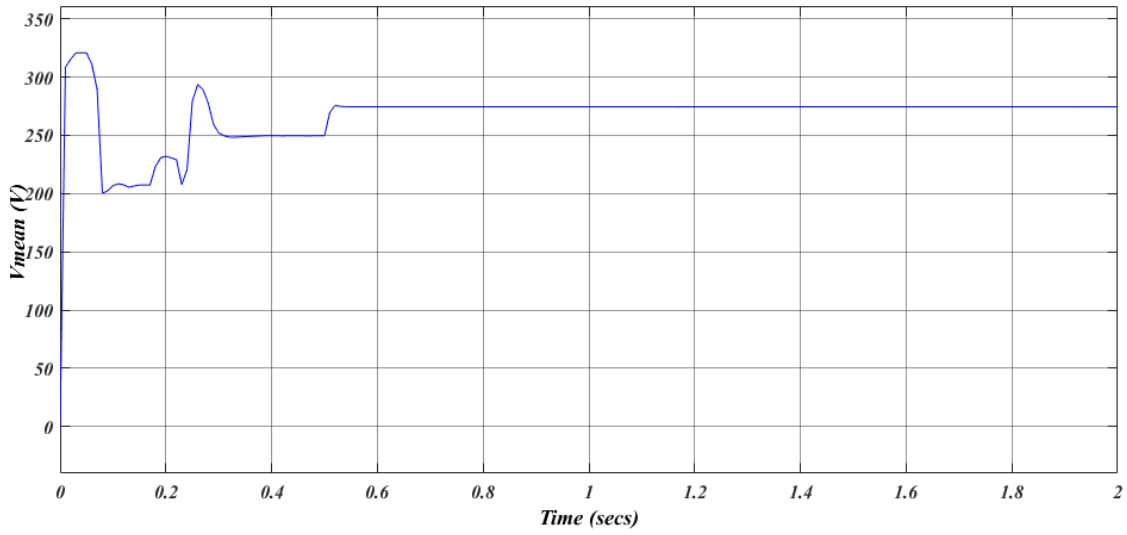

Figure 6-9. *DC Voltage output from the PV.*

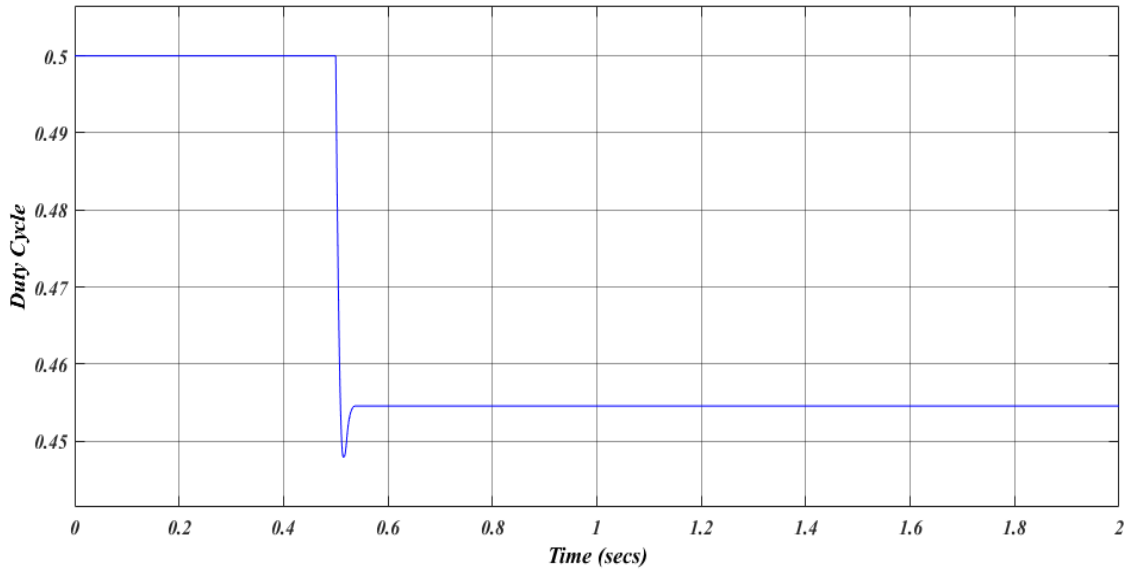

Figure 6-10. *Duty cycle of boost converter.*

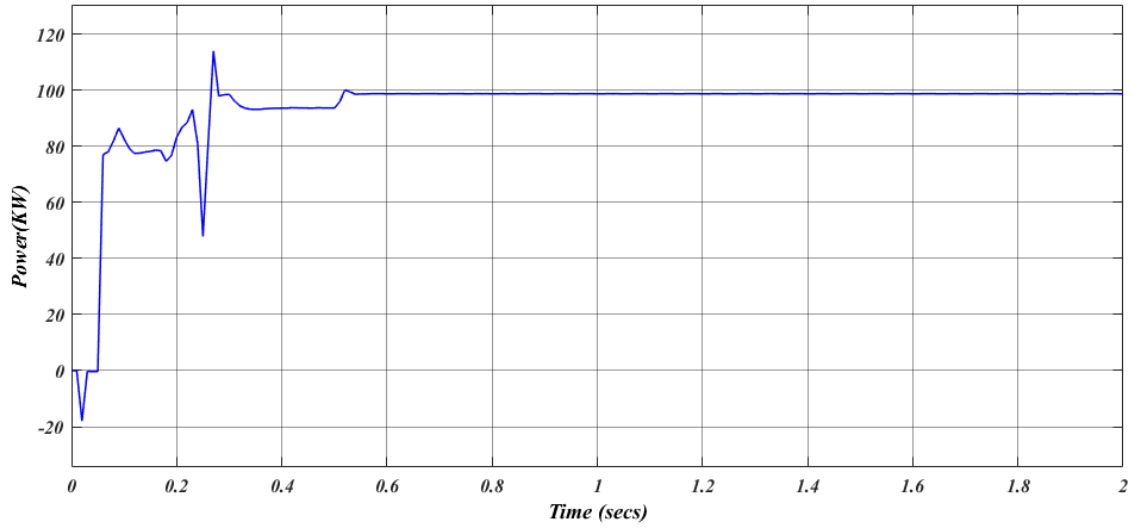

Figure 6-11. *PV System Output Power that is delivered to the load.*

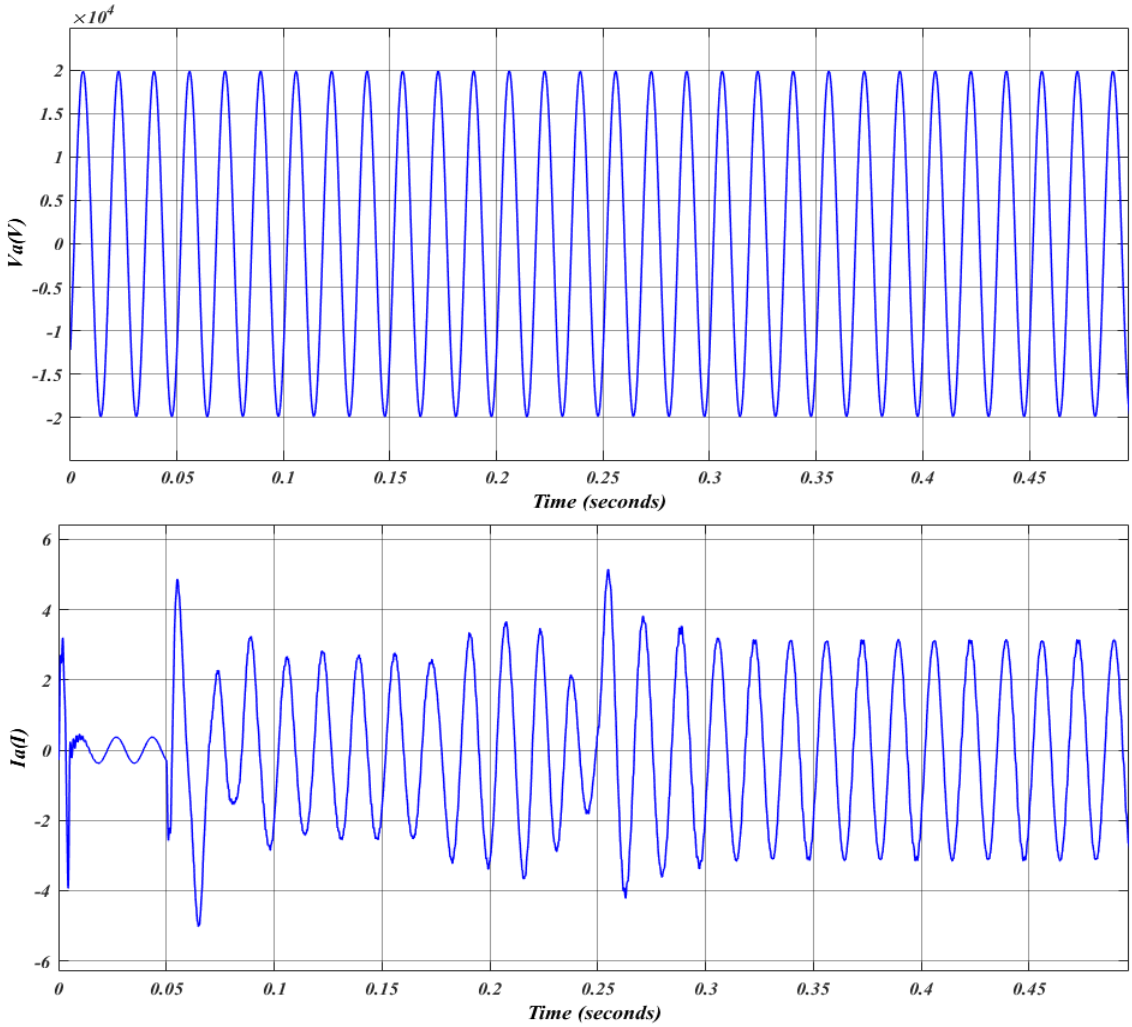

Figure 6-12. *Single-phase waveform of voltage and current at 25kV ac bus.*

6.2.2 Performance of PV Array under varying operating conditions

In this case, the irradiance and temperature are altered to see the behavior of PV system. In the case from the start of simulation to t= 0.6 sec, the irradiance is 1000 w/m^2. From t = 0.6 to t = 1.1 sec, the solar irradiance ramped down from 1000 w/m^2 to 250 w/m^2 and again from t = 1.2 sec to t = 1.6 sec, the solar irradiance ramped up from 250 w/m^2 to 1000 w/m^2 and temperature of PV array increased to 25 ◦C to 50 ◦C to observe the impact of temperature as shown in Figure 6-13.

The output of PV array follows similar behavior as in case one until t = 0.6 sec, only the difference is MPPT algorithm enable immediately as the steady state output reaches at t = 0.25 sec to get maximum power. As the irradiance ramped down from 1000 w/m^2 to 250 w/m^2 during t = 0.6 sec to t = 1.1 sec and restored back from 250 w/m^2 to 1000 w/m^2 during t = 1.2 sec to t = 1.7 sec, the MPPT continue to track maximum power. At t = 1.2 sec, the duty cycle is 0.461, when the irradiance is decreased to 250 w/m^2, the output mean power and voltage are 268V and 24.3 KW. Impact of temperature has been analyzed when it is increased up to 50 ◦C at t = 2 sec, the output power decreases from 100.7 KW to 93 KW. Output behavior of above description as shown in Figure 6-14 and Figure 6-18.

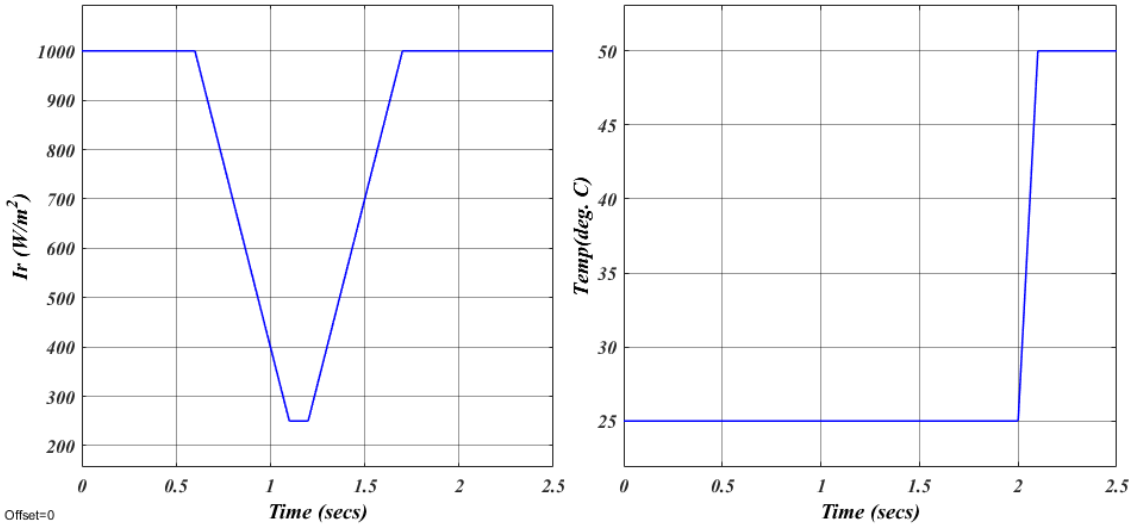

Figure 6-13. *The irradiance and temperature pattern on PV array.*

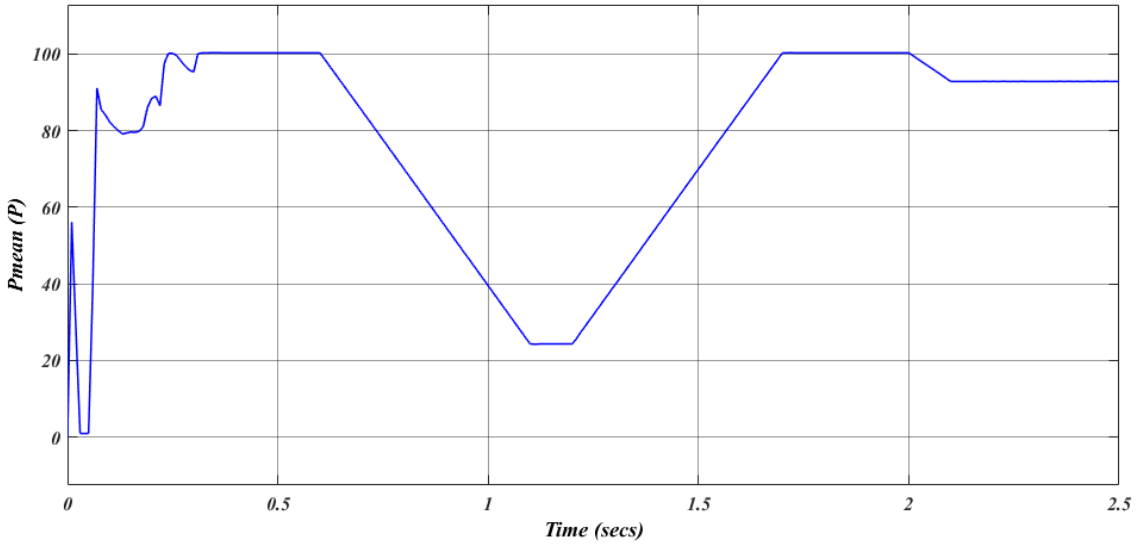

Figure 6-14. *Mean power from the PV array.*

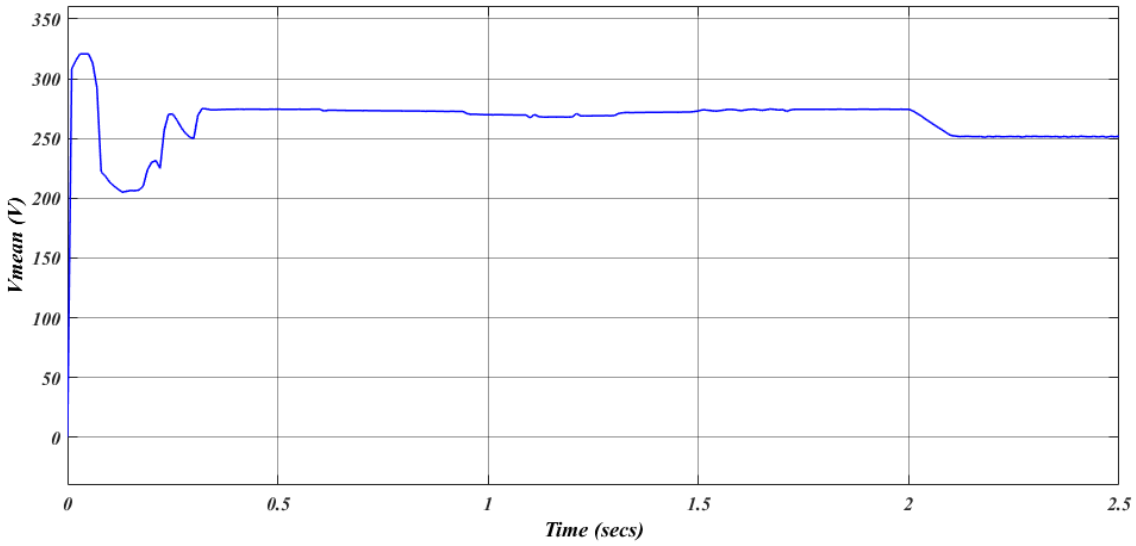

Figure 6-15. *Mean voltage from the PV.*

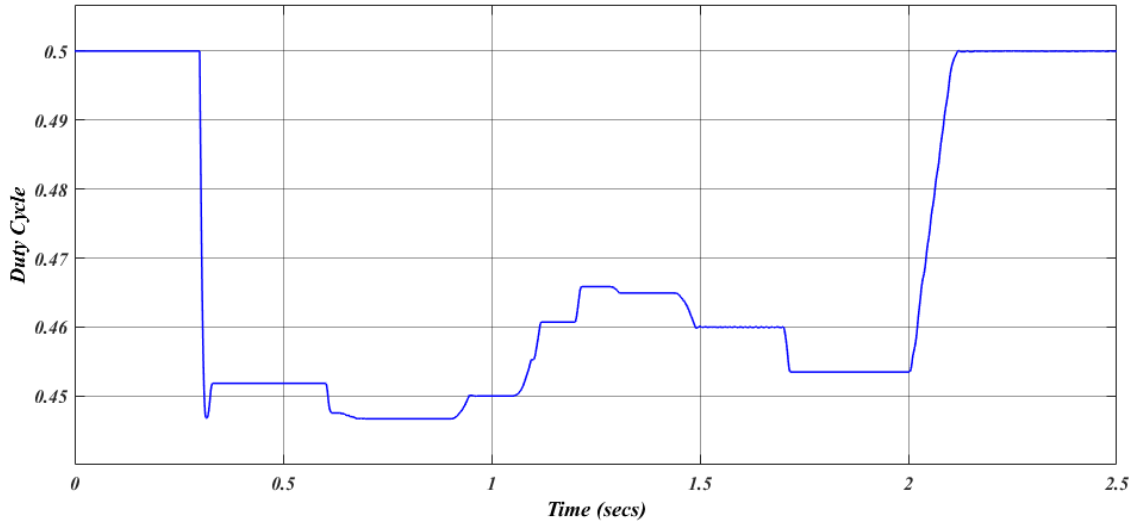

Figure 6-16. *Duty cycle variation.*

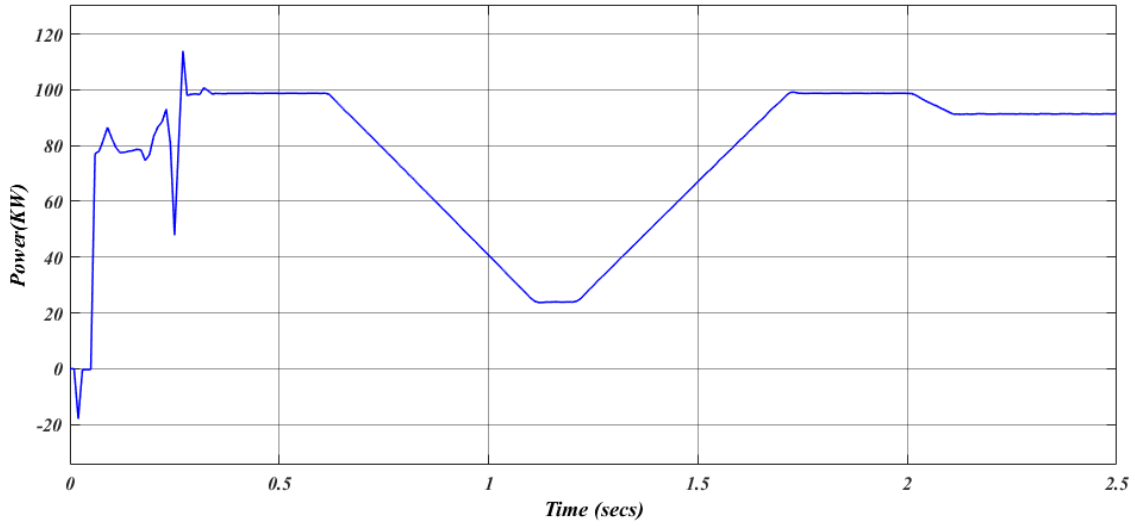

Figure 6-17. *AC Power Output of the PV System.*

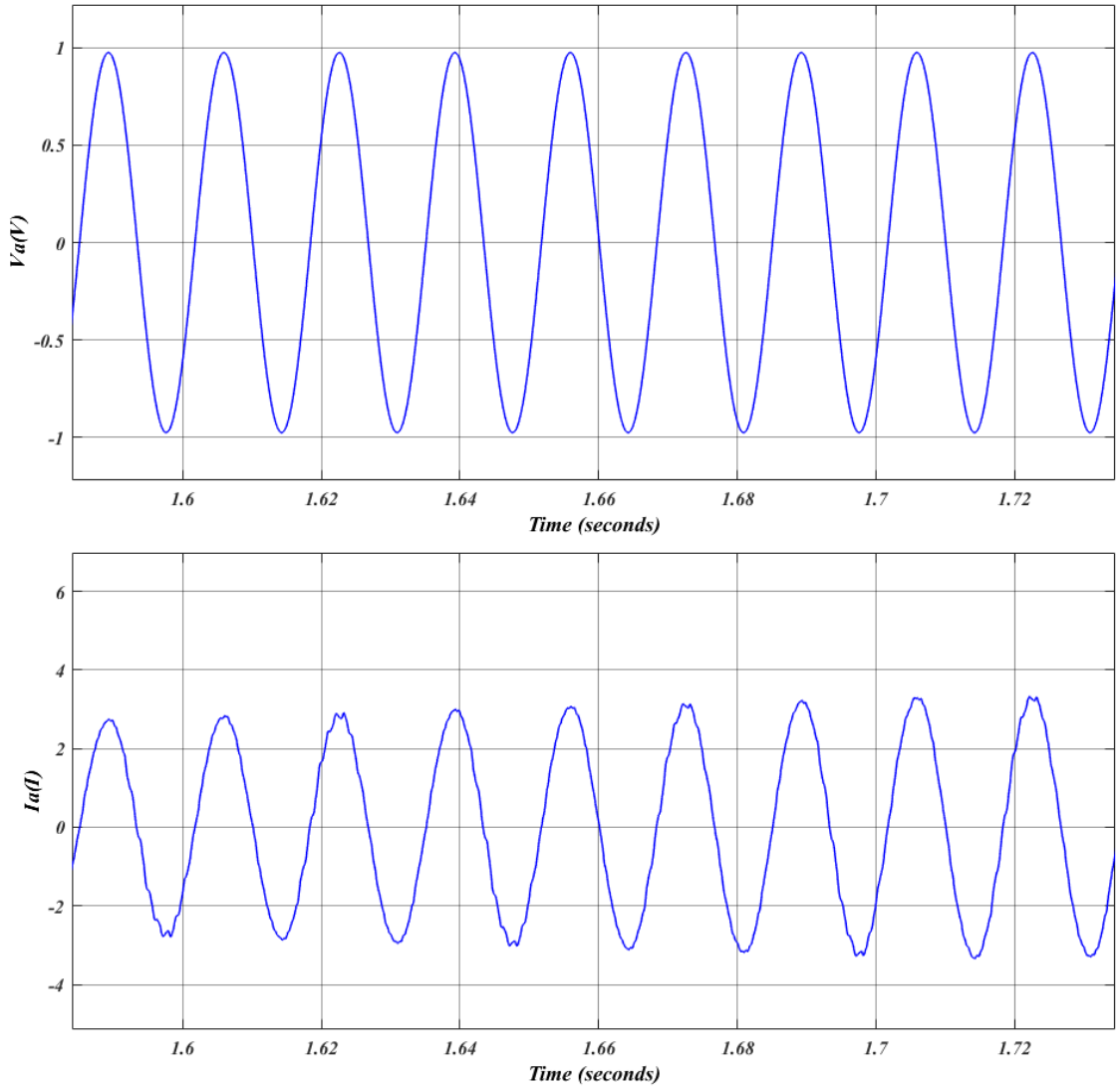

Figure 6-18. *Single-phase waveform of voltage and current at 25kV ac bus.*

6.2.3 Simulation results for PV-BESS

The simulation has considered three more scenarios for getting more insights of the PV-BESS system.

- When PV supplies constant power
- When PV supplies less power than required power, BESS discharging
- When PV supplies more power than required power, BESS charging

These three scenarios represent a representation of the PV-BESS operation as per the flowchart in Figure 6-19 that has been incorporated in the simulation.

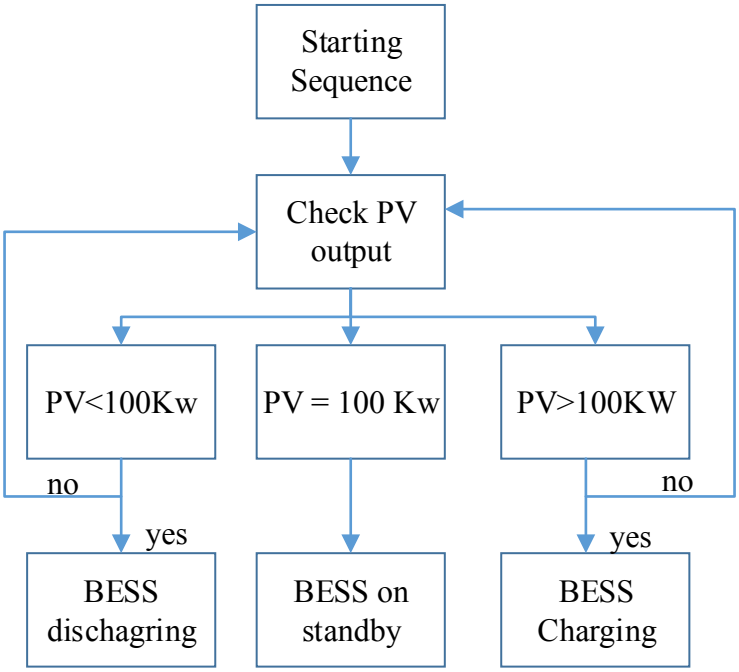

Figure 6-19. *PV-BESS operational flow chart.*

6.3 Case 2: PV supplies constant power, BESS has no impact

In the case, PV system and BESS system are connected in parallel with utility grid and load. The PV array generates electricity at its optimum capacity of 100 kW. For this scenario, the role of the battery is almost negligible. The battery response only during settling time of PV system. The power flow diagram has been shown in Figure 6-20 and power output from PV, BESS, PV-BESS (or power delivered to load) and grid shown in Figure 6-21.

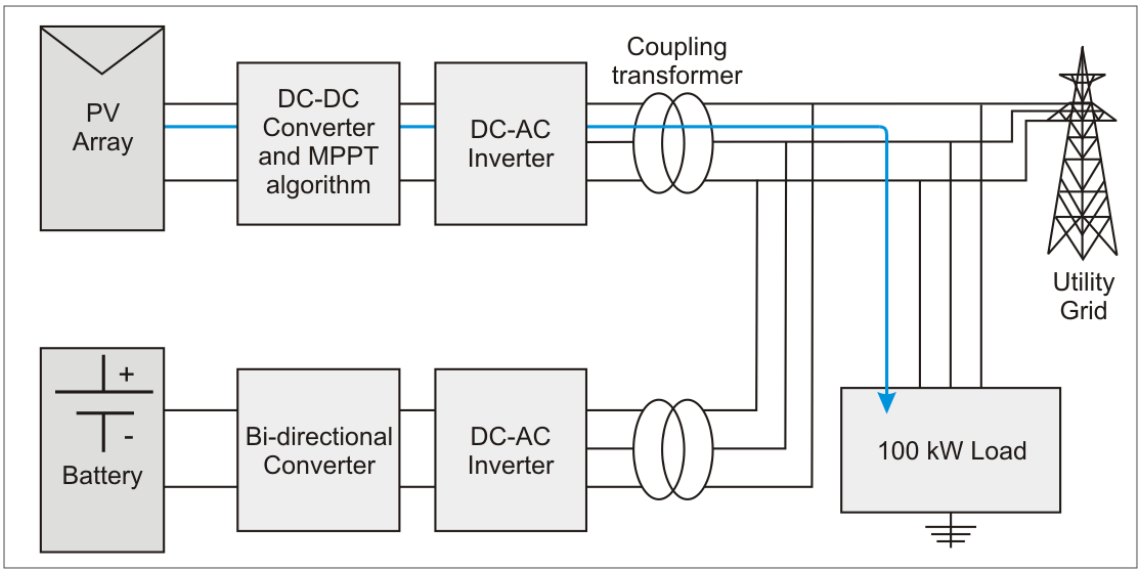

Figure 6-20. *Energy flow for PV-BESS System.*

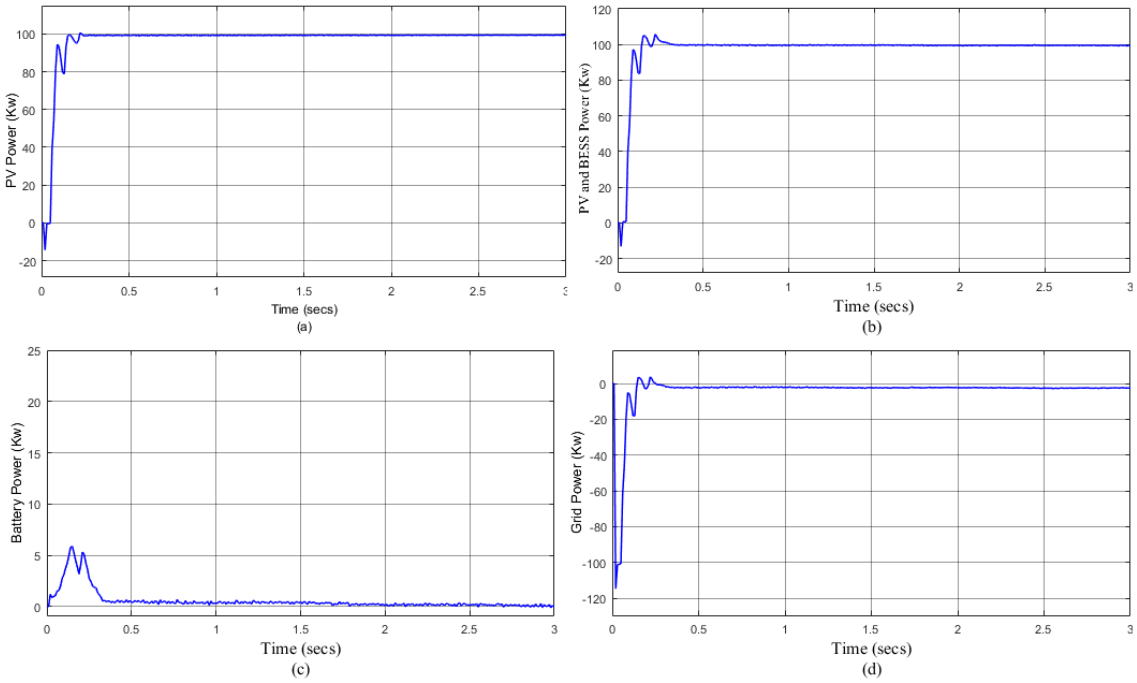

Figure 6-21. *Power (a) PV (b) Battery (c) PV and Battery (d) Grid.*

6.4 Case 3: BESS discharging due to change in PV

For this scenario, simulation assumed that the PV output power fluctuates due to change in irradiance during certain intervals from 1000 W/m^2 to 150 W/m^2. To supply the required amount of power to the load, BESS delivers power to the load by discharging the battery; assume the battery was previously charged. This ensures continuous power to the load. Overall power flow diagram has been shown in Figure 6-22.

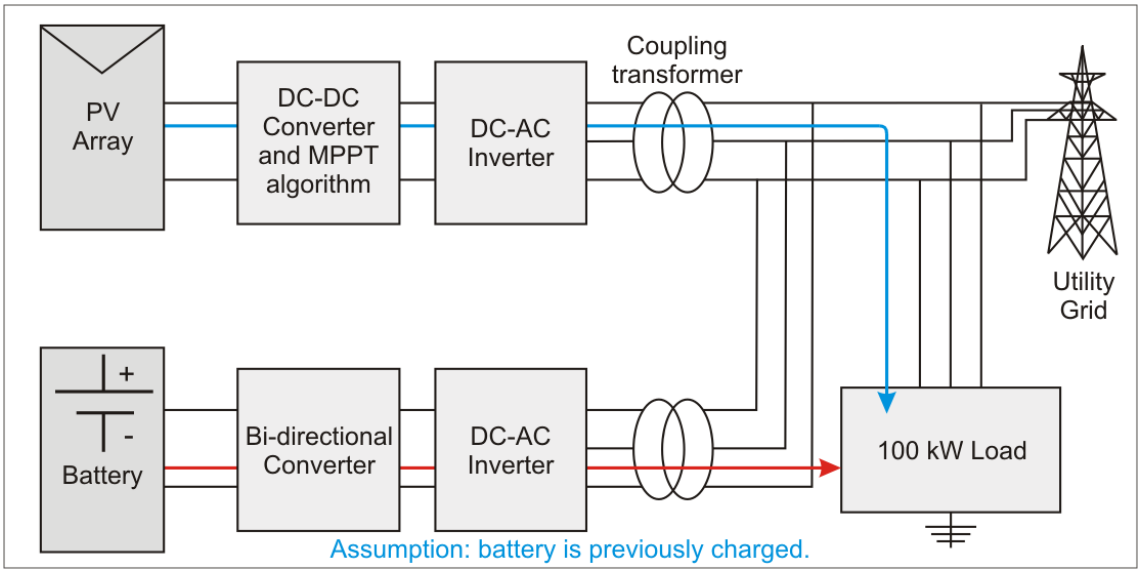

Figure 6-22. *Energy flow for the PV-BESS System.*

For Case 3, battery discharge compensates the shortfall of electricity generation by the PV array. Total load requirements are met both by the battery discharge and by the PV. Figure 6-23 (a) shows that the power generated from PV under varying irradiance pattern from t = 0 sec to t = 8 sec, total power delivered varies from 100 kW to 15 kW. Figure 6-23(b) shows power drawn from the battery to supply constant power to the load. Figure 6-23(c) shows the total power delivered from PV and BESS to the load and Figure 6-23(d) shows the power supplied by the grid. Figure 6-24 the overall impact of combined power in a single diagram. As the power drawn the battery, the state of charge of the also decreases from 79.32% to 79.23% as shown in Figure 6-25. Figure 6-26 shows the single-phase voltage and current waveform at the point of coupling. Although these are in phase, not purely sinusoidal which requires being improved through precise control of BESS controller.

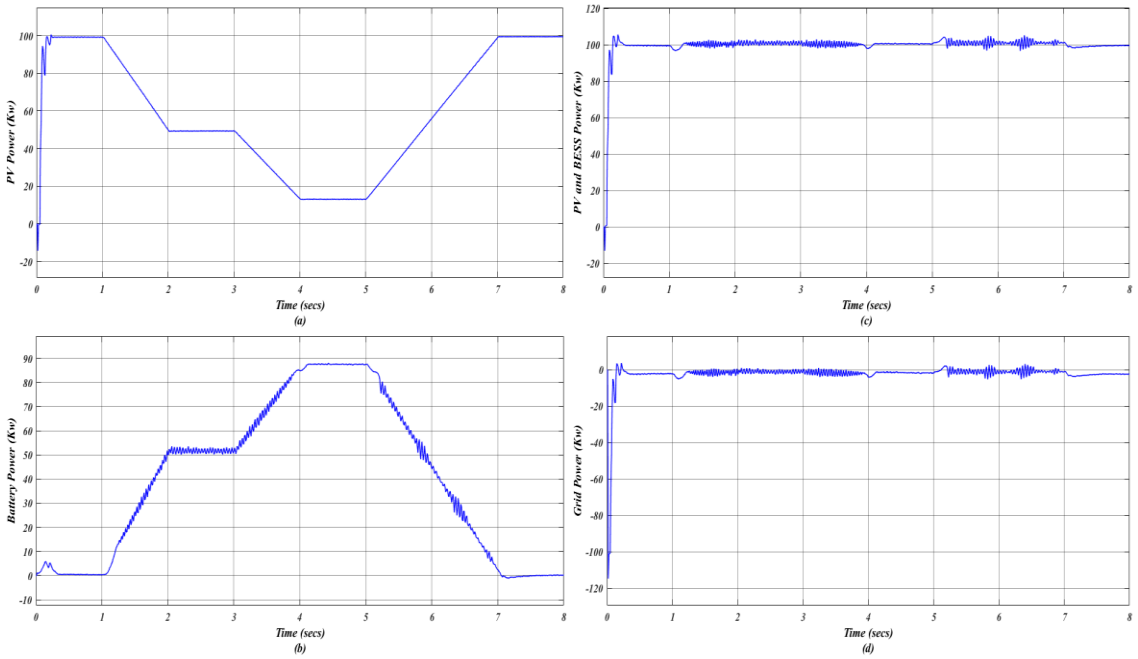

Figure 6-23. *Power generated from (a) PV (b) Battery (c) PV and Battery (d) Grid.*

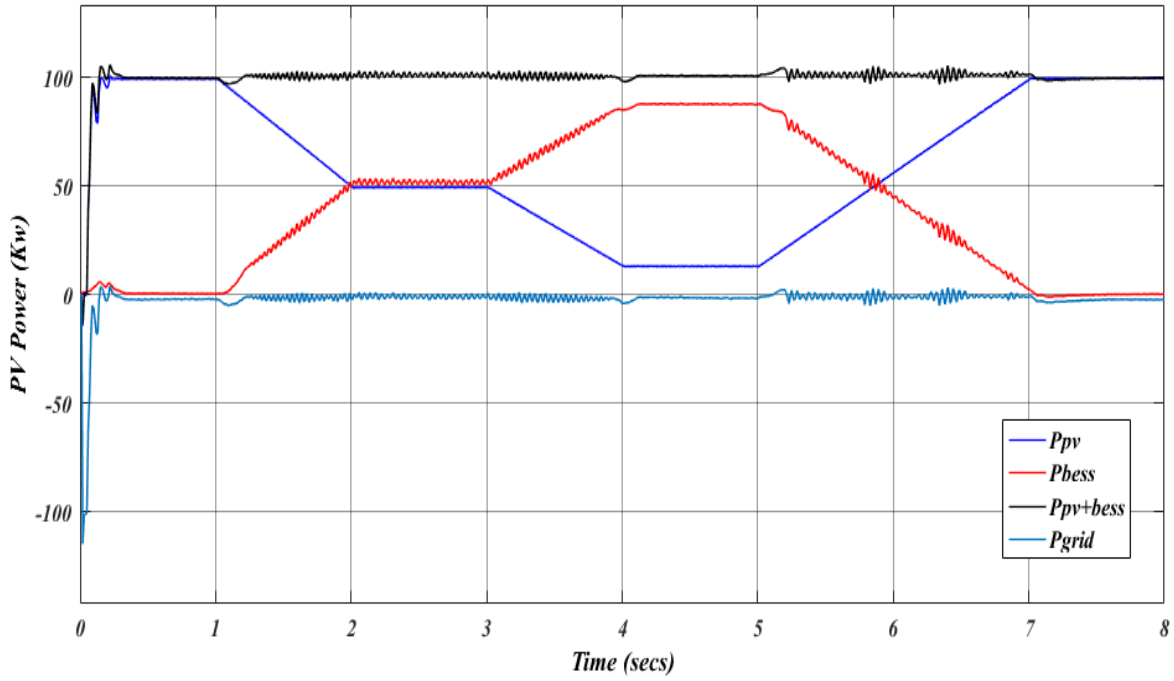

Figure 6-24. *Power generation of the whole system in one diagram.*

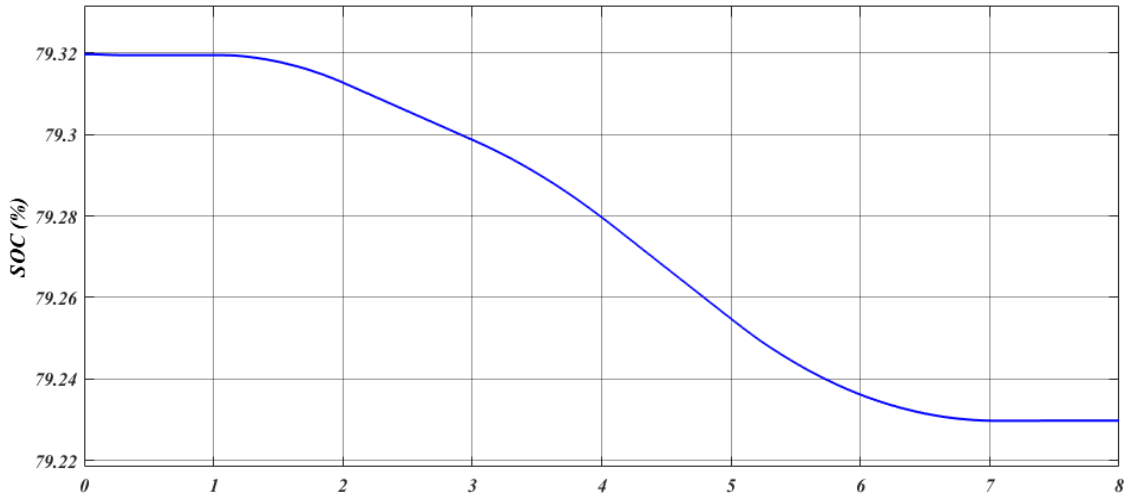

Figure 6-25. *State of Charge (in %) of battery bank.*

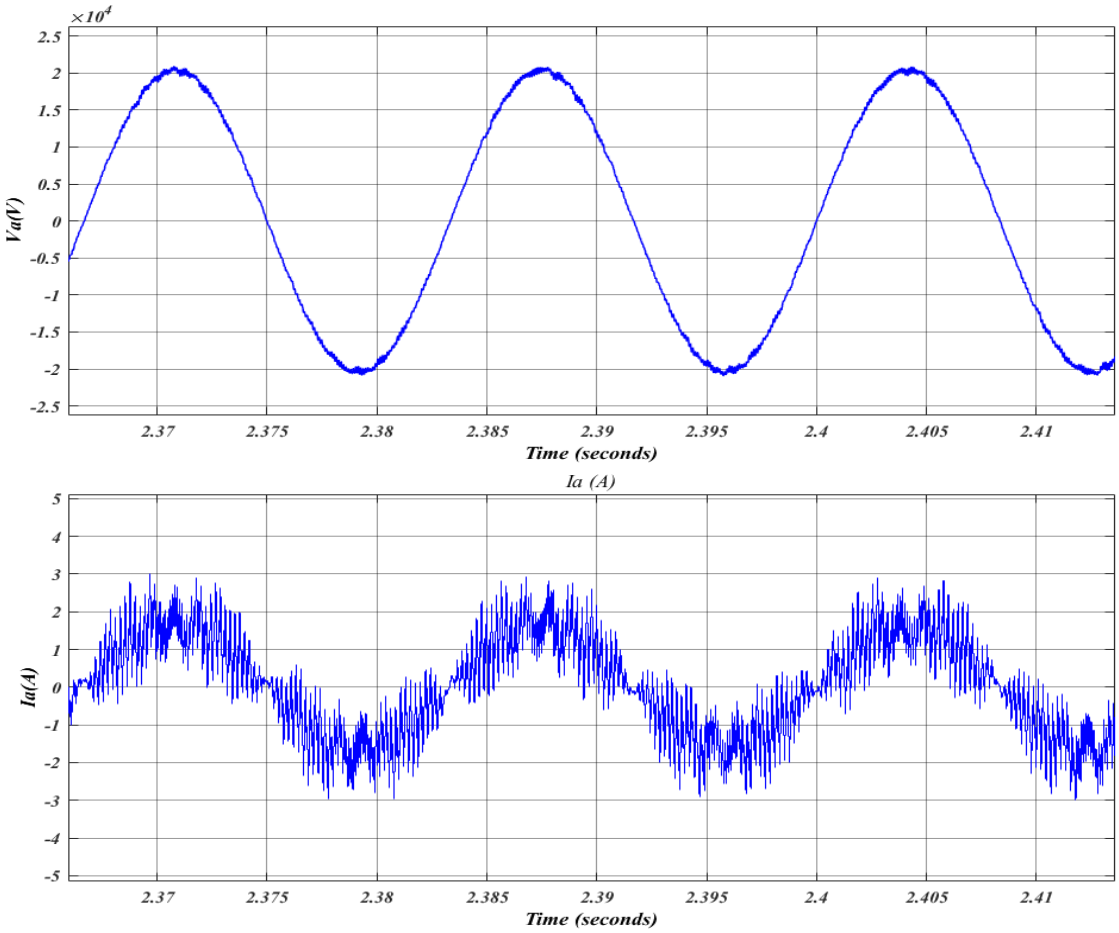

Figure 6-26. *Voltage and current waveform at the point of PCC for Case 3.*

6.5 Case 4: Battery charging from access PV power

In this case, the load is considered as 50 KW to analysis the charging behavior batteries when power generated from PV more than the required power. Overall power flow is shown in Figure 6-27.

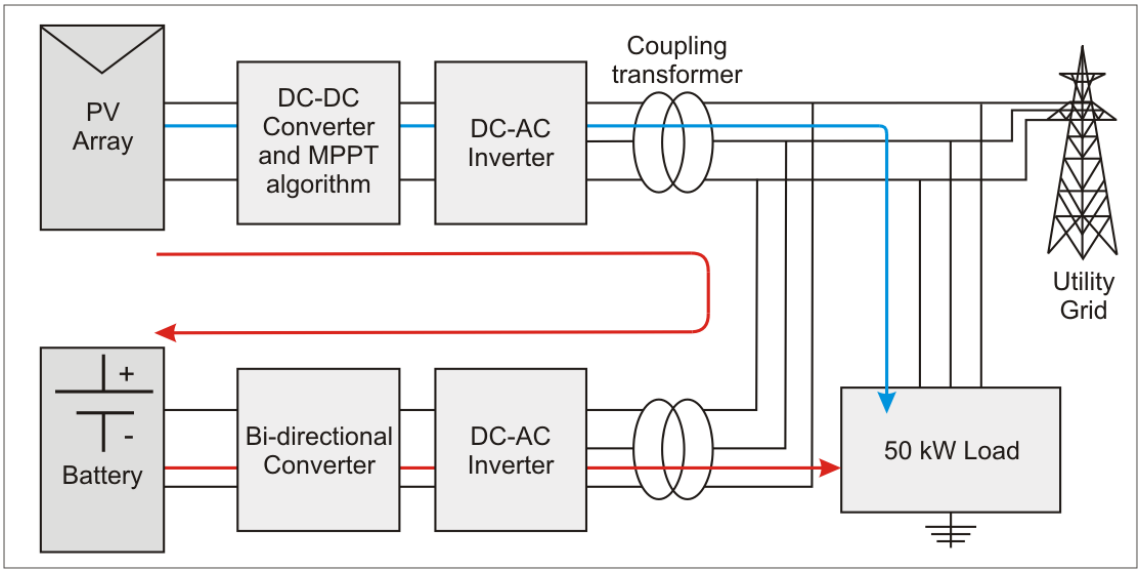

Figure 6-27. *Energy flow showing battery charging and discharge to the load.*

In the case, PV power starts to generator 100 KW of power, the load connected is 50 KW, remaining power charges the batteries as shown in Figure 6-28. For t=0 sec to t = 3 sec, constant power generated from PV, the batteries start to charge during that time. Although it takes less than one second for steady-state charging of batteries from the PV system, it can be improved by improving the control of BESS system. Precise controlling is complicated and thus not discussed in the thesis. Improving the controller can enhance the overall power quality of the PV-BESS system. For the short period of time, at t=6 sec, power generated from PV is almost 0 and whole power provided by BESS to the load. Similarly discharging and charging characteristics can be observed in Figure 6-28. The voltage and current waveforms are shown in Figure 6-31 as in phase but not pure sinusoidal as discussed in the previous case also and it can be improved the improving the precisely controlling the BESS controller.

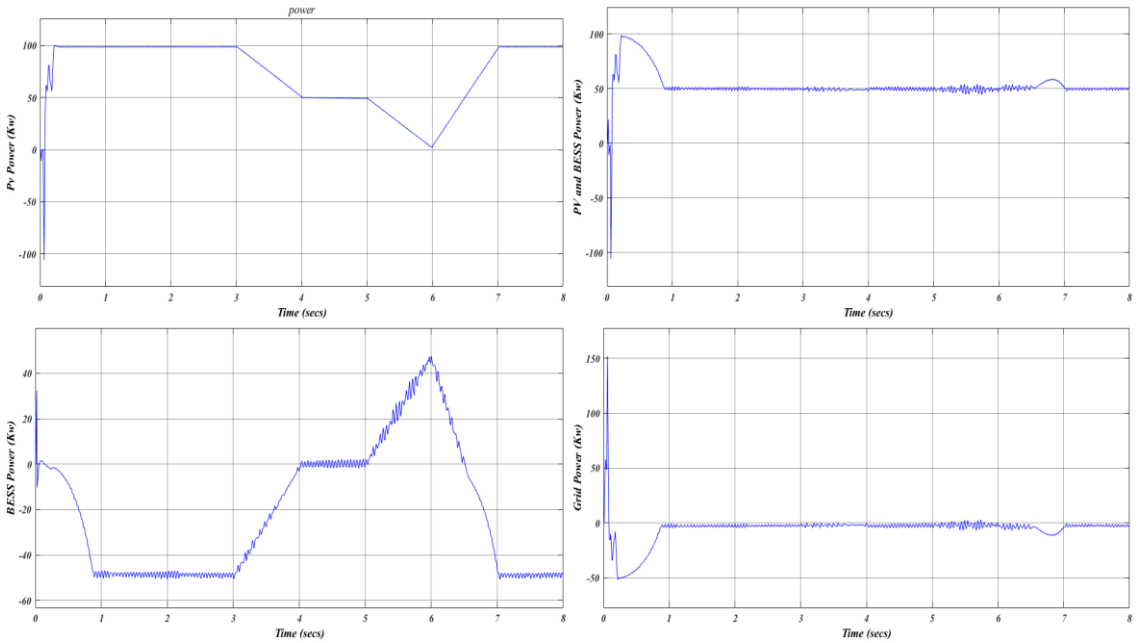

Figure 6-28. *Power delivery to the load from the PV array, battery system and the AC grid.*

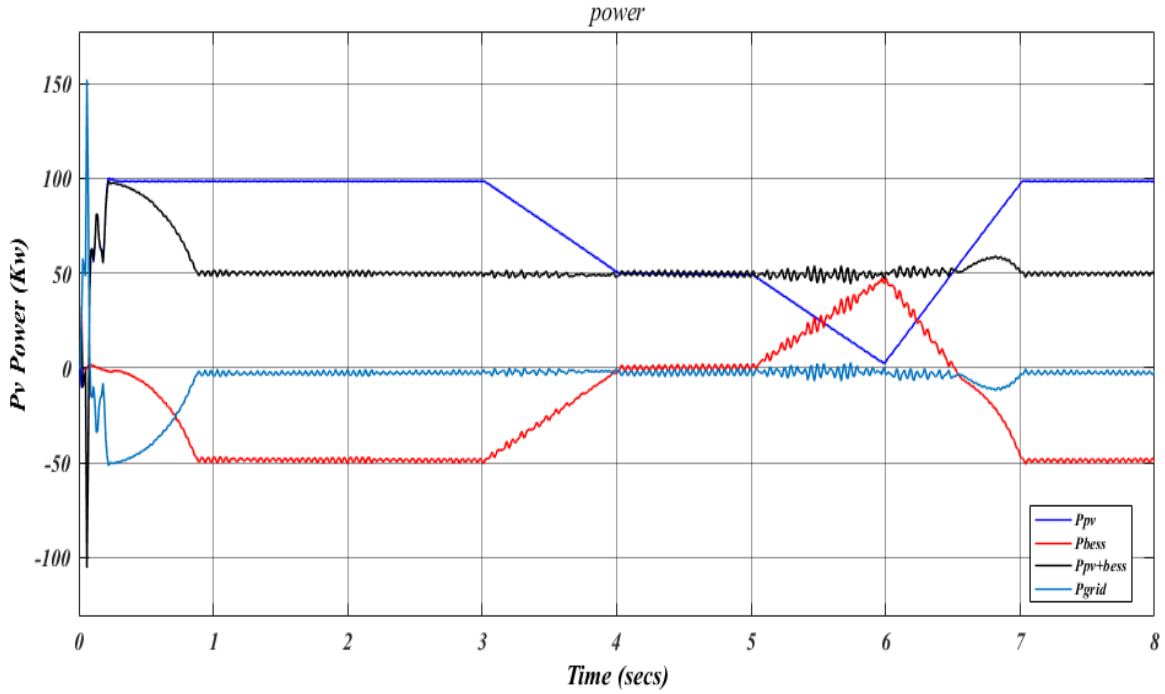

Figure 6-29. *Power generation of the whole system in one diagram.*

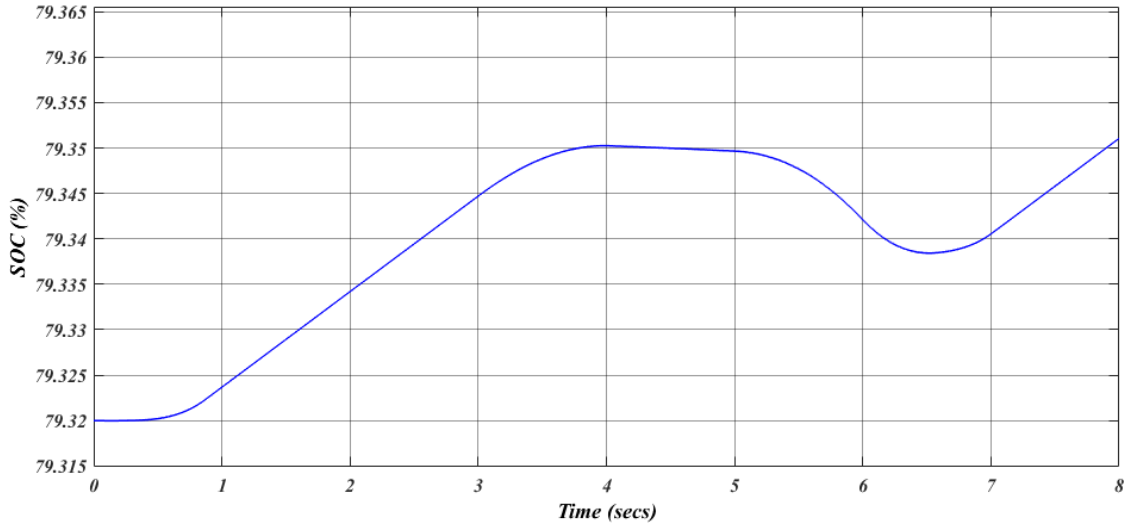

Figure 6-30. *State of charge (%) of the battery.*

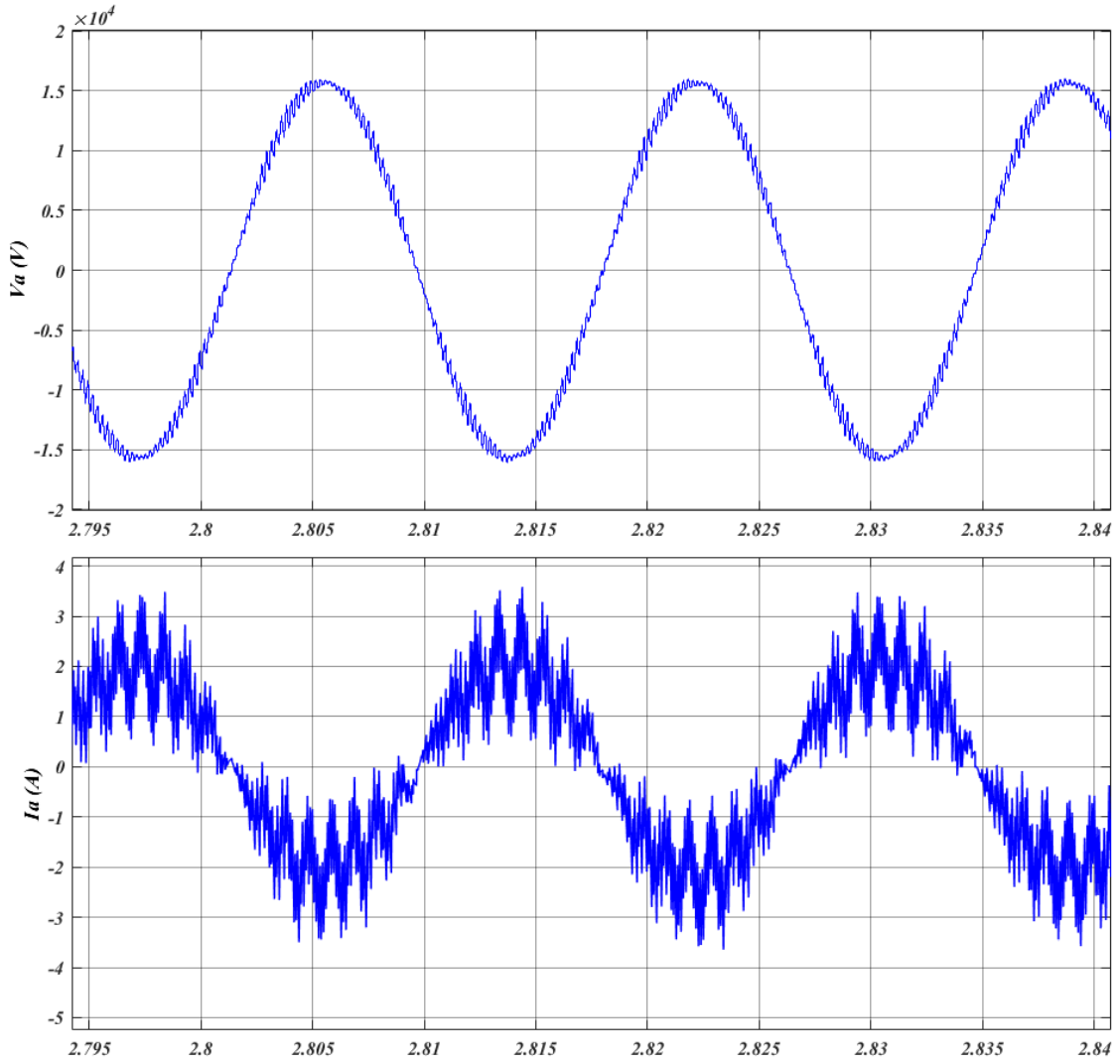

Figure 6-31. *Voltage and current waveform at the point of PCC for Case 4.*

6.6 Summary

Simulation test results of the proposed PV-BESS have been discussed in Chapter 6. MATLAB/Simulink has played a significant role to investigate the performance. The study showed that PV-BESS is a feasible approach to provide electric power to a load consistently in different irradiance conditions. Test results of PV-BESS have been recorded that exhibited a performance improvement over that of a PV system only that do not have any batteries. Further improvement in the controller of the BESS has been a suggestion to improve the overall power quality of PV-EBSS system. The simulation results provided in the thesis are taken for a short period of time because MATLAB takes a long time to run the simulation. But it provides the analogy with original changes in the atmosphere. The irradiance changes can be taken as an effect of moving clouds on the PV panel and thus the temperature.

7. CONCLUSIONS AND FUTURE PROSPECTS

The MATLAB/Simulink environment has been used in this thesis to carry out a wide range of simulations of the compound PV-BESS system. The design of the PV system model comprises the PV array, a boost-type DC/DC converter with a MPPT algorithm using incremental conductance and integral regulator technique, three-phase VSC-type DC/AC inverter and its coupling transformer to connect to a load point and a point of common coupling of an equivalent power grid. The design of BESS model comprises the battery pack, a Cuk-type bi-directional DC/DC converter, a VSC-type DC/AC inverter and a coupling transformer connecting to the point of common coupling.

The main objective of the thesis was to investigate the effectiveness of an integrated PV-BESS system capable to provide a reasonable constant power to an AC load point, in the presence of changing environmental conditions, such as irradiance and temperature. During the development stage, it was found that connecting the BESS in parallel with PV system reduced the modeling complexity a great deal, compared to the option of connecting the two DC/DC converters to the DC bus of a single DC/AC inverter.

The PV-BESS system model is tested for different environmental conditions to visualize their effects in the total output power. The results show that when the output power of the PV system fluctuates or when it provides less power than that required by the load, the BESS system compensates the defaulted power by discharging the right amount of power to provide a constant power supply to the load. On the other hand, when the PV system generates more power than that required by the load, the BESS system absorbs the power surplus to replenish its storage capacity and thus to be able to compensate for future power defaults by the PV system.

6.7 Future work recommendations

The research work reported in the thesis focuses mainly on active power compensation due to PV output power fluctuations. Scenarios of changes in active and reactive power requirements at the load point ought to be considered in any follow up research emanating from this thesis.

The changes in the environmental conditions assumed in this work are very contrived; future work should consider more realistic environmental scenarios of solar radiation and temperature on the PV panel and a measured daily demand curve at point of common coupling, where the load point is.

The tuning of the control parameters in the BESS was carried out by experimentation, i.e., trial and error. The use of suitable optimization techniques to tune the control parameters of the BESS should help to improve the quality of its response in terms of accuracy and time response to follow up more closely the output power variations of the of PV system.

The performance of the compound PV-BESS system should be assessed during faulted conditions on the DC circuits and in the AC circuit.

The functionality of MATLAB evolves constantly, many new blocks are readily available to reduce the simulation time and ease the complexity of the simulation process and this ought to be incorporated into the developed system to ensure its continuous improvement.

REFERENCES

[1] H. Ritchie and M. Roser, "Energy Production & Changing Energy Sources," OurWorldInData.org, 2017. [Online]. Available: https://ourworldindata.org/energy-production-and-changing-energy-sources/. [Accessed November 2017].

[2] S. Hegedus and A. Luque, "Achievements and challenges of solar electricity from photovoltaics," in *Handbook of Photovoltaic Science and Engineering*, John Wiley & Sons, Ltd, 2011, pp. 2-38.

[3] I. E. AGENCY, "World Energy Outlook 2013.," 2013. [Online]. Available: https://www.iea.org/publications/freepublications/publication/WEO2013.pdf. [Accessed November 2017].

[4] I. E. Agency, "Snapshot Of Global Photovoltaic Markets," 2016. [Online]. Available: http://www.iea-pvps.org/fileadmin/dam/public/report/statistics/IEA-PVPS_-_A_Snapshot_of_Global_PV_-_1992-2016__1_.pdf. [Accessed October 2017].

[5] REN21, "Renewables 2017 Global Status Report "Market And Industry Trends"," 2017. [Online]. Available: http://www.ren21.net/wp-content/uploads/2017/06/17-8399_GSR_2017_Full_Report_0621_Opt.pdf. [Accessed December 2017].

[6] J. V. Appen, M. Braun, T. Stetz, K. Diwold and D. Geibel, "Time in the Sun: The Challenge of High PV Penetration in the German Electric Grid," *IEEE Power and Energy Magazine,* vol. 11, no. 2, pp. 55-64, March-April, 2013.

[7] D. Spiers, "Batteries in PV Systems," in *Practical Handbook of Photovoltaics*, Elsevier, December 2012, pp. 721-776.

[8] R. Corkish, M. A. Green, M. E. Watt and S. R. Wenham, Applied Photovoltaics, 2nd ed., Earthscan, 2007.

[9] G. Dzimano, *Modeling Of Photovoltaic Systems, Doctoral Thesis,* The Ohio State University, 2008.

[10] M. R. SUNNY, "Sizing An Energy Storage To Be Used In Parallel With PV Inverter To Balance The Fluctuations In Output Power From PV Generator Msc, Thesis," Tampere University of Technology, 2014.

[11] R. Messenger and A. Abtahi, Photovoltaic Systems Engineering, Fourth ed., CRC Press, 2017.

[12] A. Luque and S. Hegedus, Handbook of Photovoltaic Science and Engineering, second ed., John Wiley & Sons, 2003.

[13] M. R. Patel, Spacecraft Power Systems, CRC Press, 2004.

[14] A. MÄKI, "Topology Of A Silicon-Based Grid-Connected, Photovoltaic Generator, Msc Thesis," Tampere University of Technology, 2010.

[15] S. Kjaer, J. Pedersen and F. Blaabjerg, "A review of single-phase grid-connected inverters for photovoltaic modules," *IEEE Transactions on Industry Applications,* vol. 41, no. 5, pp. 1292-1306, Sept.-Oct. 2005..

[16] D. T. Lobera, *Measuring actual operating conditions of a photovoltaic power generator, Msc Thesis,* Tampere University of Technology, 2010.

[17] B. Sørensen, "Chapter 33: Battery storage," in *Renewable Energy Conversion, Transmission and Storage*, 2007.

[18] D. Linden and T. B. Reddy, Handbook of Batteries, 3rd ed., McGraw-Hill, 2002, p. 1.8.

[19] D. Berndt, "Electrochemical Energy Storage," in *Battery Technology Handbook*, CRC press, 2003.

[20] P. J. Grbovic, "Ultra-capacitors in Power Conversion Systems Applications," in *Analysis And Design From Theory To Practice*, John Wiley & Sons, 2012, p. 17.

[21] "Ralph J. Brodd, "Synopsis of the Lithium-Ion Battery Markets"," in *Lithium-Ion Batteries, Science and Technologies*, Springer, 2009, p. 2.

[22] G. Blomgren, R. Powers and D. MacArthur, "Lithium and Lithium Ion Batteries," 2002.

[23] S. Piller, M. Perrin and A. Jossen, "Methods for state-of-charge determination and their applications," *Journal of Power Sources,* pp. 113-120, 2001.

[24] X. Hu, S. Li, H. Peng and F. Sun, "Robustness analysis of State-of-Charge estimation methods for two types of Li-ion batteries,," *Journal of Power Sources,* vol. 217, pp. 209-219, November 2012.

[25] R. Huggins, Advanced Batteries Materials Science Aspects, 2010.

[26] K. Young, C. Wang, Y. W. Le and a. K. Strunz, "Electric Vehicle Battery Technologies," in *Electric Vehicle Integration into Modern Power Networks*, New Y ork, 2013, p. 29.

[27] B. S. Bhangu, P. Bentley and D. A. Ston, "Nonlinear Observers for Predicting State-of-Chargeand State-of-Health of Lead-Acid Batteries forHybrid-Electric Vehicles," *IEEE Transactions on Vehicular Technology,* vol. 54, no. 3, pp. 783-794, May 2005.

[28] R. A. Huggins, Energy storage, Springer, 2010.

[29] "Mathwork," [Online]. Available: http://se.mathworks.com/help/physmod/sps/powersys/ref/battery.html?requestedDomain=se.mathworks.com. [Accessed Jun 2017].

[30] O. Tremblay1 and L.-A. Dessaint, "Experimental Validation of a Battery Dynamic Model for EV," *World Electric Vehicle,* pp. 1-9, May 13 - 16, 2009.

[31] M. H. Rashid, Power Electronics Handbook, Third, Ed., Butterworth-Heinemann pu, 2011.

[32] N. Mohan, T. M. Undeland and W. P. Robbins, Power Electronics. Converters, Applications, 3rd, Ed., John Wiley and Sons, Inc, 2003.

[33] A. Pazynych, "A STUDY OF THE HARMONIC CONTENT OF DISTRIBUTION, Msc Thesis," Tampere University of Technology, 2014.

[34] M. A. G. d. Brito, L. P. Sampaio, L. G. Junior and C. A. Canesin, "Evaluation of MPPT techniques for photovoltaic applications," *IEEE International Symposium on Industrial Electronics,* pp. 1039-1044, 2011.

[35] M. Abdulkadir, A. S. Samosir and A. H. M. Yatim, "Modelling and simulation of maximum power point tracking of photovoltaic system in Simulink model," *IEEE International Conference on Power and Energy (PECon),* pp. 325-330, 2012.

[36] "Introduction to TLI technology.," Mitsubishi Electric Power Semiconductors, 2009. [Online]. Available:

http://www.pwrx.com/pwrx/app/TLI%20Series%20Application%20Note.pdf. [Accessed October 2017].

[37] N. G. Hingorani and L. Gyugyi, Understanding FACTS: Concepts and Technology of Flexible AC Transmission Systems, New York, USA: Wiley-IEEE Press, 1999.

[38] F. Blaabjerg, R. Teodorescu, M. Liserre and A. Timbus, "Overview of Control and Grid Synchronization for Distributed Power Generation Systems," *IEEE Transactions on Industrial Electronics,* vol. 53, no. 5, pp. 1398-1409, 2006.

[39] S. Yang, Q. Lei, F. Z. Peng and Z. Qian, "A Robust Control Scheme for Grid-Connected Voltage-Source Inverters," *IEEE Transactions on Industrial Electronics,* vol. 58, no. 1, pp. 202-212, January 2011.

[40] M. H. Mahlooji, H. R. Mohammadi and M. Rahimi, "A review on modeling and control of grid-connected photovoltaic inverters with LCL filter, In Renewable and Sustainable Energy Reviews," vol. 81, no. 1, pp. 563-578, 02 aug 2017.

[41] M. G. Molina, "Dynamic Modelling and Control Design of Advanced Energy Storage for Power System Applications," in *Dynamic Modelling*, A. V. Brito, Ed., InTech, 2010.

[42] K. Ahmed, S. Finney and B. Williams, "Passive Filter Design for Three-Phase Inverter Interfacing in Distributed Generation," in *Compatibility in Power Electronics*, Gdansk, 2007.

[43] "Mathwork," [Online]. Available: https://se.mathworks.com/help/physmod/sps/examples/detailed-model-of-a-100-kw-grid-connected-pv-array.html. [Accessed mar 2017].

[44] D. Linden and T. B. Reddy, "Chapter 23 - lead-acid batteries," in *Handbook of Batteries*, McGraw-Hill, 2002.